Supplementary Materials for

Molecular Jackhammers Induce Intracellular Calcium Release and Skeletal Muscle Contraction by Vibronic-Driven Action

Yuchen Rui[1,†], Bowen Li[1,†,*], Vardan Vardanyan[1], Soonyoung Kim[4], Dallin Arnold[1], Jacob L. Beckham[1], Ciceron Ayala-Orozco[1], Ana L. Santos[1], Gautam Chaudhry[1], Lixin Zhou[1], Shichen Xu[1], Tengda Si[1], Zicheng Wang[1], Angel A. Martí[1,2,3], Anatoly Kolomeisky[1,*], Jacob T. Robinson[2,4,*], James M. Tour[1,3,5,6,*]

[1]Department of Chemistry, Rice University, Houston, Texas 77005, USA.

[2]Department of Bioengineering, Rice University, Houston, Texas 77005, USA.

[3]Department of Materials Science and Nanoengineering, Rice University, Houston, Texas 77005, USA.

[4]Department of Electrical Engineering, Rice University, Houston, Texas 77005, USA.

[5]Smalley-Curl Institute, Rice University, Houston, Texas, 77005, USA.

[6]NanoCarbon Center and the Rice Advanced Materials Institute, Rice University, Houston, Texas, 77005, USA.

[†]These authors contributed equally: Yuchen Rui, Bowen Li

*Corresponding authors: libowen924@gmail.com; tolya@rice.edu; jtrobinson@rice.edu; tour@rice.edu

lead contact: James M. Tour

Synthesis of cyanine dyes and data characterization

Scheme S1: Summary of heterocyclic salts **1** used in synthesis of cyanine dyes.

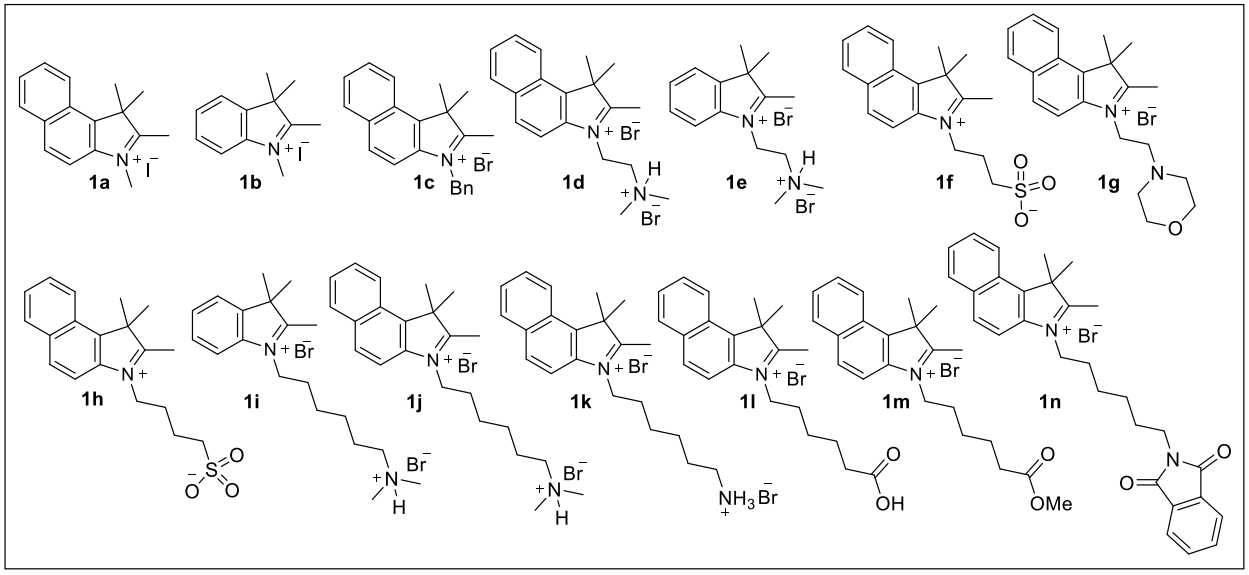

Scheme S2: Synthesis of cyanine dye **3** between heterocyclic salts **1/1'** and **2**.

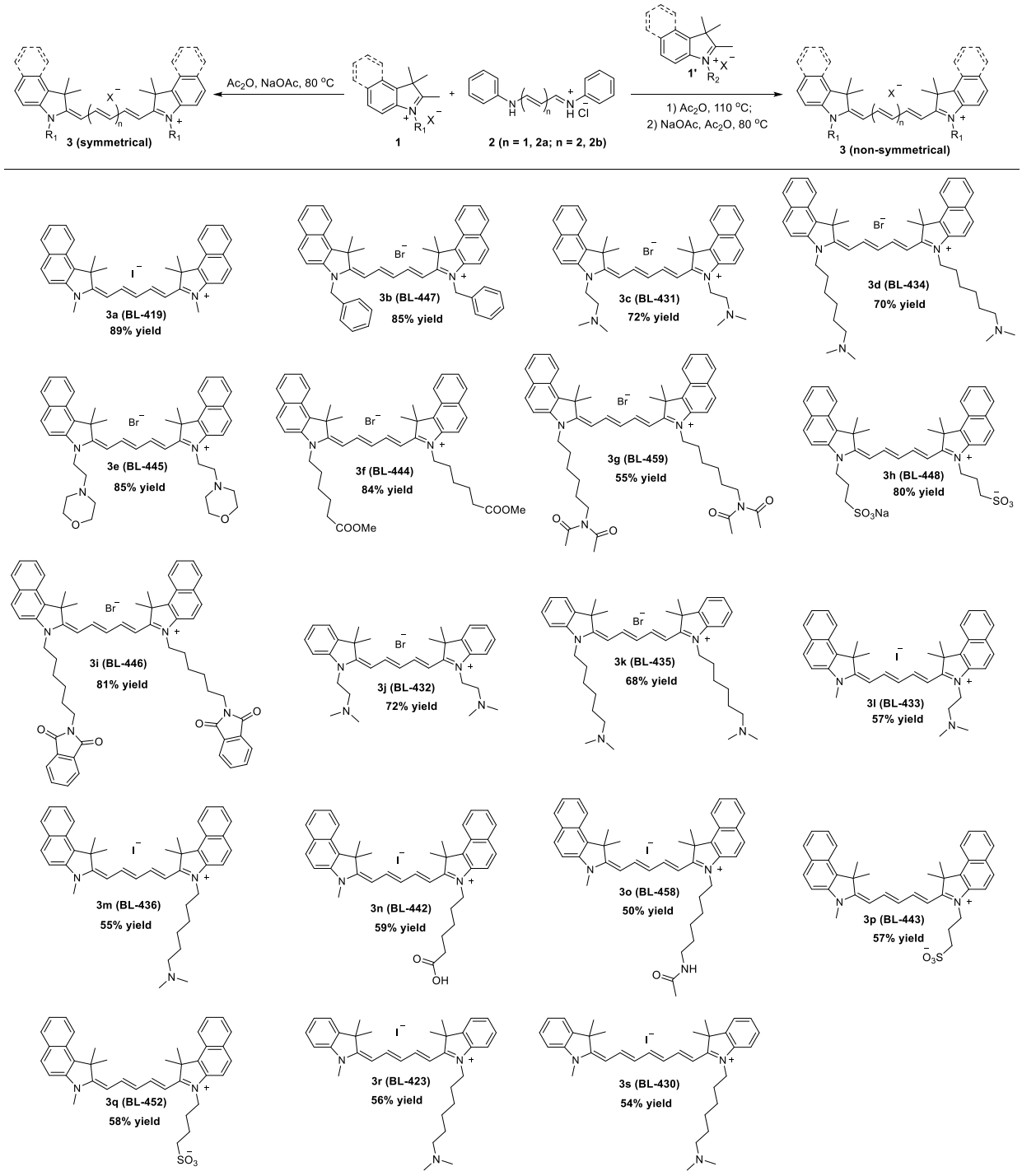

Compound **4** were synthesized according to the previous literature.[1]

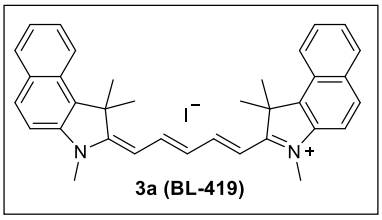

3a (BL-419)

Synthesis of 3a (BL-419): Prepared according to the general procedure **a** from **1a** (133 mg, 0.38 mmol, 2 equiv) and **2a** (49 mg, 0.19 mmol, 1 equiv). Dark blue solid. Yield: 89% (103 mg). ^{1}H-NMR (600 MHz, CD_2Cl_2) δ 8.27 – 8.20 (m, 2H), 8.20 – 8.16 (m, 2H), 7.99 – 7.94 (m, 4H), 7.66 – 7.61 (m, 2H), 7.51 – 7.47 (m, 2H), 7.45 (d, *J* = 8.8 Hz, 2H), 6.75 (t, *J* = 12.4 Hz, 1H), 6.28 (d, *J* = 13.7 Hz, 2H), 3.76 (s, 6H), 2.04 (s, 12H). ^{13}C-NMR (151 MHz, CD_2Cl_2) δ 175.27, 152.93, 140.47, 134.12, 132.30, 130.88, 130.36, 128.50, 128.11, 125.63, 125.44, 122.68, 110.93, 110.91, 103.52, 51.57, 32.66, 27.74. HRMS (ESI) calculated for [M, $C_{35}H_{35}N_2$]$^{+}$: 483.2795, found: 483.2822.

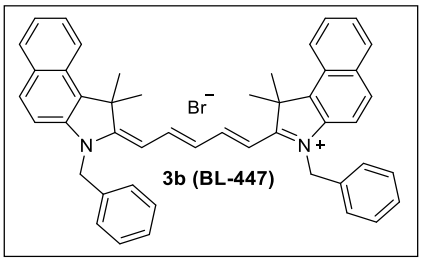

3b (BL-447)

Synthesis of 3b (BL-447): Prepared according to the general procedure **a** from **1c** (144 mg, 0.38 mmol, 2 equiv) and **2a** (49 mg, 0.19 mmol, 1 equiv). Dark blue solid. Yield: 85% (115 mg). ^{1}H-NMR (500 MHz, CD_3OD) δ 8.35 (t, *J* = 13.1 Hz, 2H), 8.24 (d, *J* = 8.5 Hz, 2H), 7.94 – 7.89 (m, 4H), 7.64 – 7.60 (m, 2H), 7.48 – 7.42 (m, 4H), 7.36 – 7.32 (m, 4H), 7.30 – 7.26 (m, 6H), 6.48 (t, *J* = 12.4 Hz, 1H), 6.31 (d, *J* = 13.7 Hz, 2H), 5.45 (s, 4H), 2.03 (s, 12H). ^{13}C-NMR (126 MHz, CD_3OD) δ 176.58, 154.90, 141.17, 136.01, 134.99, 133.45, 131.74, 131.09, 130.26, 129.43, 129.19,

128.81, 127.51, 127.12, 126.17, 123.38, 112.20, 104.66, 52.57, 48.38, 27.73. HRMS (ESI) calculated for [M, $C_{47}H_{43}N_2$]$^+$: 635.3421, found: 635.3458.

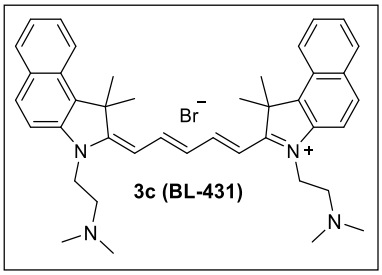

Synthesis of 3c (BL-431): Prepared according to the general procedure **a** from **1d** (167 mg, 0.38 mmol, 2 equiv) and **2a** (49 mg, 0.19 mmol, 1 equiv). Dark blue solid. Yield: 72% (92 mg). ^{1}H-NMR (600 MHz, CD_3OD) δ 8.40 (t, *J* = 12.9 Hz, 2H), 8.26 (d, *J* = 8.5 Hz, 2H), 8.03 (d, *J* = 8.7 Hz, 2H), 8.00 (d, *J* = 8.3 Hz, 2H), 7.67 – 7.63 (m, 2H), 7.61 (d, *J* = 8.8 Hz, 2H), 7.50 (t, *J* = 7.6 Hz, 2H), 6.75 – 6.68 (m, 1H), 6.38 (d, *J* = 13.6 Hz, 2H), 4.37 (t, *J* = 7.4 Hz, 4H), 2.81 (t, *J* = 7.5 Hz, 4H), 2.44 (s, 12H), 2.04 (s, 12H). ^{13}C-NMR (151 MHz, CD_3OD) δ 176.24, 154.48, 140.88, 135.04, 133.48, 131.75, 131.12, 129.46, 128.78, 127.02, 126.15, 123.38, 111.96, 104.26, 56.79, 52.51, 45.96, 43.32, 27.66. HRMS (ESI) calculated for [M, $C_{41}H_{49}N_4$]$^+$: 597.3952, found: 597.3962.

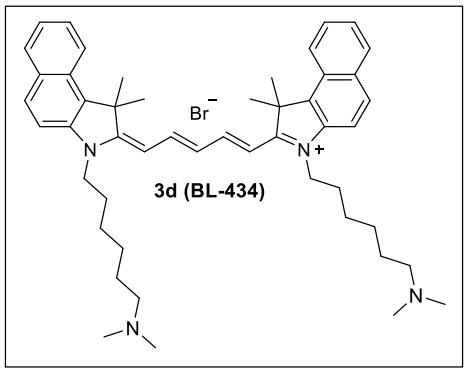

Synthesis of 3d (BL-434): Prepared according to the general procedure **a** from **1j** (188 mg, 0.38 mmol, 2 equiv) and **2a** (49 mg, 0.19 mmol, 1 equiv). Dark blue solid. Yield: 70% (105 mg). ^{1}H-

NMR (600 MHz, CD_3OD) δ 8.35 (t, *J* = 13.0 Hz, 2H), 8.19 (d, *J* = 8.5 Hz, 2H), 7.98 (d, *J* = 8.8 Hz, 2H), 7.92 (d, *J* = 8.2 Hz, 2H), 7.65 (d, *J* = 8.8 Hz, 2H), 7.58 (t, *J* = 7.5 Hz, 2H), 7.43 – 7.35 (m, 2H), 6.98 (t, *J* = 12.3 Hz, 1H), 6.43 (d, *J* = 13.6 Hz, 2H), 4.28 (t, *J* = 7.6 Hz, 4H), 3.27 – 3.20 (m, 4H), 2.92 (s, 12H), 1.95 (s, 12H), 1.91 – 1.85 (m, 4H), 1.82 – 1.77 (m, 4H), 1.67 – 1.60 (m, 4H), 1.56 – 1.49 (m, 4H). ^{13}C-NMR (151 MHz, CD_3OD) δ 175.62, 154.10, 140.84, 135.10, 133.25, 131.65, 131.01, 129.37, 128.66, 127.20, 125.95, 123.35, 112.35, 104.24, 58.92, 52.32, 45.11, 43.75, 28.54, 27.81, 27.21, 27.15, 25.48. HRMS (ESI) calculated for [M, $C_{49}H_{65}N_4$]$^+$: 709.5214, found: 709.5219.

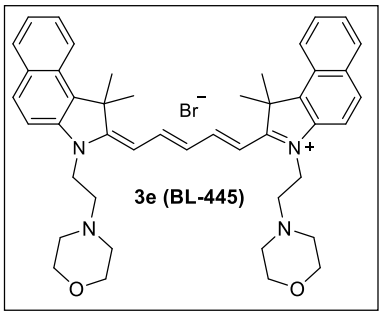

3e (BL-445)

Synthesis of 3e (BL-445): Prepared according to the general procedure **a** from **1g** (153 mg, 0.38 mmol, 2 equiv) and **2a** (49 mg, 0.19 mmol, 1 equiv). Dark blue solid. Yield: 85% (123 mg). ^{1}H-NMR (500 MHz, CD_3OD) δ 8.44 – 8.33 (m, 2H), 8.21 (d, *J* = 8.6 Hz, 2H), 7.97 (d, *J* = 8.7 Hz, 2H), 7.93 (d, *J* = 8.2 Hz, 2H), 7.61 – 7.56 (m, 4H), 7.46 – 7.39 (m, 2H) 6.70 (t, *J* = 12.3 Hz, 1H), 6.38 (d, *J* = 13.8 Hz, 2H), 4.36 (t, *J* = 6.4 Hz, 4H), 3.58 (t, *J* = 4.6 Hz, 8H), 2.80 (t, *J* = 6.4 Hz, 4H), 2.56 (t, *J* = 4.5 Hz, 8H), 1.98 (s, 12H). ^{13}C-NMR (126 MHz, CD_3OD) δ 176.36, 154.03, 140.95, 134.95, 133.30, 131.51, 131.04, 129.37, 128.68, 126.66, 126.01, 123.34, 112.29, 104.63, 67.87, 56.44, 55.04, 52.35, 43.06, 27.72. HRMS (ESI) calculated for [M, $C_{45}H_{53}N_4O_2$]$^+$: 681.4163, found: 681.4209.

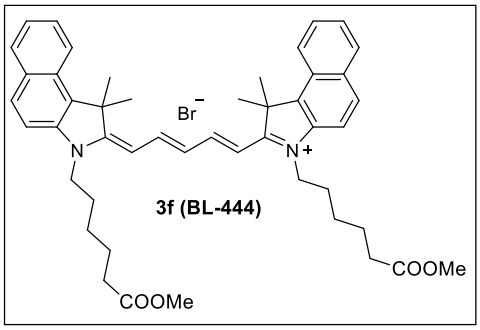

Synthesis of 3f (BL-444): Prepared according to the general procedure **a** from **1m** (158 mg, 0.38 mmol, 2 equiv) and **2a** (49 mg, 0.19 mmol, 1 equiv). Dark blue solid. Yield: 84% (126 mg). ^{1}H-NMR (500 MHz, CD_3OD) δ 8.36 (t, *J* = 13.0 Hz, 2H), 8.23 – 8.18 (m, 2H), 7.97 (d, *J* = 8.8 Hz, 2H), 7.93 (dd, *J* = 8.1, 1.2 Hz, 2H), 7.62 – 7.54 (m, 4H), 7.46 – 7.41 (m, 2H), 6.69 (t, *J* = 12.3 Hz, 1H), 6.33 (d, *J* = 13.7 Hz, 2H), 4.21 (t, *J* = 7.5 Hz, 4H), 3.60 (s, 6H), 2.34 (t, *J* = 7.3 Hz, 4H), 1.97 (s, 12H), 1.88 – 1.82 (m, 4H), 1.73 – 1.66 (m, 4H), 1.54 – 1.47 (m, 4H). ^{13}C-NMR (126 MHz, CD_3OD) δ 175.82, 175.59, 154.30, 140.89, 135.08, 133.32, 131.67, 131.06, 129.40, 128.71, 126.69, 126.03, 123.34, 112.08, 104.04, 52.36, 52.03, 44.92, 34.48, 28.41, 27.66, 27.24, 25.66, 20.86. HRMS (ESI) calculated for [M, $C_{47}H_{55}N_2O_4$]$^{+}$: 711.4156, found: 711.4200.

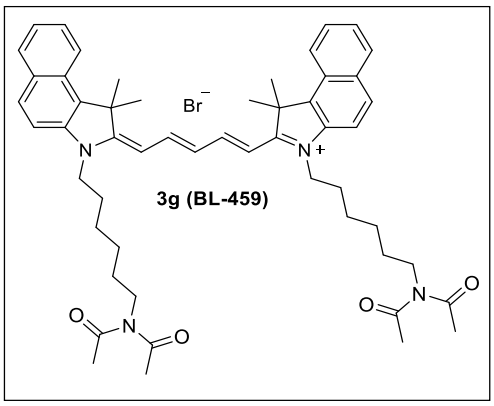

Synthesis of 3g (BL-459): Prepared according to the general procedure **a** from **1k** (178 mg, 0.38 mmol, 2 equiv) and **2a** (49 mg, 0.19 mmol, 1 equiv). Dark blue solid. Yield: 55% (94 mg). ^{1}H-NMR (600 MHz, CD_3OD) δ 8.35 (t, *J* = 13.0 Hz, 2H), 8.21 (d, *J* = 8.5 Hz, 2H). 7.99 – 7.89 (m,

4H), 7.63 – 7.52 (m, 4H), 7.44 (t, *J* = 7.5 Hz, 2H), 6.71 (t, *J* = 12.3 Hz, 1H), 6.34 (d, *J* = 13.6 Hz, 2H), 4.21 (t, *J* = 7.6 Hz, 4H), 3.69 – 3.60 (m, 4H), 2.34 (s, 12H), 1.97 (s, 12H), 1.88 – 1.81 (m, 4H), 1.61 – 1.49 (m, 8H), 1.45 – 1.39 (m, 4H). ^{13}C-NMR (151 MHz, CD_3OD) δ 175.79, 175.17, 154.22, 140.89, 135.08, 133.32, 131.69, 131.07, 129.40, 128.72, 126.74, 126.05, 123.34, 112.11, 104.07, 52.36, 45.76, 44.98, 29.73, 28.52, 27.69, 27.49, 27.28, 26.47. HRMS (ESI) calculated for [M, $C_{53}H_{65}N_4O_4$]$^+$: 821.5000, found: 821.5024.

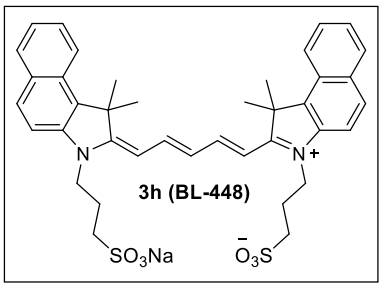

Synthesis of 3h (BL-448): Prepared according to the general procedure **a** from **1f** (126 mg, 0.38 mmol, 2 equiv) and **2a** (49 mg, 0.19 mmol, 1 equiv). Dark blue solid. Yield: 80% (109 mg). ^{1}H-NMR (600 MHz, CD_3OD) δ 8.34 (t, *J* = 13.0 Hz, 2H), 8.18 (d, *J* = 8.5 Hz, 2H), 7.96 (d, *J* = 8.7 Hz, 2H), 7.89 (d, *J* = 8.3 Hz, 2H), 7.70 (d, *J* = 8.8 Hz, 2H), 7.61 – 7.53 (m, 2H), 7.40 (t, *J* = 7.5 Hz, 2H), 6.73 (t, *J* = 12.3 Hz, 1H), 6.40 (d, *J* = 13.7 Hz, 2H), 4.43 (t, *J* = 8.0 Hz, 4H), 3.07 (t, *J* = 6.9 Hz, 4H), 2.31 (t, *J* = 7.9 Hz, 4H), 1.91 (s, 12H). ^{13}C-NMR (151 MHz, CD_3OD) δ 175.73, 154.86, 141.01, 134.84, 133.37, 131.71, 131.01, 129.51, 128.58, 127.26, 125.91, 123.35, 112.18, 103.98, 52.40, 44.25, 27.54, 24.47. HRMS (ESI) calculated for [M-H, $C_{39}H_{42}N_2O_6S_2$]$^-$: 697.2412, found: 697.2381.

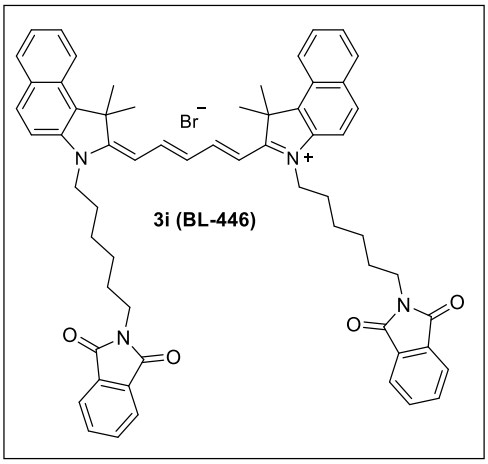

Synthesis of 3i (BL-446): Prepared according to the general procedure **a** from **1n** (197 mg, 0.38 mmol, 2 equiv) and **2a** (49 mg, 0.19 mmol, 1 equiv). Dark blue solid. Yield: 81% (153 mg). ^{1}H-NMR (500 MHz, CD_2Cl_2) δ 8.48 (t, *J* = 13.0 Hz, 2H), 8.20 (d, *J* = 8.5 Hz, 2H), 7.96 – 7.90 (m, 4H), 7.83 – 7.73 (m, 4H), 7.71 – 7.66 (m, 4H), 7.62 – 7.56 (m, 2H), 7.47 – 7.39 (m, 4H), 6.73 (t, *J* = 12.4 Hz, 1H), 6.27 (d, *J* = 13.7 Hz, 2H), 4.15 (t, *J* = 7.5 Hz, 4H), 3.65 (t, *J* = 7.1 Hz, 4H), 2.07 (s, 12H), 1.89 – 1.81 (m, 4H), 1.71 – 1.63 (m, 4H), 1.57 – 1.50 (m, 4H), 1.46 – 1.38 (m, 4H). ^{13}C-NMR (126 MHz, CD_2Cl_2) δ 174.72, 168.50, 153.33, 139.71, 134.34, 134.18, 132.33, 132.03, 130.65, 130.13, 128.38, 127.84, 125.73, 125.19, 123.16, 122.64, 110.91, 103.13, 51.53, 44.60, 37.85, 28.54, 27.78, 27.62, 26.76, 26.61. HRMS (ESI) calculated for [M, $C_{60}H_{63}N_4O_4$]$^{+}$: 913.4687, found: 913.4767.

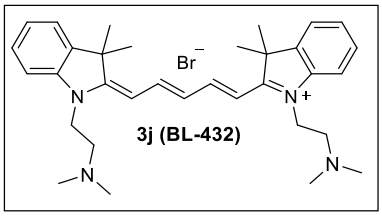

Synthesis of 3j (BL-432): Prepared according to the general procedure **a** from **1e** (148 mg, 0.38 mmol, 2 equiv) and **2a** (49 mg, 0.19 mmol, 1 equiv). Dark blue solid. Yield: 72% (79 mg). ^{1}H-

NMR (600 MHz, CD_3OD) δ 8.32 (t, *J* = 13.0 Hz, 2H), 7.50 (d, *J* = 7.5 Hz, 2H), 7.46 – 7.39 (m, 2H), 7.36 (d, *J* = 7.9 Hz, 2H), 7.27 (t, *J* = 7.4 Hz, 2H), 6.77 (t, *J* = 12.1 Hz, 1H), 6.40 (d, *J* = 13.5 Hz, 2H), 4.32 (t, *J* = 7.3 Hz, 4H), 2.95 – 2.82 (m, 4H), 2.53 (s, 12H), 1.74 (s, 12H). ^{13}C-NMR (151 MHz, CD_3OD) δ 175.00, 155.75, 143.30, 142.57, 129.77, 127.50, 126.36, 123.50, 111.93, 104.86, 56.03, 56.00, 50.63, 45.58, 45.56, 42.61, 42.58, 27.98. HRMS (ESI) calculated for [M, $C_{33}H_{45}N_4$]$^+$: 497.3639, found: 497.3646.

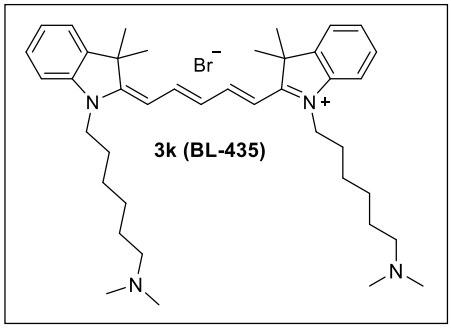

Synthesis of 3k (BL-435): Prepared according to the general procedure **a** from **1i** (169 mg, 0.38 mmol, 2 equiv) and **2a** (49 mg, 0.19 mmol, 1 equiv). Dark blue solid. Yield: 68% (65 mg). ^{1}H-NMR (600 MHz, CD_3OD) δ 8.27 (t, *J* = 13.0 Hz, 2H), 7.49 (d, *J* = 6.9 Hz, 2H), 7.43 – 7.37 (m, 2H), 7.36 – 7.29 (m, 2H), 7.28 – 7.22 (m, 2H), 6.97 (t, *J* = 12.4 Hz, 1H), 6.45 (d, *J* = 13.6 Hz, 2H), 4.16 (t, *J* = 7.6 Hz, 4H), 3.24 – 3.14 (m, 4H), 2.91 (s, 12H), 1.89 – 1.82 (m, 4H) 1.81 – 1.75 (m, 4H), 1.73 (s, 12H), 1.63 – 1.56 (m, 4H), 1.55 – 1.47 (m, 4H). ^{13}C-NMR (151 MHz, CD_3OD) δ 174.53, 155.32, 143.47, 142.70, 129.73, 127.32, 126.15, 123.41, 112.14, 104.65, 58.97, 50.52, 44.89, 43.74, 43.73, 28.24, 28.08, 27.26, 27.16, 25.53. HRMS (ESI) calculated for [M, $C_{41}H_{61}N_4$]$^+$: 609.4891, found: 609.4901.

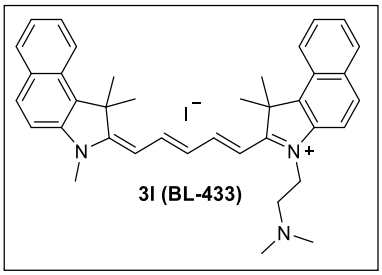

Synthesis of 3l (BL-433): Prepared according to the general procedure **b** from **1a** (67 mg, 0.19 mmol, 1 equiv), **1d** (84 mg, 0.19 mmol, 1 equiv) and **2a** (49 mg, 0.19 mmol, 1 equiv). Dark blue solid. Yield: 57% (72 mg). ^{1}H-NMR (600 MHz, CD_3OD) δ 8.41 – 8.32 (m, 2H), 8.26 – 8.19 (m, 2H), 8.04 – 7.92 (m, 4H), 7.65 – 7.59 (m, 3H), 7.57 (d, *J* = 8.8 Hz, 1H), 7.49 – 7.43 (m, 2H), 6.70 (t, *J* = 12.3 Hz, 1H), 6.38 (d, *J* = 13.9 Hz, 1H), 6.30 (d, *J* = 13.5 Hz, 1H), 4.32 (t, *J* = 7.4 Hz, 2H), 3.78 (s, 3H), 2.81 – 2.73 (m, 2H) , 2.43 (s, 6H), 2.00 (s, 12H). ^{13}C-NMR (151 MHz, CD_3OD) δ 177.14, 175.36, 154.77, 141.53, 140.96, 135.25, 134.64, 133.54, 133.29, 131.68, 131.64, 131.09, 131.07, 129.49, 129.33, 128.76, 128.69, 126.82, 126.18, 125.92, 123.42, 123.32, 112.07, 111.85, 104.76, 103.54, 56.73, 52.55, 52.25, 45.99, 43.18, 32.22, 27.72, 27.49. HRMS (ESI) calculated for [M, $C_{38}H_{42}N_3$]$^{+}$: 540.3373, found: 540.3385.

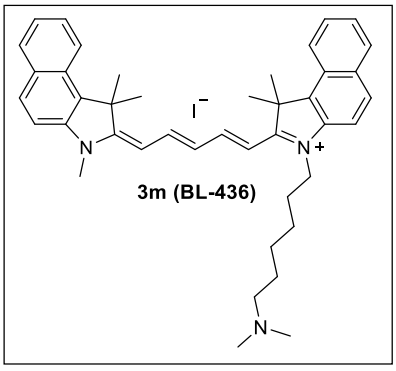

Synthesis of 3m (BL-436): Prepared according to the general procedure **b** from **1a** (67 mg, 0.19 mmol, 1 equiv), **1j** (94 mg, 0.19 mmol, 1 equiv) and **2a** (49 mg, 0.19 mmol, 1 equiv). Dark blue solid. Yield: 55% (76 mg). ^{1}H-NMR (600 MHz, CD_3OD) δ 8.36 (t, *J* = 13.0 Hz, 2H), 8.26 – 8.19

(m, 2H), 8.01 (d, *J* = 8.8 Hz, 2H), 7.98 – 7.92 (m, 2H), 7.65 – 7.58 (m, 4H), 7.49 – 7.43 (m, 2H), 6.80 (t, *J* = 12.3 Hz, 1H), 6.39 (dd, *J* = 27.9, 13.7 Hz, 2H), 4.27 (t, *J* = 7.6 Hz, 2H), 3.77 (s, 3H), 3.16 – 3.12 (m, 2H), 2.86 (s, 6H), 2.01 (s, 6H), 2.00 (s, 6H), 1.94 – 1.88 (m, 2H),1.79 – 1.74 (m, 2H), 1.64 – 1.59 (m, 2H), 1.54 – 1.49 (m, 2H). ^{13}C-NMR (151 MHz, CD_3OD) δ 176.53, 175.72, 154.36, 154.28, 141.63, 140.97, 135.07, 134.95, 133.43, 133.36, 131.70, 131.63, 131.08, 129.46, 129.40, 128.73, 128.71, 126.78, 126.03, 123.36, 112.21, 111.97, 104.25, 104.02, 59.03, 52.37, 45.01, 43.70, 32.16, 28.59, 27.73, 27.57, 27.35, 27.30, 25.67. HRMS (ESI) calculated for [M, $C_{42}H_{50}N_3]^+$: 596.3999, found: 596.4013.

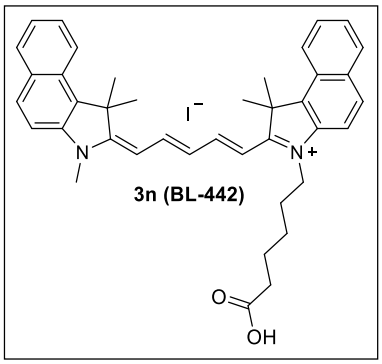

Synthesis of 3n (BL-442): Prepared according to the general procedure **b** from **1a** (67 mg, 0.19 mmol, 1 equiv), **1l** (77 mg, 0.19 mmol, 1 equiv) and **2a** (49 mg, 0.19 mmol, 1 equiv). Dark blue solid. Yield: 59% (80 mg). ^{1}H-NMR (600 MHz, CD_3OD) δ 8.35 (t, *J* = 13.0 Hz, 2H), 8.21 (d, *J* = 8.6 Hz, 2H), 7.98 (dd, *J* = 8.8, 3.3 Hz, 2H), 7.94 (d, *J* = 8.2 Hz, 2H), 7.63 – 7.56 (m, 4H), 7.45 – 7.41 (m, 2H), 6.69 (t, *J* = 12.3 Hz, 1H), 6.31 (t, J = 13.0 Hz, 2H), 4.22 (t, *J* = 7.4 Hz, 2H), 3.74 (s, 3H), 2.33 (t, *J* = 7.3 Hz, 2H), 1.99 – 1.94 (m, 12H), 1.89 – 1.84 (m, 2H), 1.73 – 1.68 (m, 2H), 1.57 – 1.52 (m, 2H). ^{13}C-NMR (151 MHz, CD_3OD) δ 177.61, 176.46, 175.79, 154.32, 141.62, 140.95, 135.08, 134.91, 133.40, 133.36, 131.67, 131.60, 131.07, 129.44, 129.39, 128.69, 126.66, 126.01, 125.99, 123.36, 112.10, 111.96, 104.14, 103.95, 52.39, 52.34, 44.98, 34.83, 32.09, 30.73, 28.47,

27.70, 27.57, 27.35, 25.80. HRMS (ESI) calculated for [M, $C_{40}H_{43}N_2O_2$]$^+$: 583.3319, found: 583.3336.

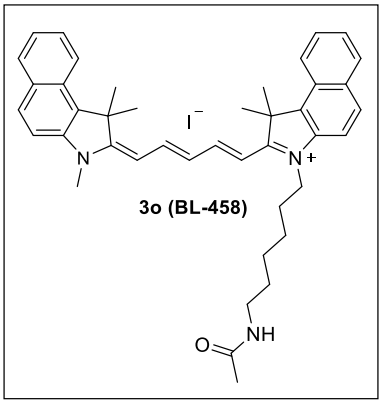

Synthesis of 3o (BL-458): Prepared according to the general procedure **b** from **1a** (67 mg, 0.19 mmol, 1 equiv), **1k** (89 mg, 0.19 mmol, 1 equiv) and **2a** (49 mg, 0.19 mmol, 1 equiv). Dark blue solid. Yield: 50% (70 mg). ^{1}H-NMR (600 MHz, CD_3OD) δ 8.33 (t, *J* = 13.0 Hz, 2H), 8.20 (d, *J* = 7.0 Hz, 2H), 8.02 – 7.83 (m, 4H), 7.66 – 7.48 (m, 4H), 7.46 – 7.36 (m, 2H), 6.67 (t, *J* = 12.3 Hz, 1H), 6.30 (d, *J* = 13.7 Hz, 2H), 4.21 (t, *J* = 7.6 Hz, 2H), 3.73 (s, 3H), 3.16 (t, *J* = 7.1 Hz, 2H), 2.01 – 1.79 (m, 17H), 1.56 – 1.47 (m, 4H), 1.46 – 1.40 (m, 2H). ^{13}C-NMR (151 MHz, CD_3OD) δ 176.37, 175.74, 175.18, 173.15, 154.32, 154.28, 141.58, 140.91, 135.09, 135.05, 134.85, 133.34, 133.32, 131.66, 131.58, 131.05, 129.41, 129.35, 128.70, 128.67, 126.60, 126.00, 125.96, 123.33, 112.09, 111.93, 104.12, 104.03, 103.94, 52.32, 52.27, 45.03, 40.26, 32.01, 30.22, 28.68, 27.67, 27.65, 27.52, 27.45, 22.63. HRMS (ESI) calculated for [M, $C_{42}H_{48}N_3O$]$^+$: 610.3792, found: 610.3822.

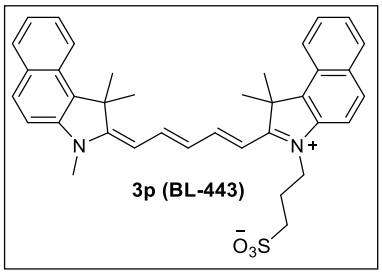

Synthesis of 3p (BL-443): Prepared according to the general procedure **b** from **1a** (67 mg, 0.19 mmol, 1 equiv), **1f** (63 mg, 0.19 mmol, 1 equiv) and **2a** (49 mg, 0.19 mmol, 1 equiv). Dark blue solid. Yield: 57% (64 mg). ^{1}H-NMR (600 MHz, CD_3OD) δ 8.29 (t, *J* = 13.0 Hz, 2H), 8.18 (dd, *J* = 16.7, 8.5 Hz, 2H), 8.02 – 7.83 (m, 4H), 7.67 (d, *J* = 8.8 Hz, 1H), 7.62 – 7.51 (m, 3H), 7.43 (t, *J* = 7.5 Hz, 1H), 7.37 (t, *J* = 7.5 Hz, 1H), 6.67 (t, *J* = 12.3 Hz, 1H), 6.41 (d, *J* = 13.7 Hz, 1H), 6.27 (d, *J* = 13.8 Hz, 1H), 4.44 (t, *J* = 8.2 Hz, 2H), 3.73 (s, 3H), 3.07 (t, *J* = 6.7 Hz, 2H), 2.36 – 2.24 (m, 2H), 2.04 – 1.75 (m, 12H). ^{13}C-NMR (151 MHz, CD_3OD) δ 176.65, 175.42, 154.68, 154.46, 141.62, 141.04, 135.00, 134.65, 133.44, 133.34, 131.74, 131.59, 131.05, 129.53, 129.40, 128.67, 128.61, 126.96, 126.00, 125.88, 123.37, 123.29, 112.05, 111.96, 104.26, 103.86, 52.34, 52.31, 44.24, 31.92, 30.74, 27.54, 27.47, 24.37. HRMS (ESI) calculated for [M+H, $C_{37}H_{39}N_2O_3S$]$^{+}$: 591.2603, found: 591.2689.

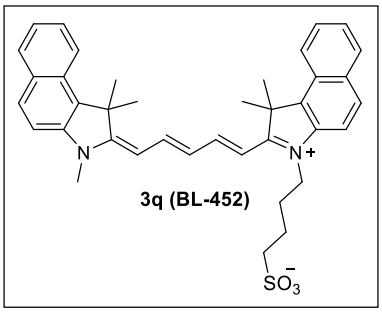

Synthesis of 3q (BL-452): Prepared according to the general procedure **b** from **1a** (67 mg, 0.19 mmol, 1 equiv), **1h** (66 mg, 0.19 mmol, 1 equiv) and **2a** (49 mg, 0.19 mmol, 1 equiv). Dark blue solid. Yield: 58% (67 mg). ^{1}H-NMR (600 MHz, CD_3OD) δ 8.24 – 8.01 (m, 4H), 7.94 – 7.75 (m, 4H), 7.60 – 7.45 (m, 4H), 7.37 – 7.28 (m, 2H), 6.58 (t, *J* = 12.3 Hz, 1H), 6.28 (d, *J* = 13.6 Hz, 1H), 6.18 (d, *J* = 13.7 Hz, 1H), 4.25 – 4.09 (m, 2H), 3.66 (s, 3H), 2.99 – 2.87 (m, 2H), 2.07 – 1.96 (m, 4H), 1.91 – 1.70 (m, 12H). ^{13}C-NMR (151 MHz, CD_3OD) δ 176.11, 175.63, 154.21, 154.09, 141.54, 140.86, 134.92, 134.74, 133.25, 131.66, 131.52, 130.99, 129.35, 129.30, 128.63, 128.60,

126.71, 125.91, 125.89, 123.28, 123.25, 112.12, 111.93, 104.09, 104.04, 52.23, 52.12, 51.78, 44.96, 31.90, 27.57, 27.46, 23.52. HRMS (ESI) calculated for [M+H, $C_{38}H_{41}N_2O_3S$]$^+$: 605.2760, found: 605.2837.

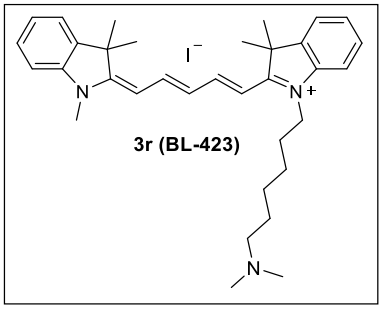

Synthesis of 3r (BL-423): Prepared according to the general procedure **b** from **1b** (57 mg, 0.19 mmol, 1 equiv), **1i** (85 mg, 0.19 mmol, 1 equiv) and **2a** (49 mg, 0.19 mmol, 1 equiv). Dark blue solid. Yield: 56% (66 mg). ^{1}H-NMR (600 MHz, CD_3OD) δ 8.31 – 8.19 (m, 2H), 7.51 – 7.45 (m, 2H), 7.42 – 7.38 (m, 2H), 7.34 (d, *J* = 7.9 Hz, 1H), 7.30 (d, *J* = 7.9 Hz, 1H), 7.27 – 7.22 (m, 2H), 6.80 (t, *J* = 12.4 Hz, 1H), 6.40 (d, *J* = 13.7 Hz, 1H), 6.33 (d, *J* = 13.7 Hz, 1H), 4.15 (t, *J* = 7.6 Hz, 2H), 3.64 (s, 3H), 3.21 – 3.16 (m, 2H), 2.90 (s, 6H), 1.87 – 1.82 (m, 2H), 1.80 – 1.76 (m, 2H), 1.75 – 1.66 (m, 12H), 1.61 – 1.56 (m, 2H), 1.53 – 1.48 (m, 2H). ^{13}C-NMR (151 MHz, CD_3OD) δ 175.26, 174.50, 155.41, 144.23, 143.51, 142.68, 142.54, 131.03, 129.73, 129.67, 126.95, 126.18, 126.13, 123.41, 123.27, 118.34, 112.13, 111.83, 104.57, 104.48, 58.93, 50.51, 50.48, 44.89, 43.66, 31.84, 28.25, 28.08, 28.06, 27.89, 27.29, 27.18, 25.50. HRMS (ESI) calculated for [M, $C_{46}H_{57}N_4$]$^+$: 496.3686, found: 496.3693.

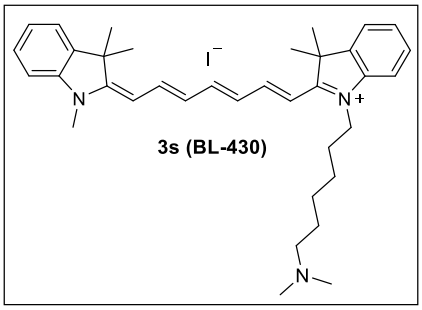

Synthesis of 3s (BL-430): Prepared according to the general procedure **b** from **1b** (57 mg, 0.19 mmol, 1 equiv), **1i** (85 mg, 0.19 mmol, 1 equiv) and **2b** (54 mg, 0.19 mmol, 1 equiv). Dark blue solid. Yield: 54% (66 mg). ^{1}H-NMR (600 MHz, CD_3OD) δ 7.93 (t, *J* = 13.0 Hz, 2H), 7.67 (brs, 1H), 7.46 (d, *J* = 7.4 Hz, 2H), 7.41 – 7.34 (m, 2H), 7.31 (d, *J* = 8.0 Hz, 1H), 7.27 (d, *J* = 7.9 Hz, 1H), 7.24 – 7.18 (m, 2H), 6.68 (t, *J* = 12.4 Hz, 1H), 6.59 (t, *J* = 12.5 Hz, 1H), 6.38 (d, *J* = 13.6 Hz, 1H), 6.28 (d, *J* = 13.6 Hz, 1H), 4.14 (t, *J* = 7.6 Hz, 2H), 3.22 – 3.14 (m, 2H), 2.90 (s, 6H), 1.87 – 1.80 (m, 2H), 1.79 – 1.74 (m, 2H), 1.68 (s, 12H), 1.60 – 1.54 (m, 2H), 1.53 – 1.47 (m, 2H). ^{13}C-NMR (151 MHz, CD_3OD) δ 173.75, 172.92, 157.75, 152.92, 144.35, 143.67, 142.45, 142.35, 129.73, 129.68, 127.21, 125.95, 125.89, 123.38, 123.24, 111.97, 111.66, 104.95, 58.91, 50.25, 50.23, 44.91, 43.64, 31.78, 28.26, 28.13, 27.98, 27.29, 27.19, 25.46. HRMS (ESI) calculated for [M, $C_{41}H_{49}N_4$]$^+$: 522.3843, found: 522.3854.

Synthesis of **3t (BL-470)**

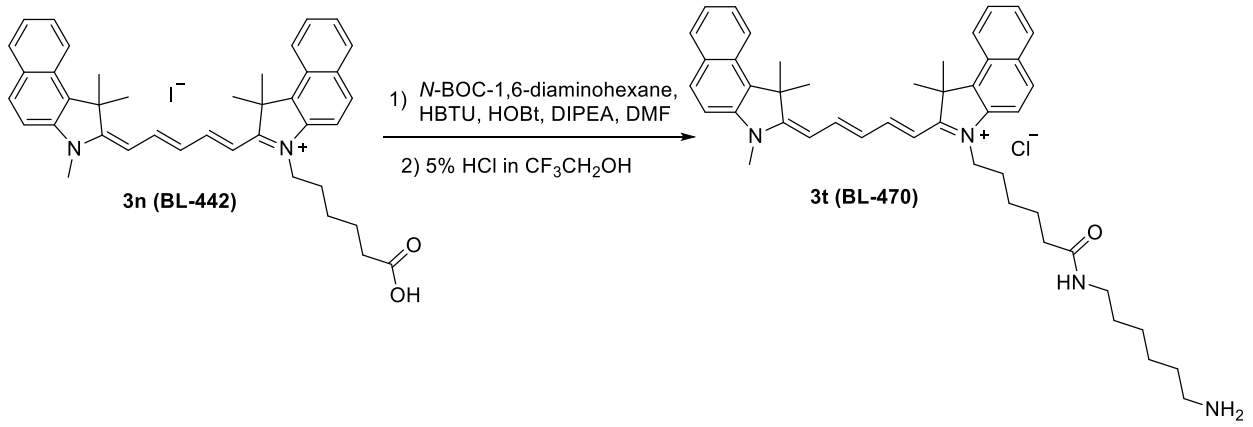

3n (BL-442) (100 mg, 0.14 mmol, 1 equiv), *N*-Boc-1,6-diaminohexane (37 mg, 0.17 mmol, 1.2 equiv), HBTU (106 mg, 0.28 mmol, 2 equiv), HOBt (38 mg, 0.28 mmol, 2 equiv) and DIPEA (122 μL, 0.7 mmol, 5 equiv) were dissolved in DMF. The mixture was stirred at room temperature for 3 h under the argon atmosphere. After reaction completed, DCM was added and the mixture was extracted with H_2O.The organic layer was dried over Na_2SO_4, filtered, and evaporated. The residue was purified by silica gel column chromatography to obtain the Boc-protected Cy5.5 amine. Boc-protected Cy5.5 amine in a solution of 5% HCI (37%) in 2,2,2-trifluoroethanol (5 mL) was stirred overnight at room temperature. After reaction completed, the solvent was evaporated and redissolved in MeOH. The crude product was purified by prep-HPLC using water and MeOH as mobile phases A and B to afford 42 mg **3t (BL-470)** as dark blue solid with 40% yield for two steps.

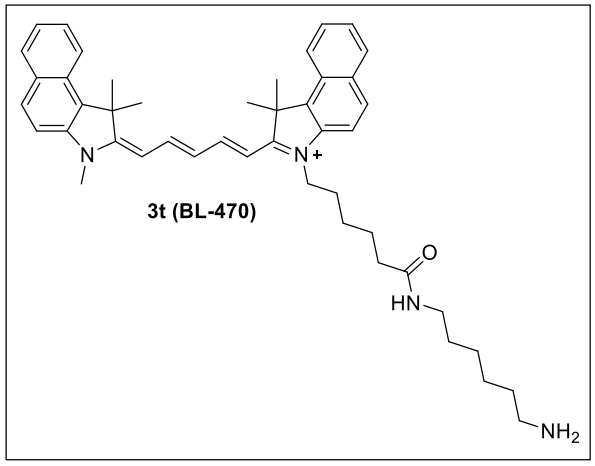

3t (BL-470): ^{1}H-NMR (600 MHz, CD_3OD) δ 8.41 – 8.28 (m, 2H), 8.26 – 8.16 (m, 2H), 8.04 – 7.88 (m, 4H), 7.70 – 7.53 (m, 4H), 7.50 – 7.38 (m, 2H), 6.67 (t, *J* = 12.3 Hz, 1H), 6.32 (d, *J* = 13.7 Hz, 2H), 4.23 (t, *J* = 7.4 Hz, 2H), 3.75 (s, 3H), 3.10 (t, *J* = 7.2 Hz, 2H), 2.87 (t, *J* = 7.7 Hz, 2H), 2.22 (t, *J* = 7.3 Hz, 2H), 2.08 – 1.80 (m, 14H), 1.75 – 1.67 (m, 2H), 1.66 – 1.59 (m, 2H), 1.54 – 1.41 (m, 4H), 1.38 – 1.27 (m, 4H). ^{13}C-NMR (151 MHz, CD_3OD) δ 176.52, 175.77, 175.73, 154.39,

154.31, 141.62, 141.01, 135.02, 134.90, 133.42, 133.36, 131.69, 131.64, 131.09, 129.44, 129.38, 128.73, 128.71, 126.57, 126.05, 126.03, 123.34, 112.12, 111.95, 104.12, 103.92, 52.34, 52.33, 44.91, 40.61, 40.09, 36.73, 31.92, 30.12, 28.55, 28.51, 27.64, 27.50, 27.38, 27.35, 26.99, 26.64. HRMS (ESI) calculated for [M, $C_{33}H_{45}N_4O]^+$: 681.4527, found: 681.4546.

Photophysical properties

Table S1. Photophysical Properties of the Prepared Cyanine Dyes in Methanol

Cyanine dyes	λ_{max}(abs)/nm	λ_{max}(em)/nm	$\Delta\lambda$/nm	ε_{max}[a]	Φ_F (%)
ICG	784	812	28	2.33×10^5	6.3
3a	676	701	25	1.64×10^5	1.37
3b	685	707	22	2.27×10^5	1.92
3c	680	703	23	1.19×10^5	1.59
3d	681	702	21	1.40×10^5	2.11
3e	682	705	23	1.84×10^5	1.60
3f	681	703	22	2.20×10^5	2.10
3g	679	705	26	3.05×10^5	2.05
3h	679	703	24	1.66×10^5	1.92
3i	682	707	25	2.10×10^5	2.12
3j	642	666	24	1.80×10^5	1.90
3k	644	664	20	1.09×10^5	3.34
3l	678	705	27	1.66×10^5	1.67
3m	678	701	23	1.59×10^5	1.97
3n	678	703	25	1.92×10^5	1.73
3o	681	701	20	2.63×10^5	1.71
3p	678	701	23	1.91×10^5	1.84
3q	678	701	23	2.27×10^5	1.72
3r	639	663	24	1.58×10^5	2.49
3s	744	769	25	2.66×10^5	2.12
3t	679	702	23	1.56×10^5	1.56

All values were determined using 1 μM cyanine dye solutions at 25 °C. ε_{max}/mol^{-1} L cm^{-1}. Quantum yields were determined using ICG (Φ_F = 0.13 in DMSO) as standard.

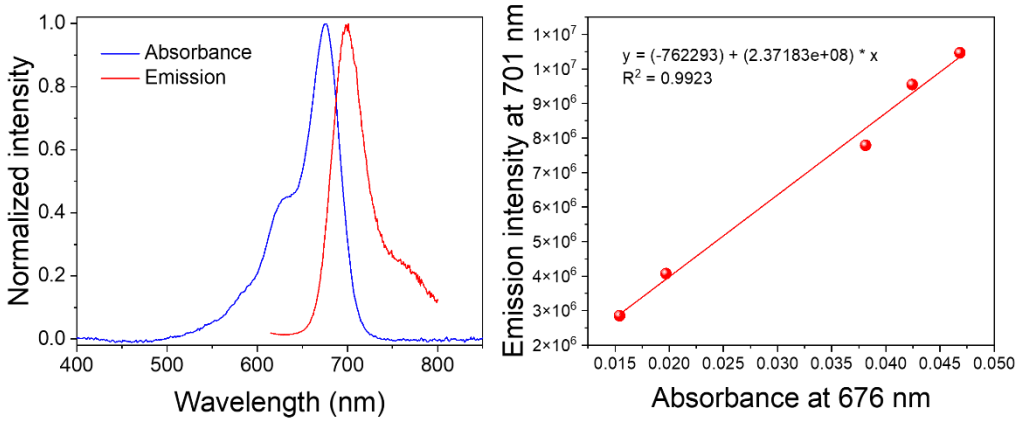

Figure S1. (left) UV-Vis absorption and emission spectra of **3a** in methanol. (right) Linear plots of integrated emission intensity at 701 nm versus absorbance at 676 nm for **3a**.

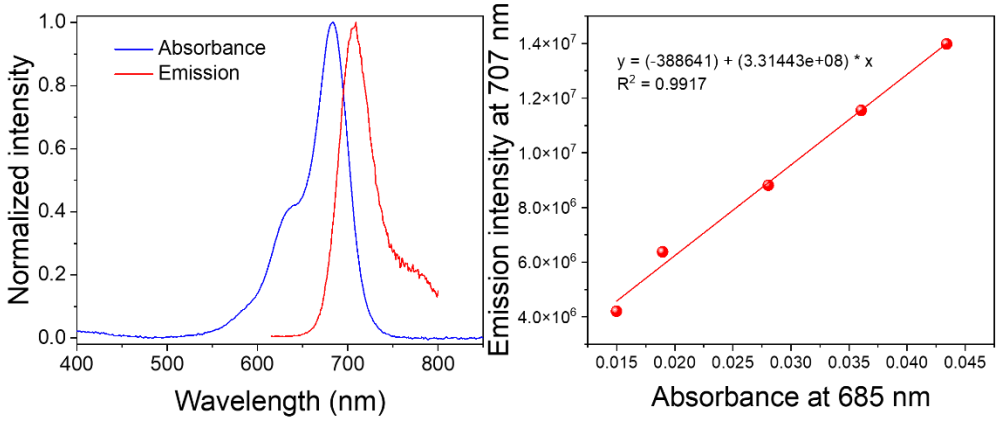

Figure S2. (left) UV-Vis absorption and emission spectra of **3b** in methanol. (right) Linear plots of integrated emission intensity at 707 nm versus absorbance at 685 nm for **3b**.

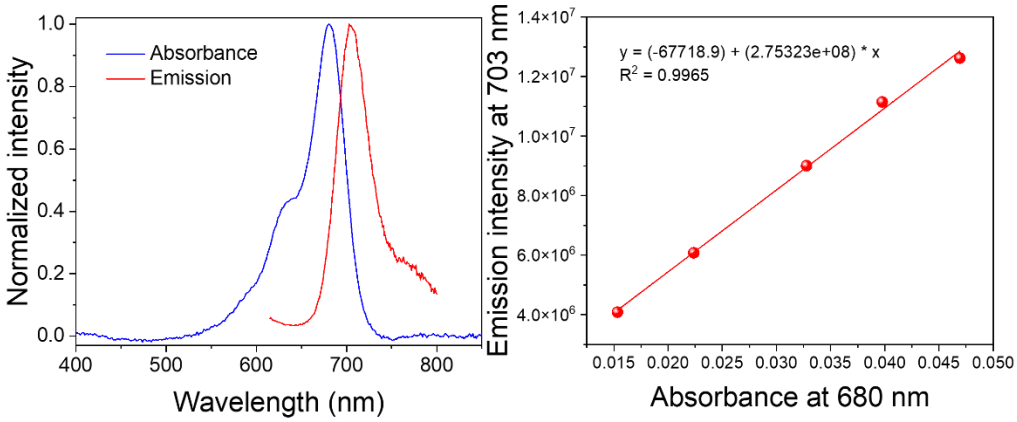

Figure S3. (left) UV-Vis absorption and emission spectra of **3c** in methanol. (right) Linear plots of integrated emission intensity at 703 nm versus absorbance at 680 nm for **3c**.

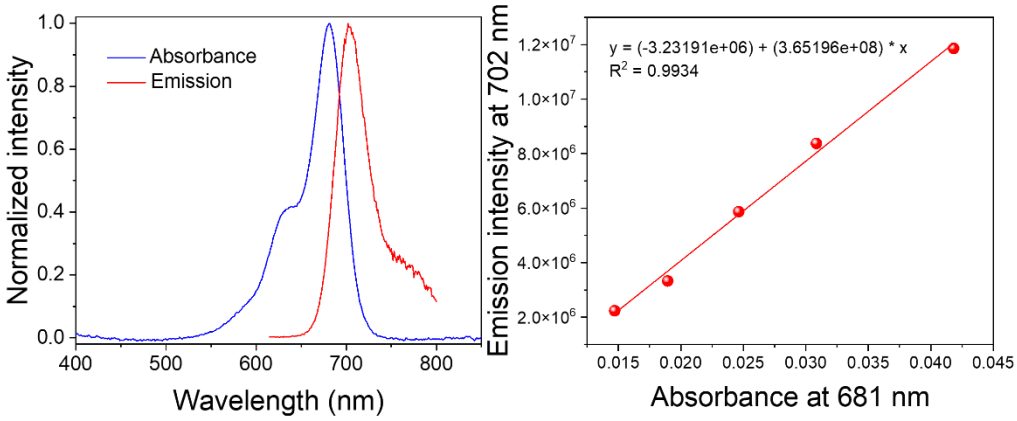

Figure S4. (left) UV-Vis absorption and emission spectra of **3d** in methanol. (right) Linear plots of integrated emission intensity at 702 nm versus absorbance at 681 nm for **3d**.

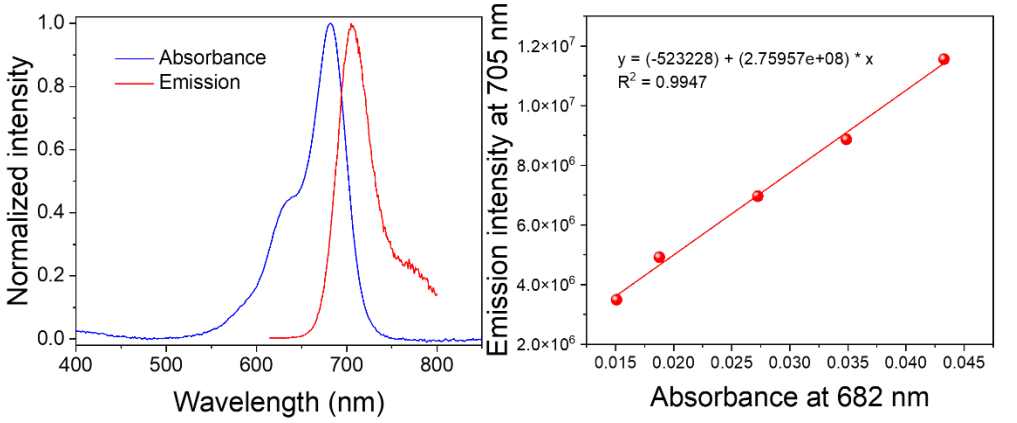

Figure S5. (left) UV-Vis absorption and emission spectra of **3e** in methanol. (right) Linear plots of integrated emission intensity at 705 nm versus absorbance at 682 nm for **3e**.

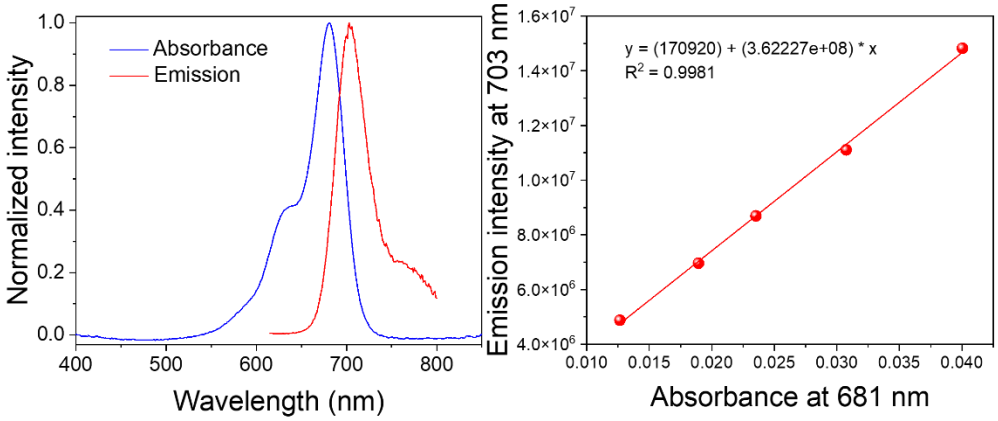

Figure S6. (left) UV-Vis absorption and emission spectra of **3f** in methanol. (right) Linear plots of integrated emission intensity at 703 nm versus absorbance at 681 nm for **3f**.

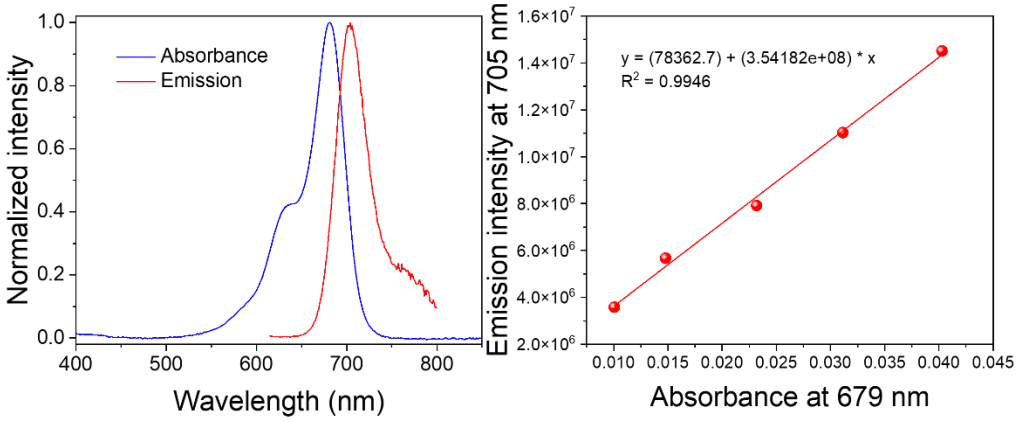

Figure S7. (left) UV-Vis absorption and emission spectra of **3g** in methanol. (right) Linear plots of integrated emission intensity at 705 nm versus absorbance at 679 nm for **3g**.

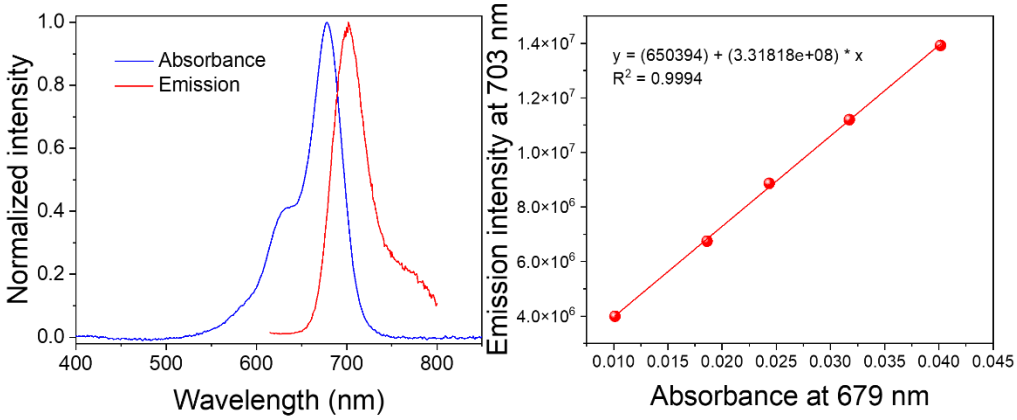

Figure S8. (left) UV-Vis absorption and emission spectra of **3h** in methanol. (right) Linear plots of integrated emission intensity at 703 nm versus absorbance at 679 nm for **3h**.

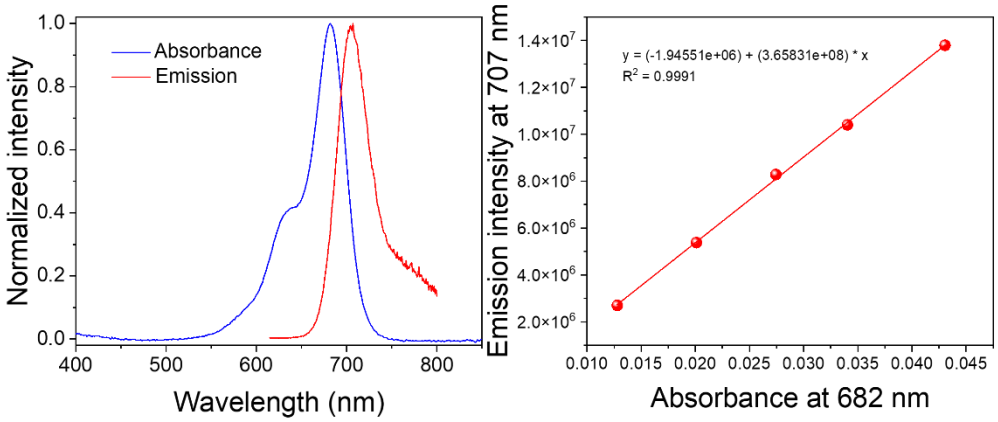

Figure S9. (left) UV-Vis absorption and emission spectra of **3i** in methanol. (right) Linear plots of integrated emission intensity at 707 nm versus absorbance at 682 nm for **3i**.

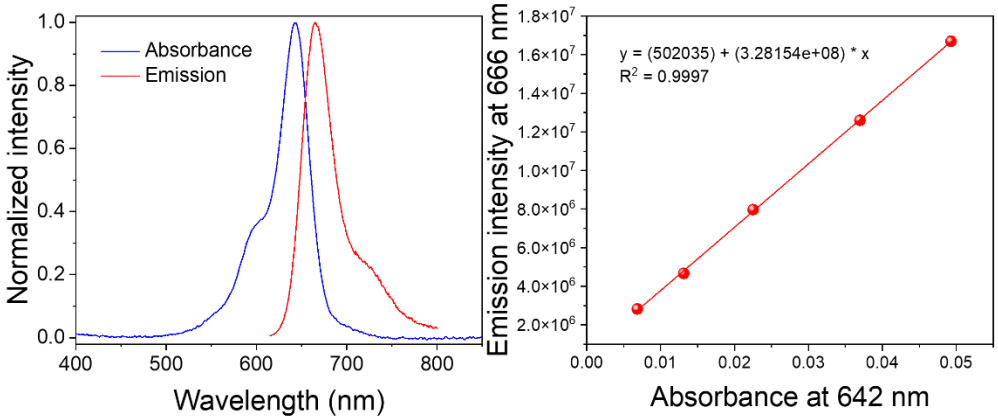

Figure S10. (left) UV-Vis absorption and emission spectra of **3j** in methanol. (right) Linear plots of integrated emission intensity at 666 nm versus absorbance at 642 nm for **3j**.

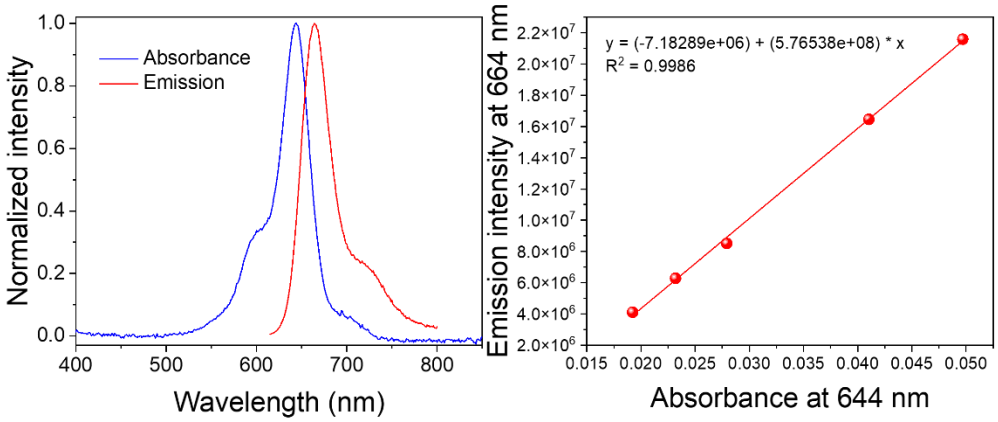

Figure S11. (left) UV-Vis absorption and emission spectra of **3k** in methanol. (right) Linear plots of integrated emission intensity at 664 nm versus absorbance at 644 nm for **3k**.

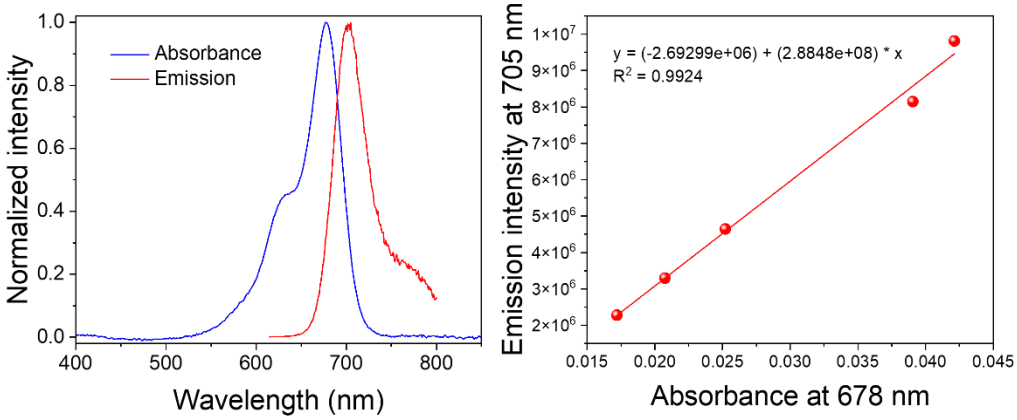

Figure S12. (left) UV-Vis absorption and emission spectra of **3l** in methanol. (right) Linear plots of integrated emission intensity at 705 nm versus absorbance at 678 nm for **3l**.

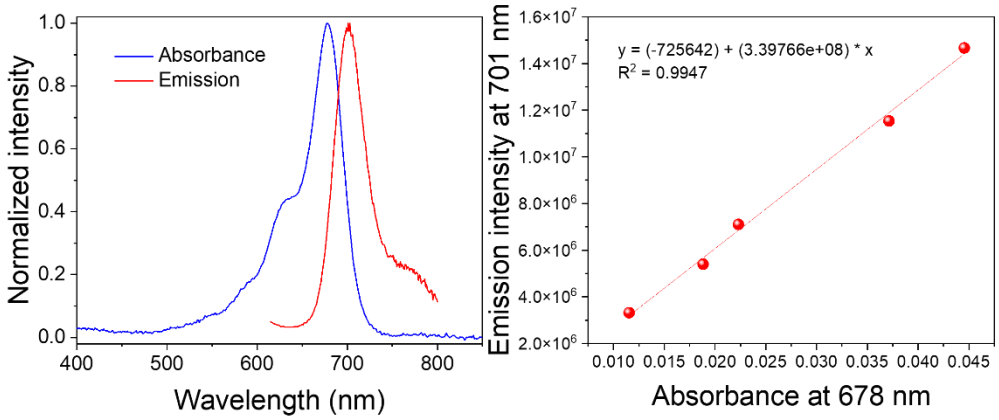

Figure S13. (left) UV-Vis absorption and emission spectra of **3m** in methanol. (right) Linear plots of integrated emission intensity at 701 nm versus absorbance at 678 nm for **3m**.

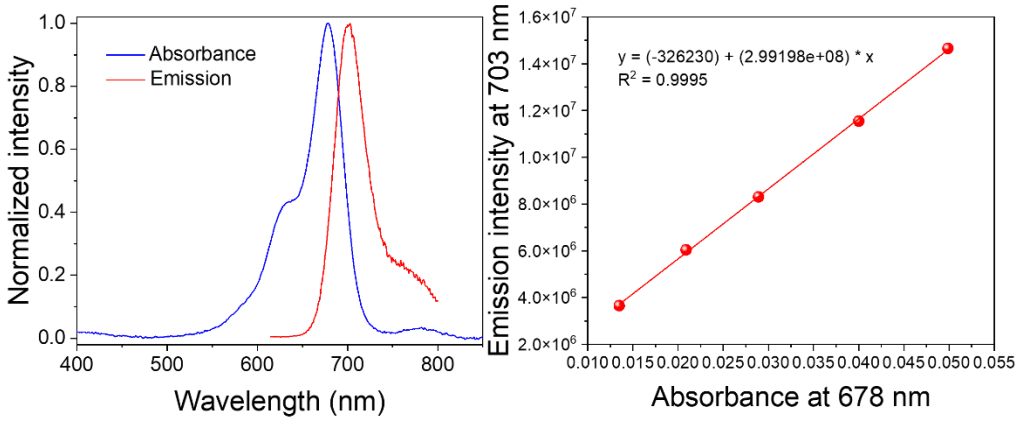

Figure S14. (left) UV-Vis absorption and emission spectra of **3n** in methanol. (right) Linear plots of integrated emission intensity at 703 nm versus absorbance at 678 nm for **3n**.

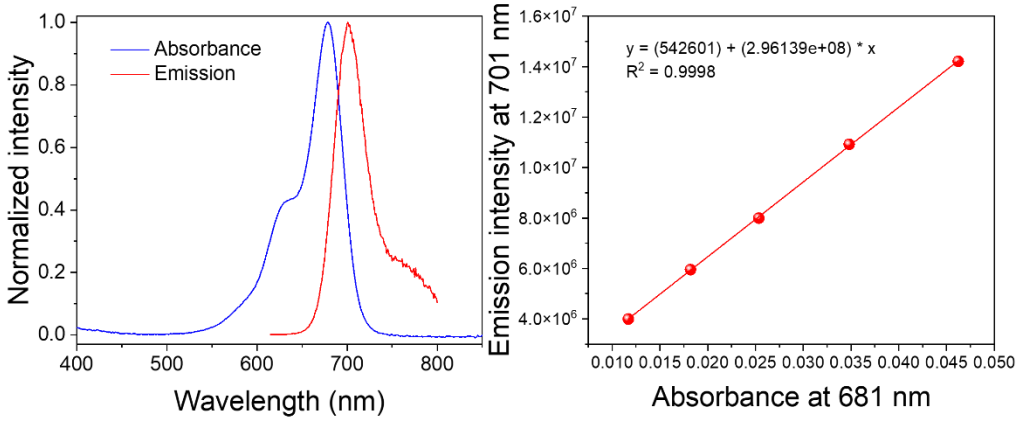

Figure S15. (left) UV-Vis absorption and emission spectra of **3o** in methanol. (right) Linear plots of integrated emission intensity at 701 nm versus absorbance at 681 nm for **3o**.

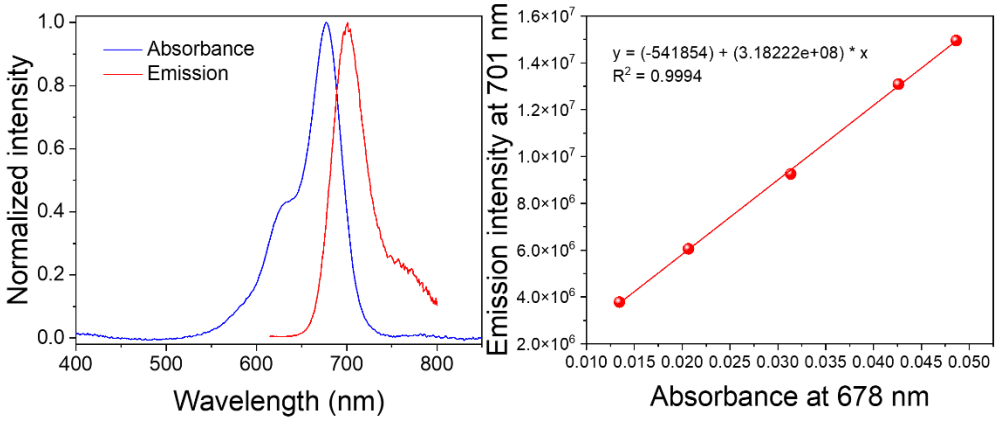

Figure S16. (left) UV-Vis absorption and emission spectra of **3p** in methanol. (right) Linear plots of integrated emission intensity at 701 nm versus absorbance at 678 nm for **3p**.

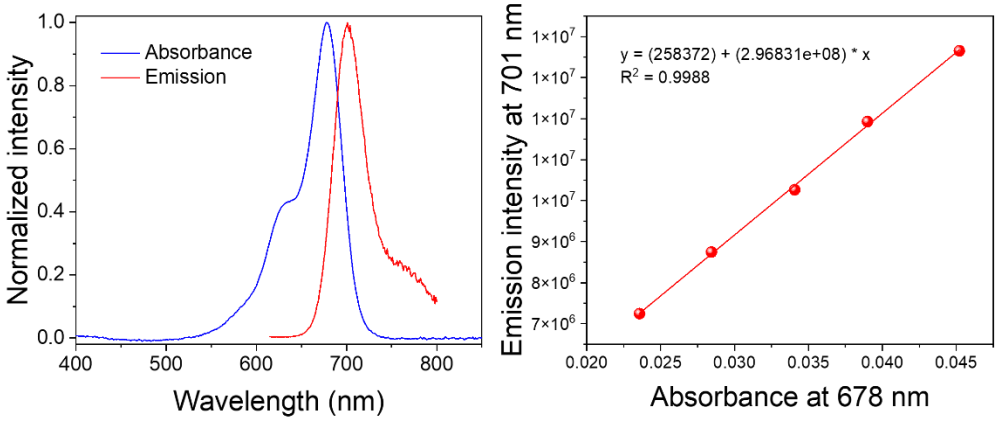

Figure S17. (left) UV-Vis absorption and emission spectra of **3q** in methanol. (right) Linear plots of integrated emission intensity at 701 nm versus absorbance at 678 nm for **3q**.

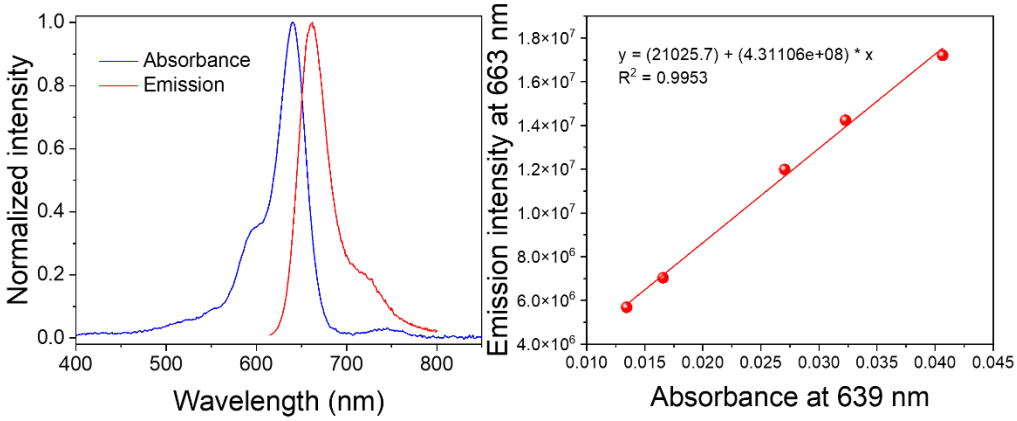

Figure S18. (left) UV-Vis absorption and emission spectra of **3r** in methanol. (right) Linear plots of integrated emission intensity at 663 nm versus absorbance at 639 nm for **3r**.

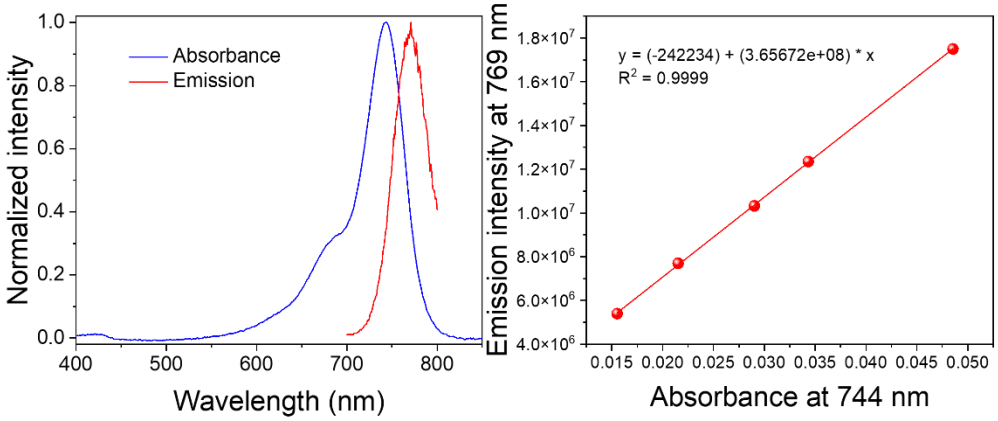

Figure S19. (left) UV-Vis absorption and emission spectra of **3s** in methanol. (right) Linear plots of integrated emission intensity at 769 nm versus absorbance at 744 nm for **3s**.

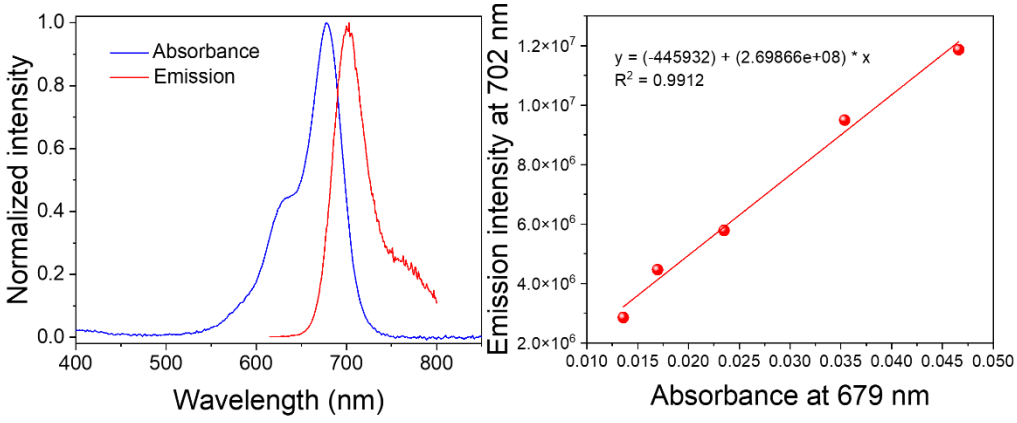

Figure S20. (left) UV-Vis absorption and emission spectra of **3t** in methanol. (right) Linear plots of integrated emission intensity at 702 nm versus absorbance at 679 nm for **3t**.

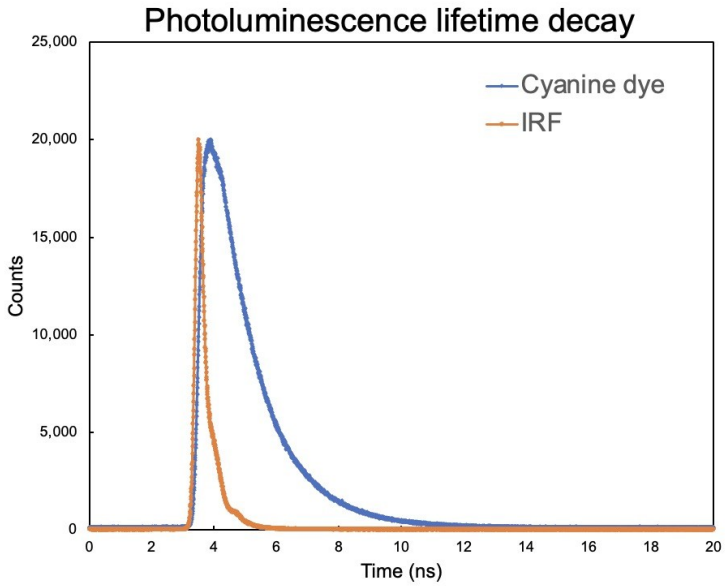

Figure S21. Photoluminescence lifetime decay of Cyanine dye (blue) and instrument response function (IRF, orange). The decay traces of the cyanine dye sample result in a biexponential decay with τ_1 = 495 ps (18%), τ_2 = 1470 ps (82%), τ_{avg} ~ 1.29 ns.

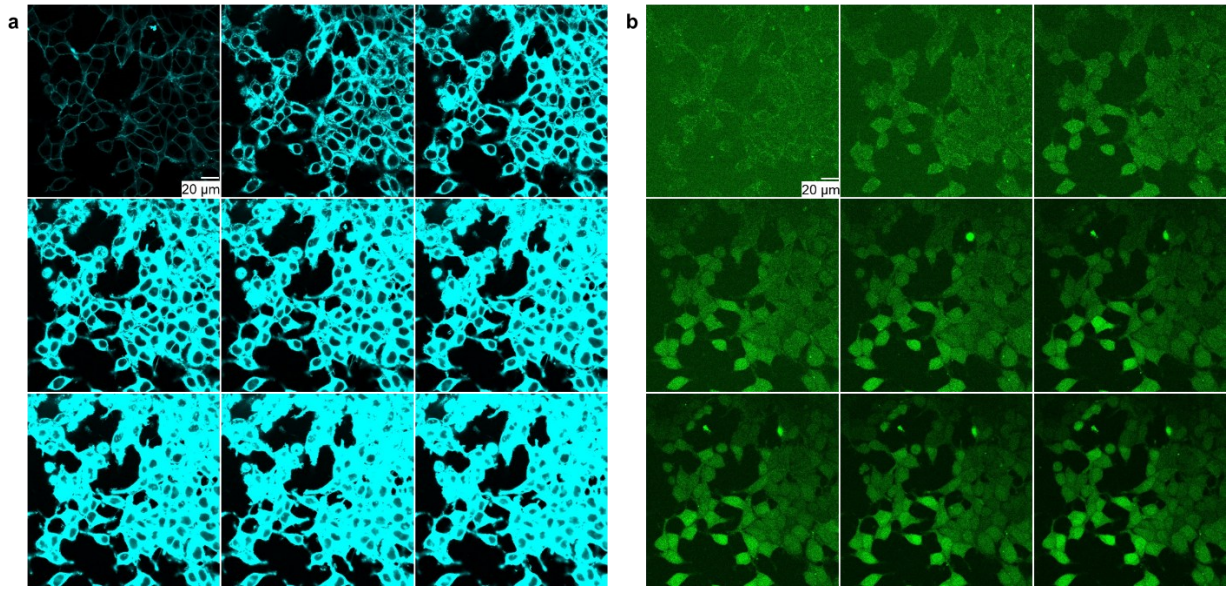

Figure S22. Confocal images of uptake of **3p** (a, 2 μM) and Fluo-4 (b, 2 μM) by HEK293 cells under 37 ℃ and 5% CO_2 incubation. Images were taken every 5 min after molecules were added.

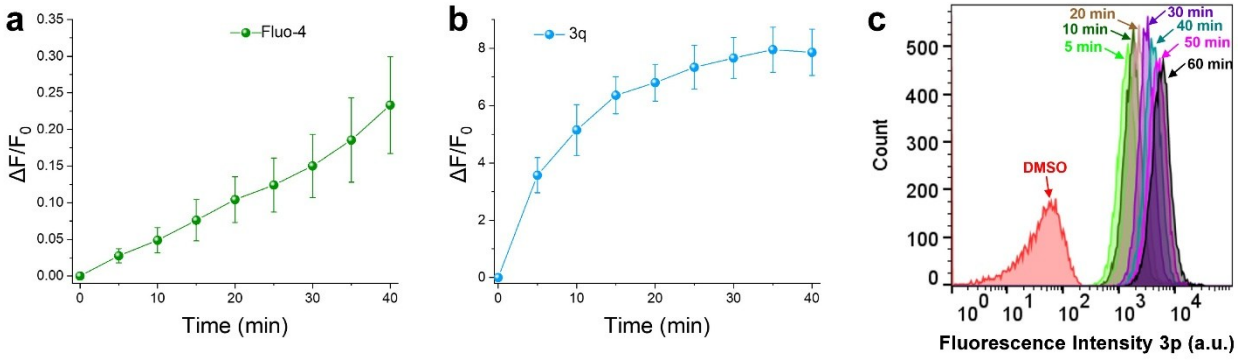

Figure S23. a), b) Quantitative data analyzed from Figure S21of the fluorescence intensity of **3p** (a, 2 μM) and Fluo-4 (b, 2 μM) taken up by HEK293 cells under 37 ℃ and 5% CO_2 incubation. c) Flow cytometry analysis of cell uptake of **3p** (2 μM) taken up by HEK293 cells under 37 ℃ and 5% CO_2 incubation with a DMSO control.

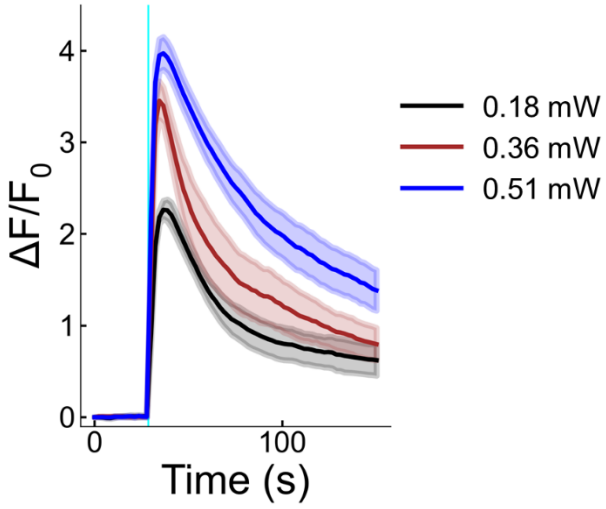

Figure S24. Normalized fluorescence intensity traces of HEK293 cells treated with **3p** (2 μM) and Fluo-4 (2 μM) and stimulated with 640 nm light with different laser power.

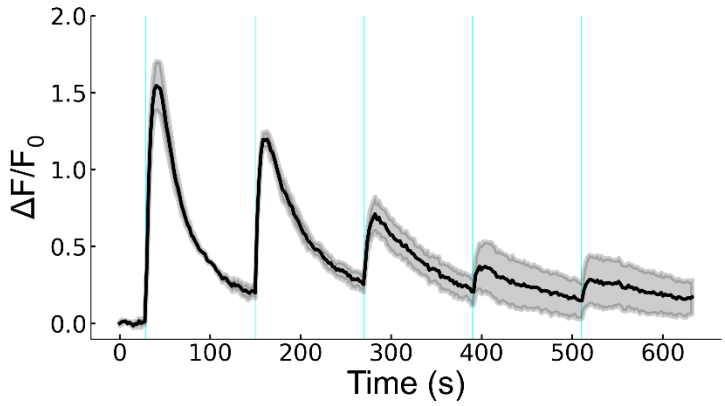

Figure S25. Multiple laser stimuli delivered to HEK293 cells treated with **3p** (2 μM). Plot shows normalized fluorescence intensity trace of Fluo-4 in HEK293 cells. The solid line represents the average responses of n = 6 independent cells and the shaded area represents the standard error of the mean. All the stimuli were delivered with a 640 nm laser of 250 ms with a power of 0.73 mW to a circular area of diameter 5 μm. The cyan lines indicate the time of stimulus presentation.

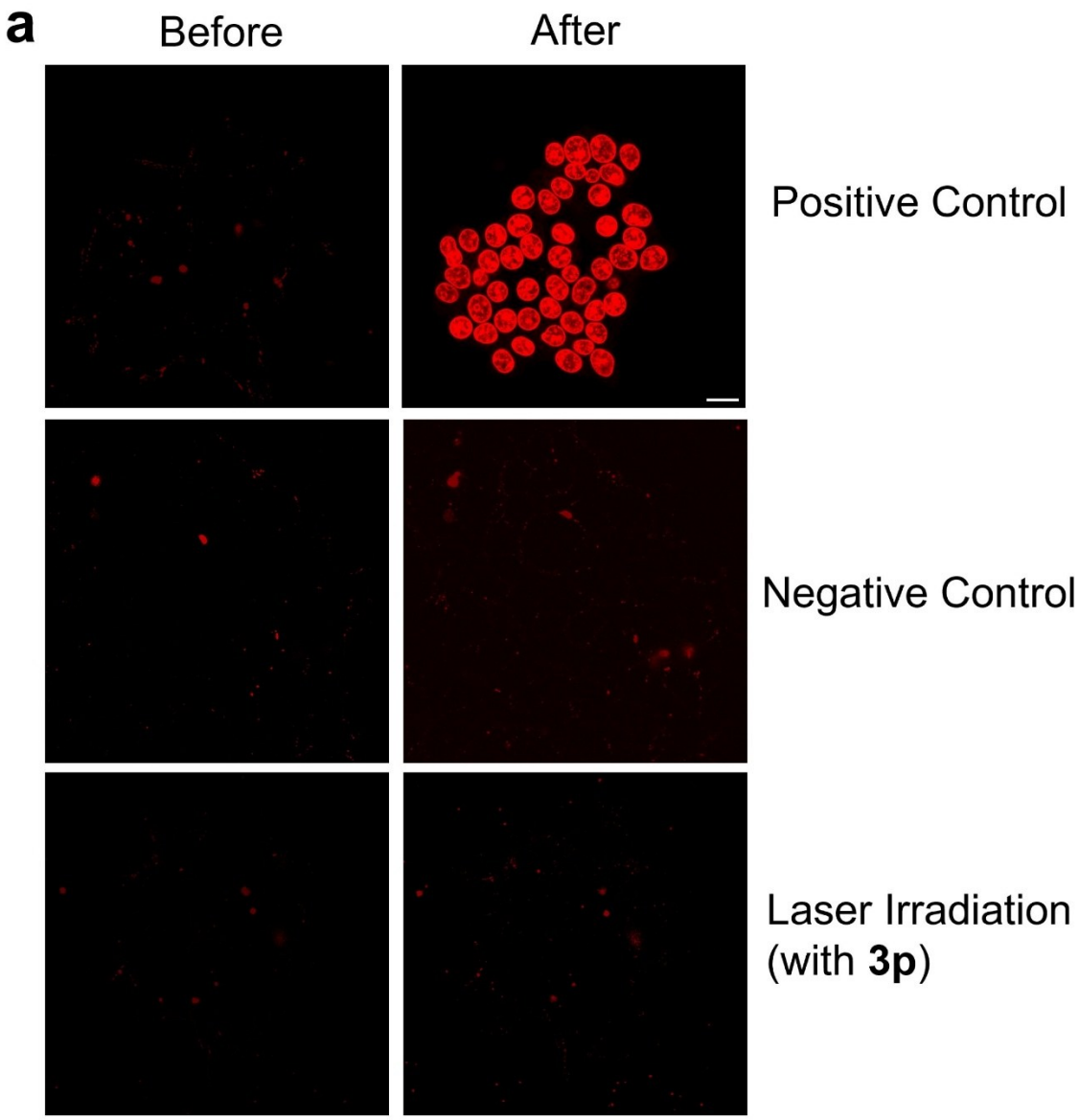

b

	PC	NC	**3p** + 640 nm Light
After	655.435	271.946	271.637
Before	268.271	268.217	270.469
Ratio	2.44	1.01	1.00

Figure S26. a) The fluorescence of propidium iodide (PI) in cells in positive control group (488 nm light, 60 W cm^{-2} treatment for 30 min), negative control (640 nm laser only) and cells treated

with **3p** and 640 nm laser. The scale bar is 20 µm and is the same for all images. b) The quantitative results of a) showing fluorescence changed before and after treatment. The ratio is given, showing that the laser conditions we used do not cause cell death, compared to negative control (NC) and positive control (PC).

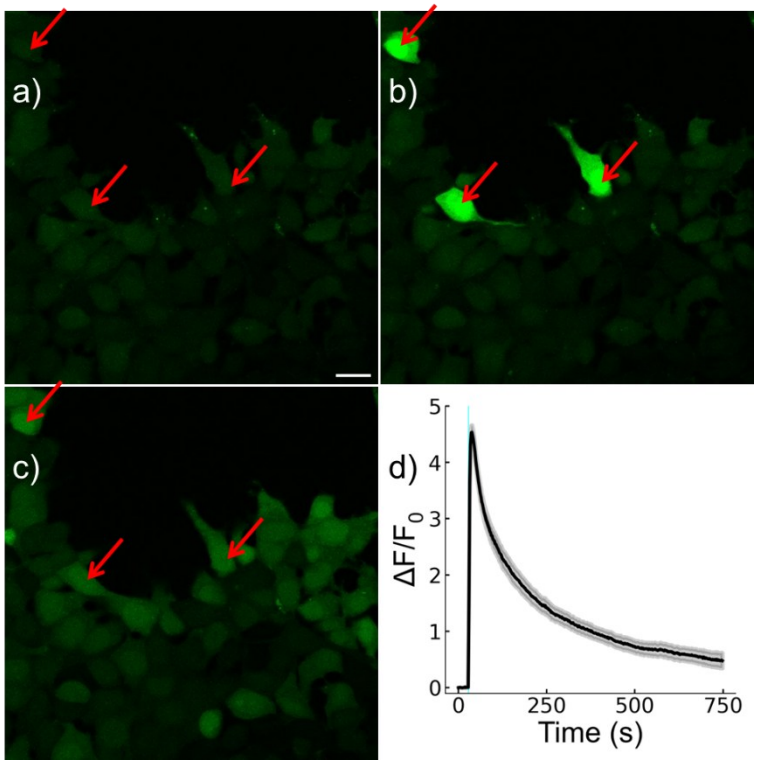

Figure S27. After stimulation, intracellular calcium level approaches baseline after a period of rest. a)– c) Bright field of confocal microscopy images of HEK293 cells treated with **3p** (2 µM) and Fluo-4 (2 µM). Images of t = 0 s (a), 35 s (b) and 750 s (c) were taken while laser stimulation takes place at t = 30 s. (d) Normalized fluorescence intensity traces of Fluo-4 in stimulated cells. The solid line represents the average responses of n = 18 independent cells and the shaded area represents the standard error of the mean. Stimulated cells are indicated by red arrows. Scale bar = 20 µm and is the same for all images. Stimulated cell was irradiated with a 640 nm laser of 0.25 s with a power of 0.73 mW to a circular area of diameter 5 µm.

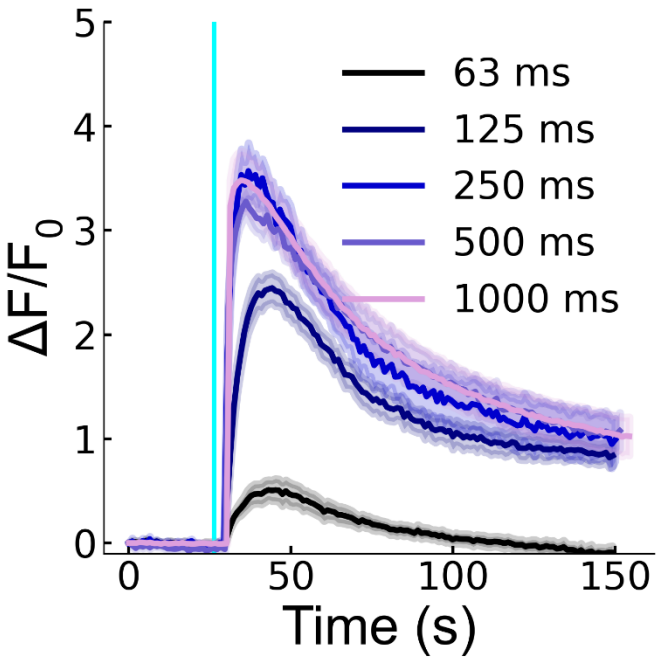

Figure S28. Normalized fluorescence intensity traces of HEK293 cells treated with 3p (2 μM) and Fluo-4 (2 μM) and stimulated with 640 nm light with a power of 0.73 mW to a circular area of diameter 5 μm, with different duration.

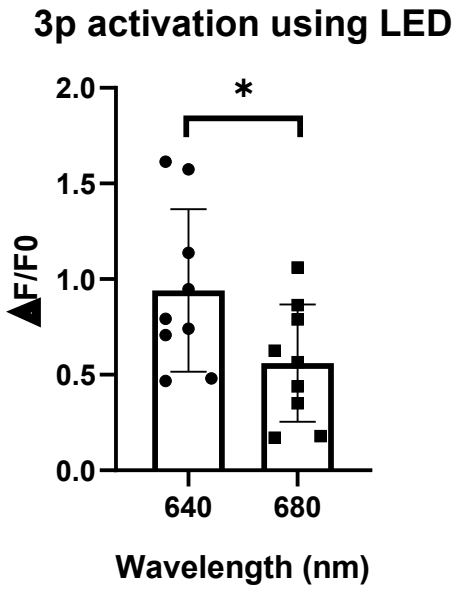

Figure S29. Normalized fluorescence intensity increases in HEK293 cells treated with 3p (2 μM) and Fluo-4 (2 μM) and stimulated with 640 or 680 nm LED light at 200 mW/cm². Each data point represents a HEK293 cell colony.

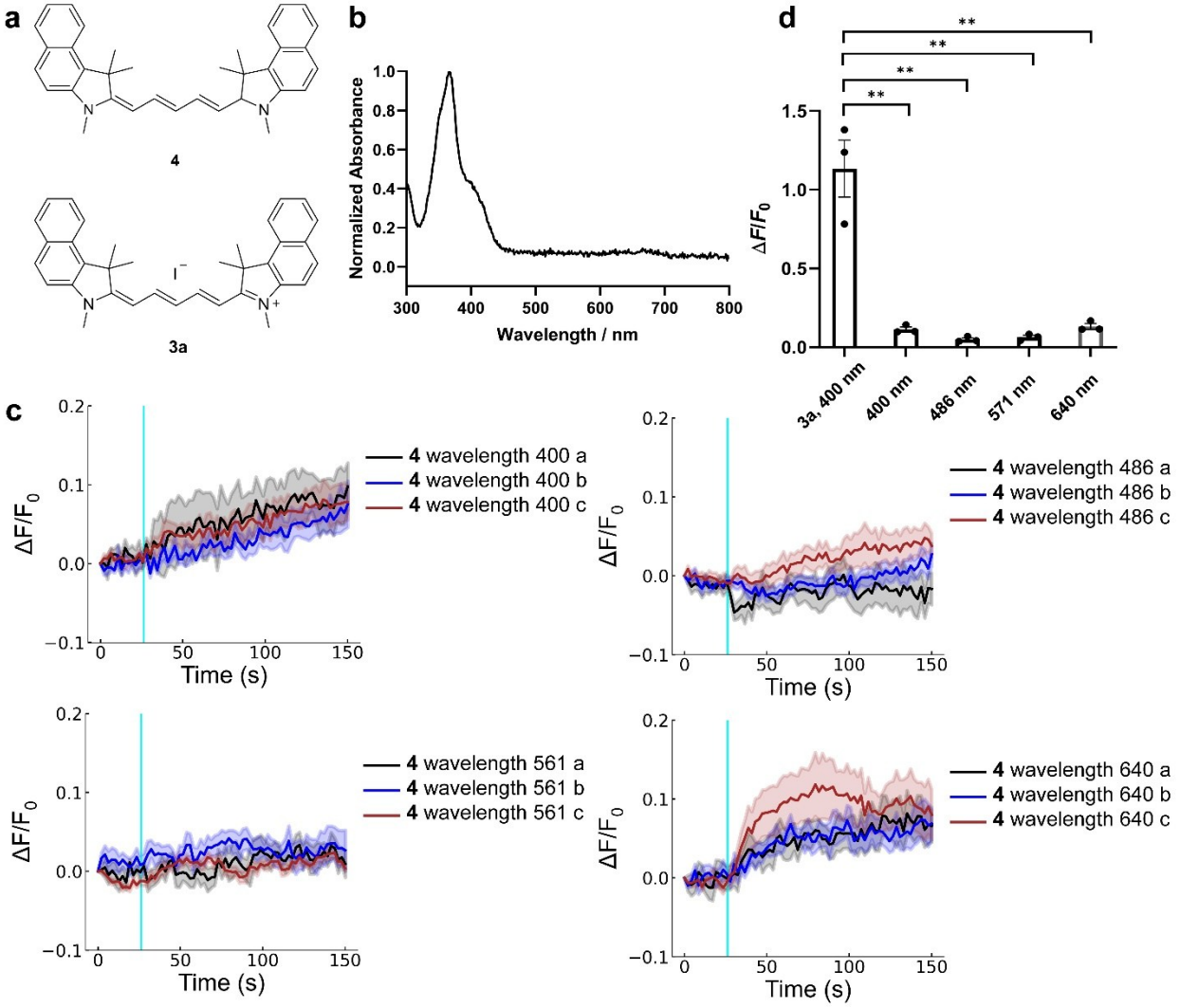

Figure S30. a) Structures of **4** and **3a**. Compared to **3a** and other MJHs, the (right) nitrogen atom in the conjugated systems of **4** lacks a positive charge, eliminating the vibronic action in the molecule. b) UV-vis absorption spectra of **4**. c) Normalized fluorescence intensity traces of HEK293 cells treated with **4** (2 μM) and Fluo-4 (2 μM) and stimulated by light with different wavelengths. a, b and c in the legends represent three replications. d) Bar graph summarizing the

result of c). The error bars represent the standard error of the mean of n = 3 experiments (six stimulated cells per experiment).

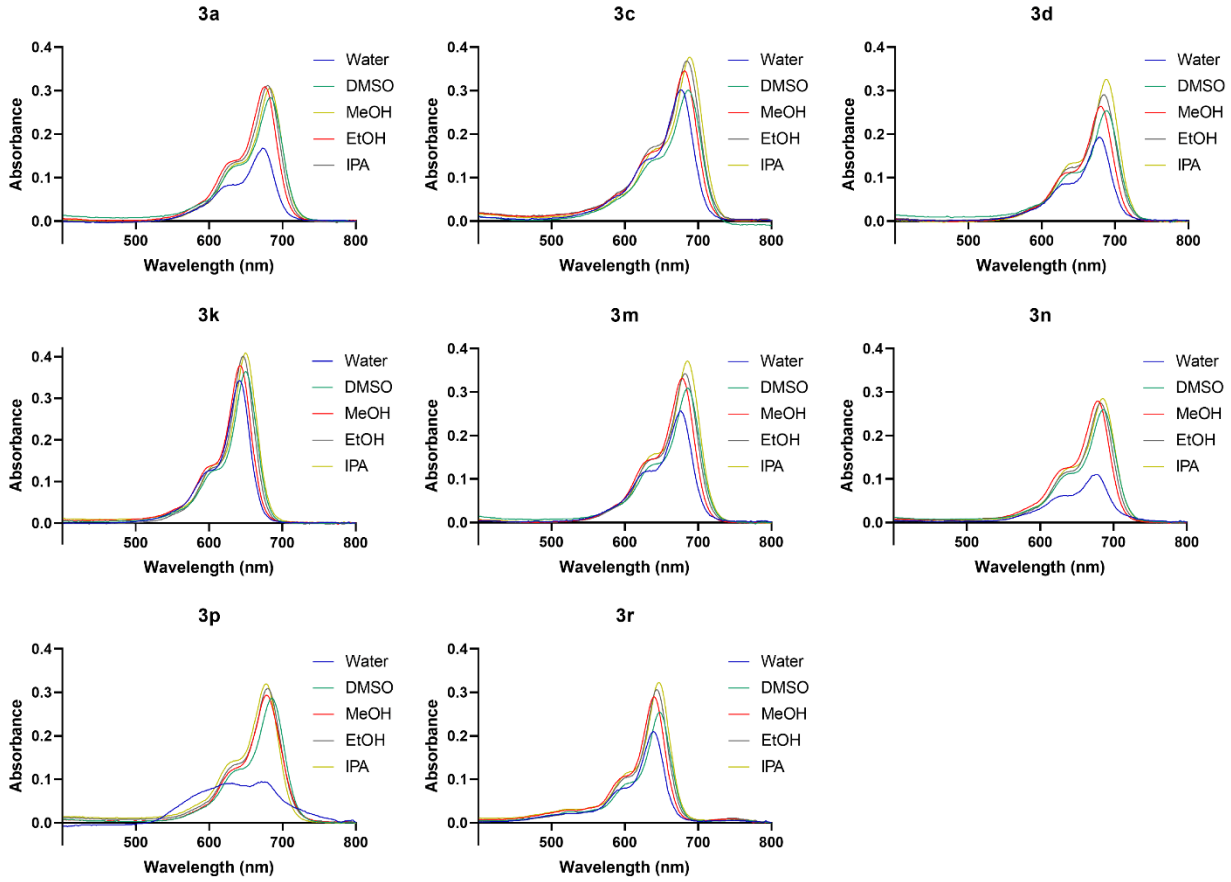

Figure S31. UV–vis absorption spectra of selected MJHs recorded in solvents with varying dielectric constants. Each compound displays solvent-dependent changes in both absorption intensity and peak position, indicating the sensitivity of its electronic excitation to the dielectric environment. These solvatochromic responses were used to calculate the EPI. Solvents include water, methanol, ethanol, isopropanol, and DMSO.

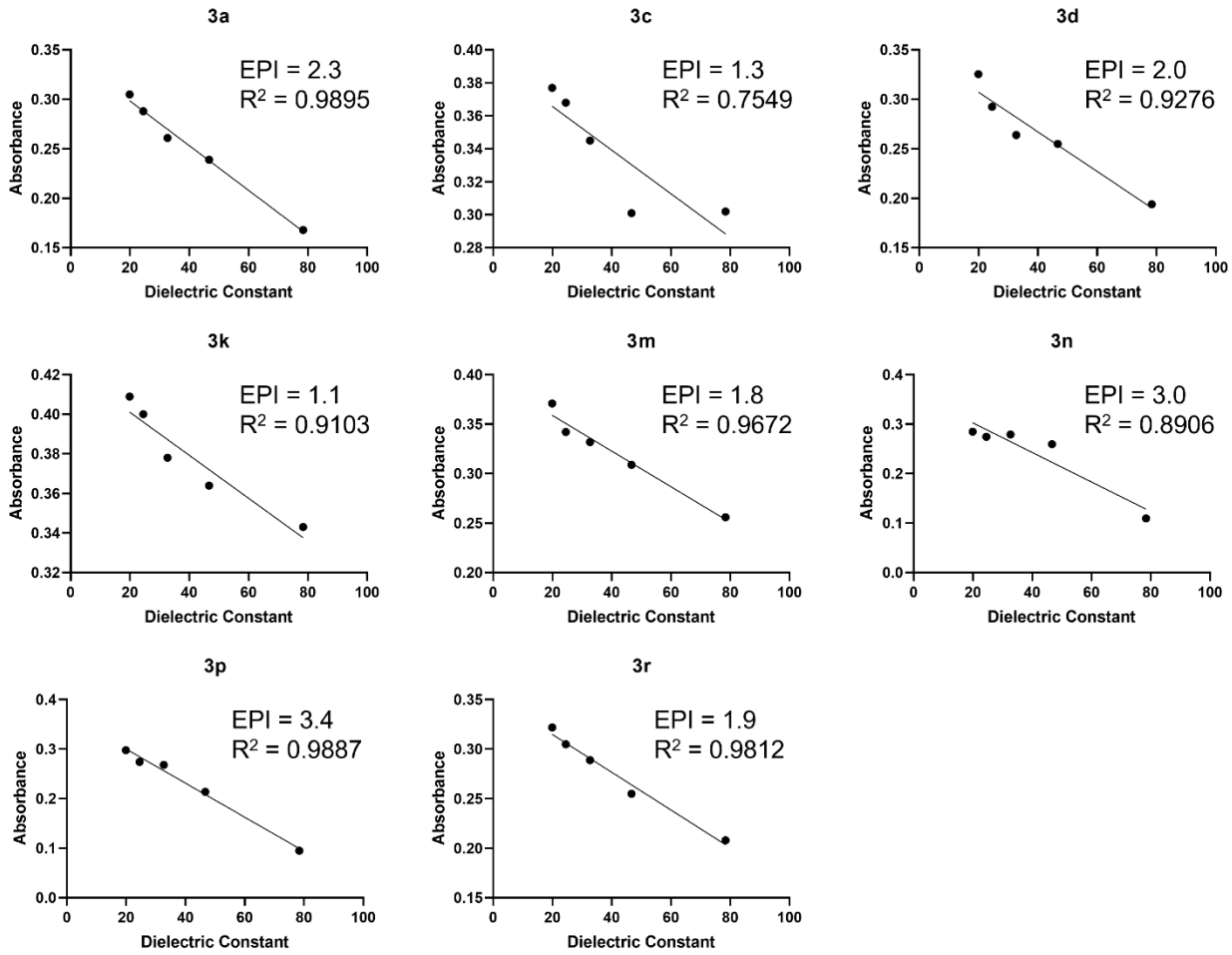

Figure S32. EPI measurement for selected MJHs. The absorption spectra of each molecule were recorded in solvents spanning a range of dielectric constants including water, DMSO, methanol, ethanol and isopropanol. The EPI was derived from the slope of the linear relationship (R^2 is given) between the maximum absorbance and the dielectric constant of each solvent, scaled by a factor of −1000 to facilitate comparison.

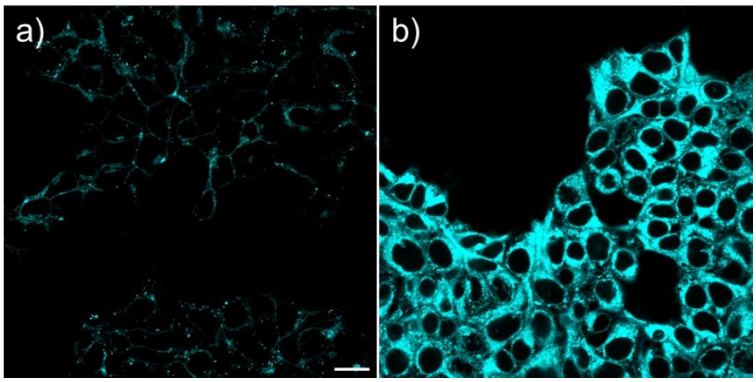

Figure S33. Uptake of **3h** (2 μM) (a) and **3p** (2 μM) (b) in HEK293 cells under same concentration and brightness.

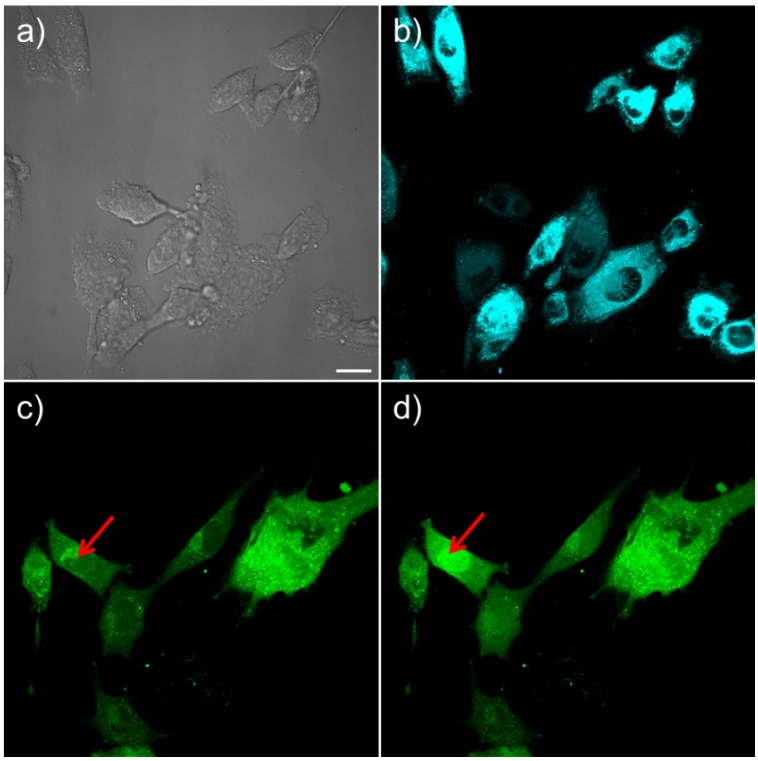

Figure S34. Confocal microscopy images show **3p** induces calcium release in C2C12 myoblasts. a) Bright field of C2C12 myoblasts. b) C2C12 myoblasts treated with **3p** (2 μM). c), d), C2C12 myoblasts treated with **3p** (2 μM) and Fluo-4 (2 μM), and images of t = 0 s (c) and 35 s (d) were taken while laser stimulation takes place at t = 30 s. Stimulated cell is indicated by red arrows.

Scale bar = 20 µm and is the same for all images. Stimulated cell was irradiated with a 640 nm laser of 1.5 s with a power of 0.73 mW to a circular area of diameter 5 µm.

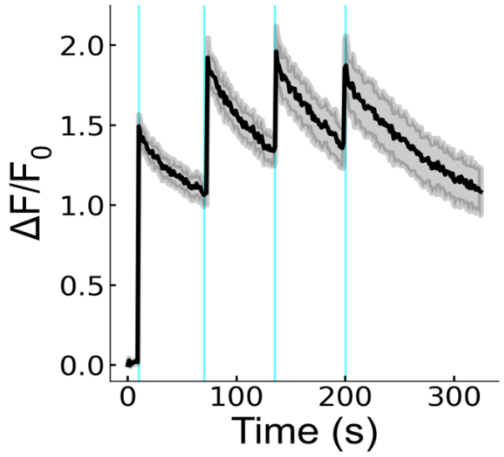

Figure S35. Multiple laser stimuli delivered to C2C12 cells treated with 3p (2 µM). Plot shows normalized fluorescence intensity trace of Fluo-4 in C2C12 cells. The solid line represents the average responses of n = 6 independent cells and the shaded area represents the standard error of the mean. All the stimuli were delivered with a 640 nm laser of 500 ms with a power of 0.73 mW to a circular area of diameter 5 µm. The cyan lines indicate the time of stimulus presentation.

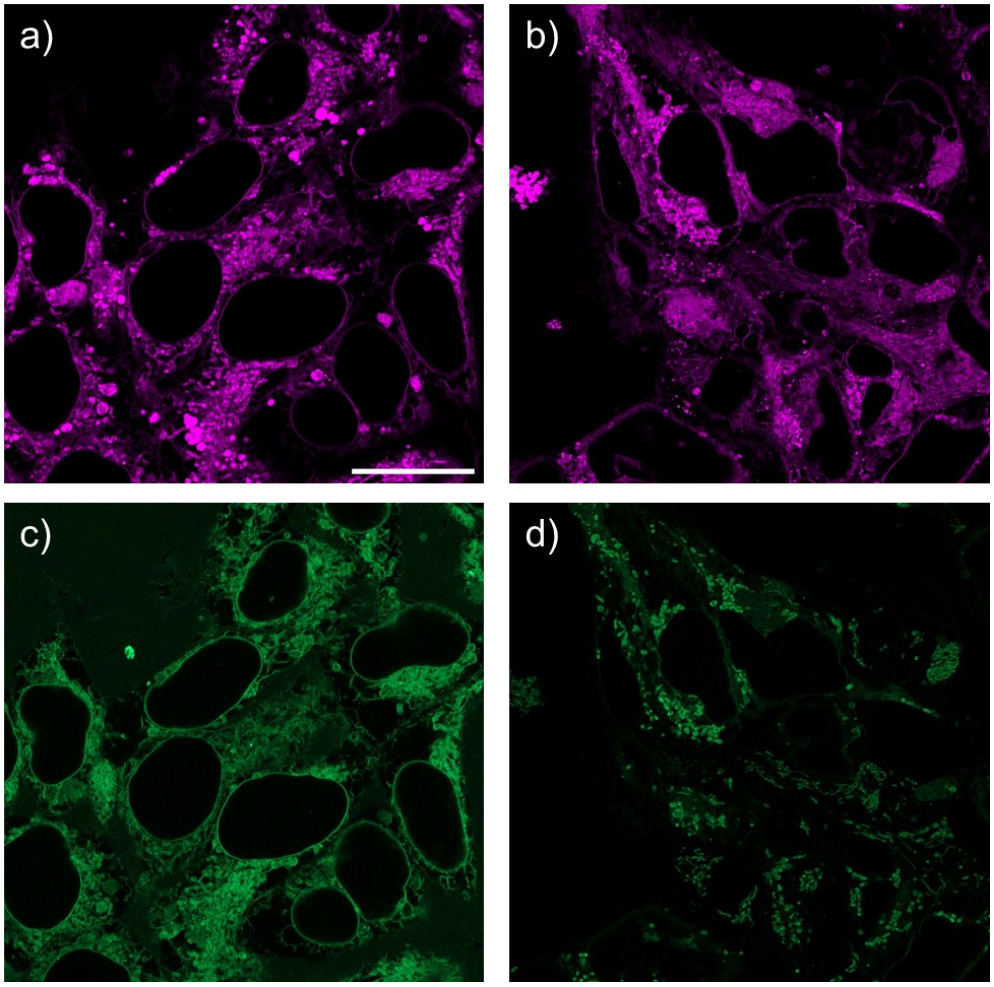

Figure S36. Zeiss LSM980 Airyscan microscopy images of HEK293 cells treated with **3p** and MitoTracker Green or ER-Tracker Green. All molecules were treated at 2 μM. a), b) Fluorescence of **3p**. c) Fluorescence of ER indicator, ER-Tracker Green. d) Fluorescence of Mitochondria indicator, MitoTracker. Scale bar = 20 μm and is the same for all figures.

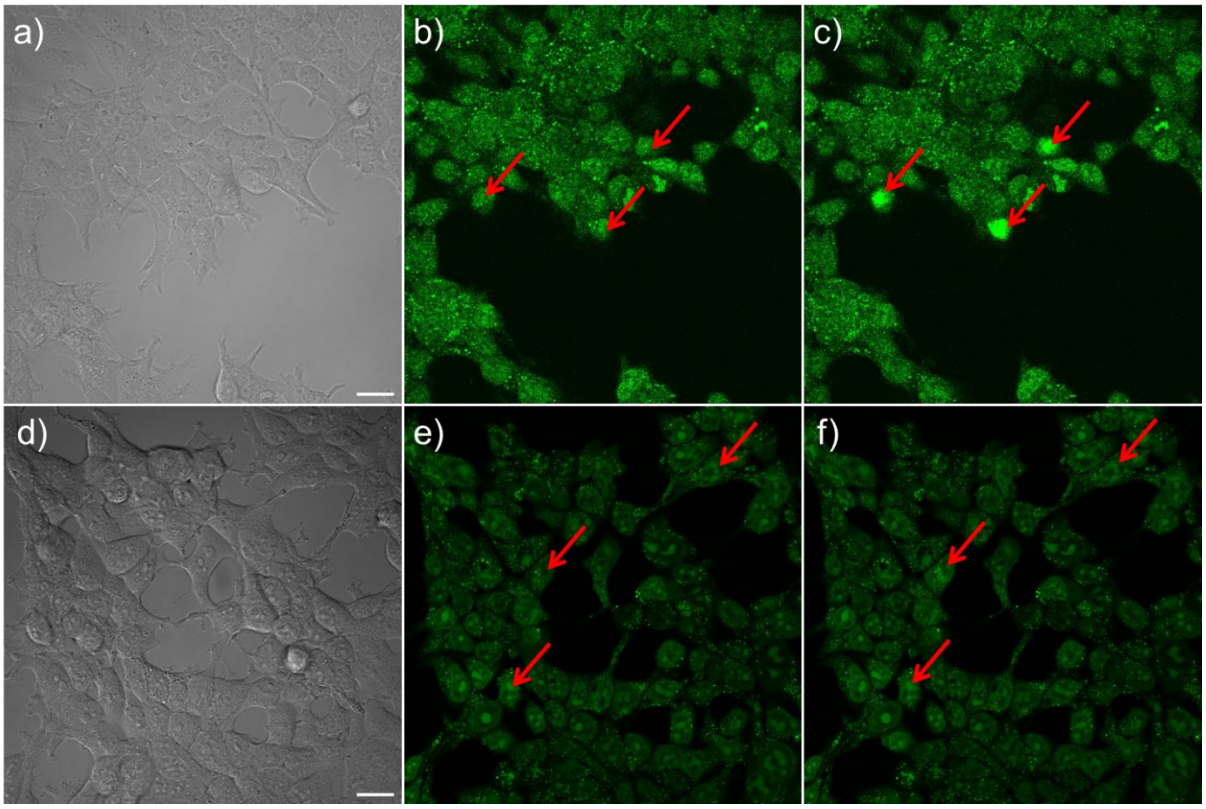

Figure S37. ROS measuring in HEK293 cells during laser stimulation. a), d) Bright field of confocal microscopy images of HEK293 cells. b), c), e), f) HEK293 cells treated with ROS indicator CellROX (2 µM) and **3a** (2 µM) (b, c) or **3p** (2 µM) (e, f), and images of t = 0 s (b, e) and 35 s (c, f) were taken while laser stimulation takes place at t = 30 s. Stimulated cell is indicated by red arrows. Scale bar = 20 µm and is the same for all images. Stimulated cell was irradiated with a 640 nm laser of 0.25 s with a power of 0.73 mW to a circular area of diameter 5 µm.

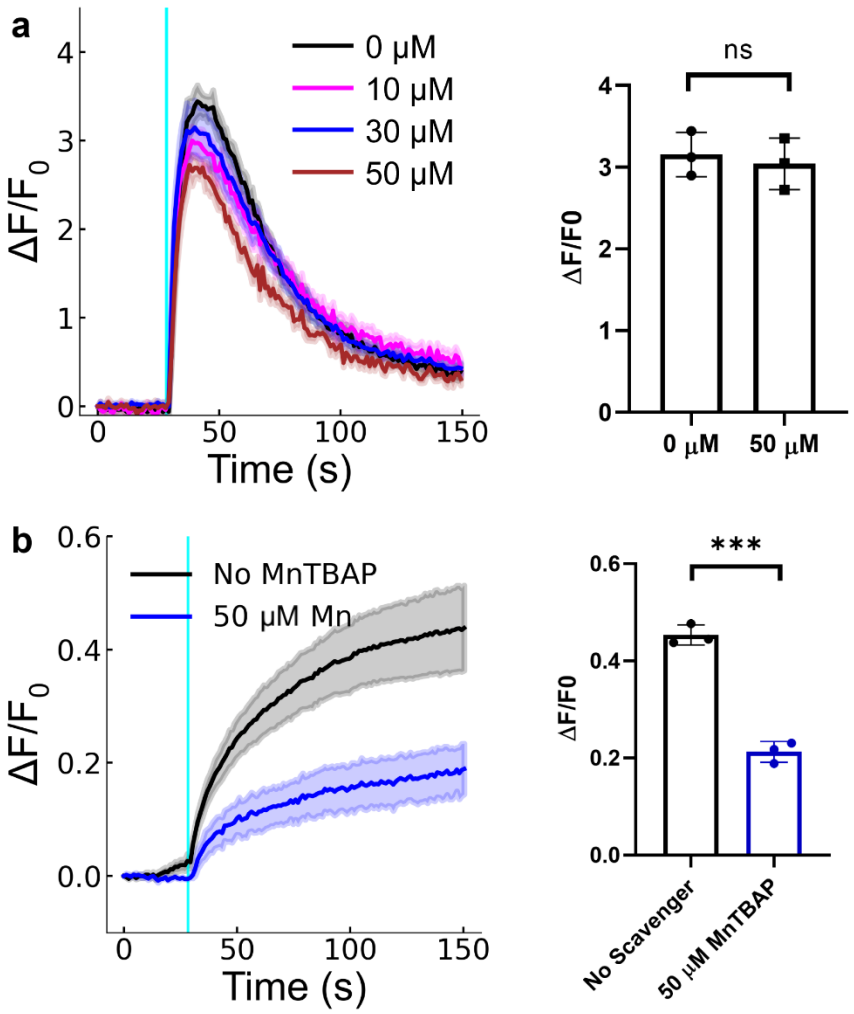

Figure S38. Calcium release and ROS level in **3p**-treated (2 μM) HEK293 cells with ROS scavengers MnTBAP. a) Normalized Fluo-4 (2 μM) fluorescence intensity traces and bar graph with different concentration of MnTBAP. b) Normalized CellROX Green Reagent (2 μM) and bar graph fluorescence in HEK293 cells treated with **3p** (2 μM) and MnTBAP.

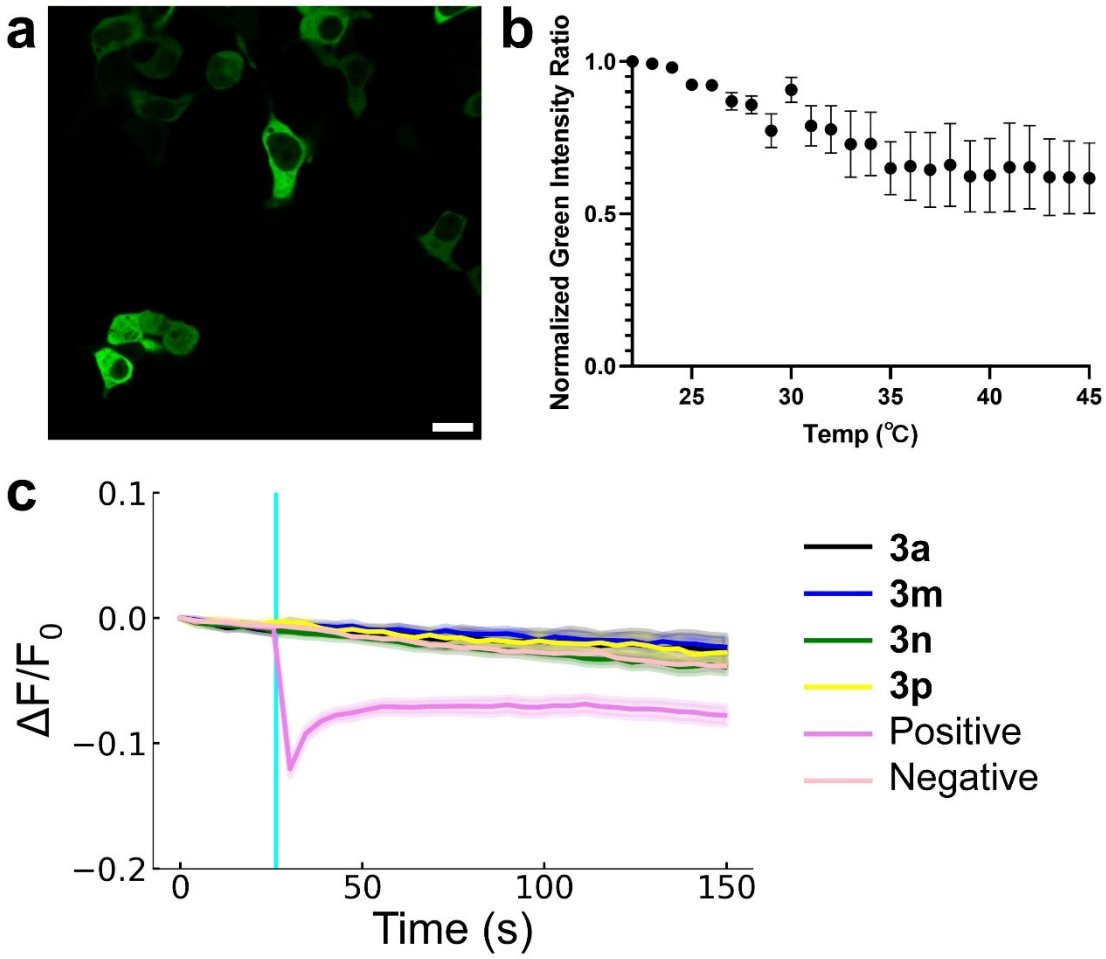

Figure S39. a) Green channel of confocal images of transfected HEK293 cells expressing ELP-TEMP fluorescent proteins. Scale bar = 20 μm. b) Normalized green intensity ratio between the intensity at the different temperatures and initial temperature (22℃), from 22 ℃ to 45 ℃. The error bars represent the standard error of mean of n = 3 experiments. c) Normalized fluorescence intensity traces of HEK293 cells treated with different MJHs (2 μM) and stimulated by 640 nm light ($n \geq 20$). Positive control condition: 0.1% DMSO stimulated by 400 nm laser at a power of 0.49 mW for 500 ms in a 5-μm diameter circular stimulation area. Negative control condition: 0.1% DMSO stimulated by 640 nm light.

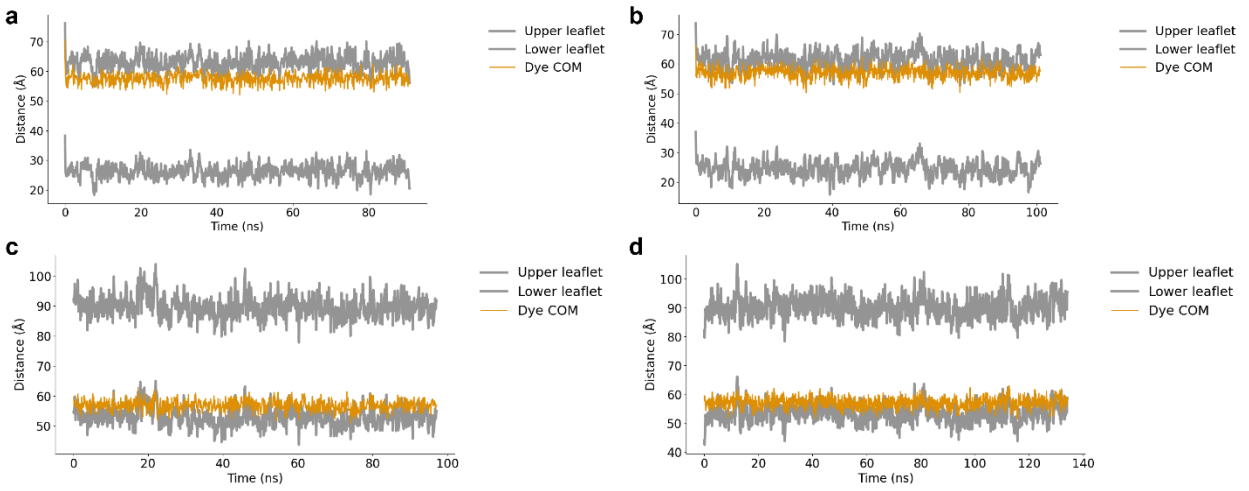

Figure S40. The simulated position of the center of mass (COM) of the MJH molecules **3a** (a), **3m** (b), **3p** (c) and **3q** (d) in the cell membrane.

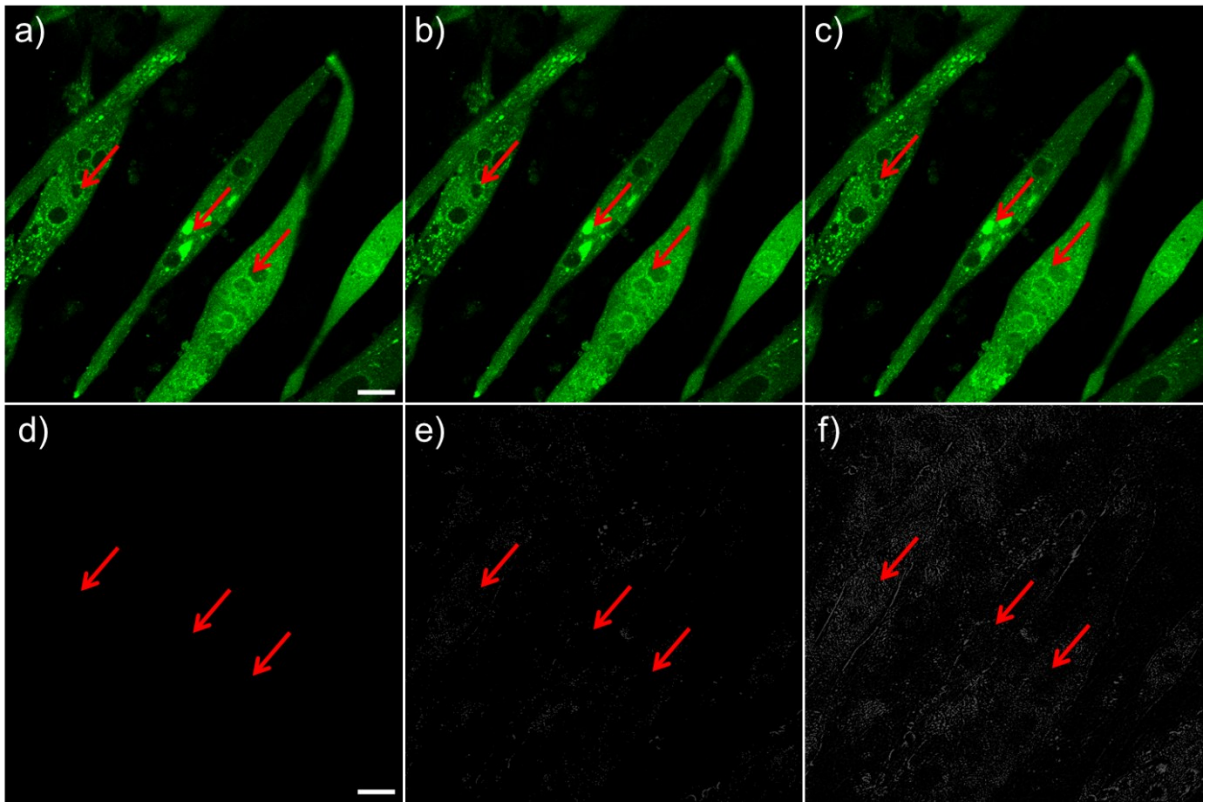

Figure S41. 3n does not induce strong calcium release or cellular contraction in C2C12 myotubes. a)– c), Confocal microscopy images of C2C12 myotubes treated with Fluo-4 (2 μM) and **3n** (2

μM). d)–f), Brightfield images after image-subtraction process of C2C12 myotubes treated with Fluo-4 (2 μM) and **3n** (2 μM). Images of t = 0 s (a, d), 35 s (b, e) and 140 s (c, f) were taken while laser stimulation takes place at t = 30 s. Stimulated myotubes are indicated by red arrows. Scale bar = 20 μm and is the same for all images. Stimulated cells were irradiated with a 640 nm laser of 1.5 s with a power of 0.73 mW to a circular area of diameter 5 μm.

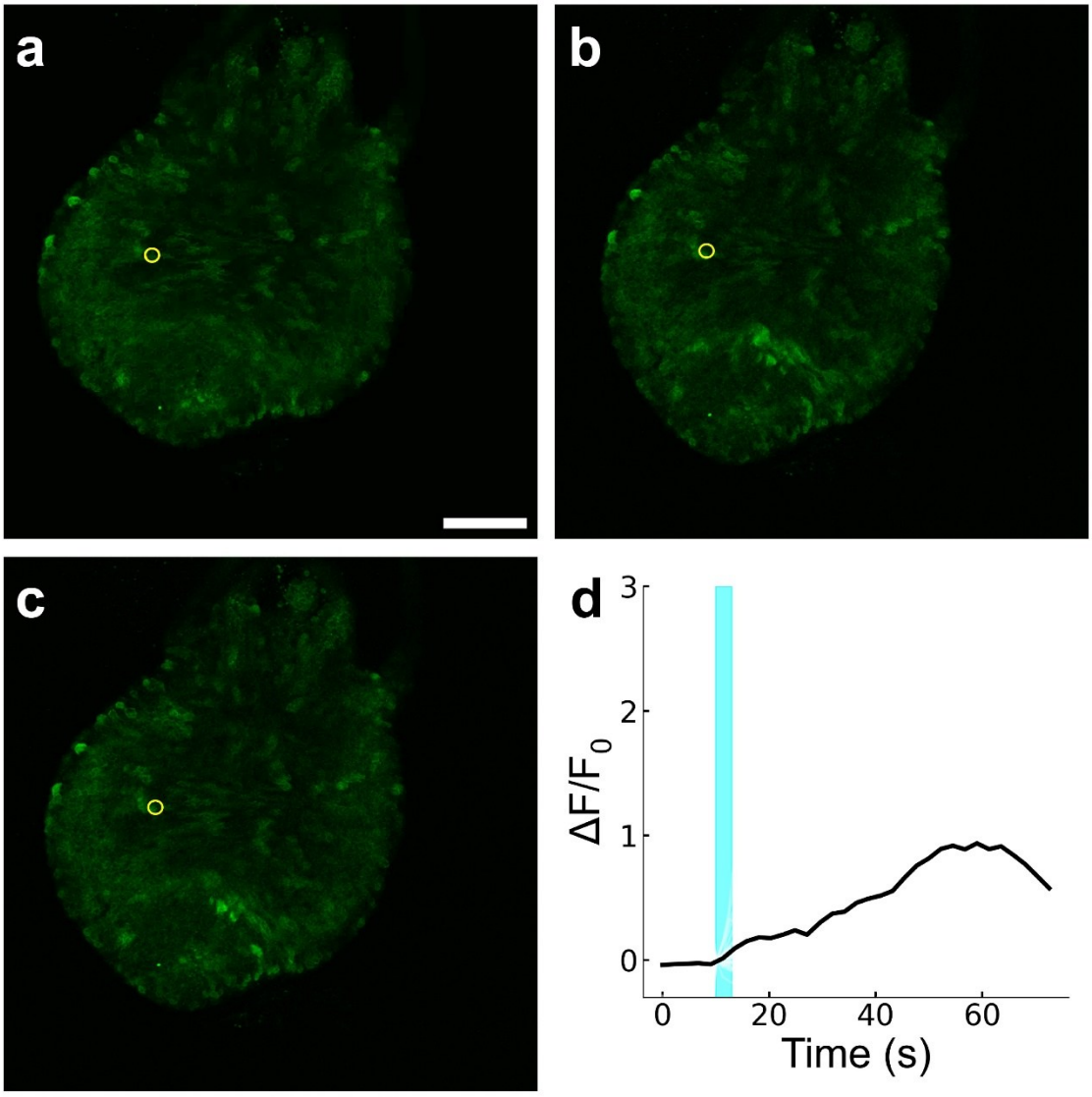

Figure S42. a)-c) Representative confocal microscopy images of *Hydra* treated with **3m** (1 μM). Images captured pre-stimulation and at t = 5 s, and t = 15 s; laser stimulation at t = 0 s. yellow circles indicate stimulated areas. Scale bar = 100 μm and is the same for all images. d) Normalized

GCaMP7b fluorescence intensity traces of *Hydra* treated with MJH **3m**. The bold, black-colored traces represent the average trace (n = 25 across five *Hydra*). For all the plots, the cyan lines indicate the time of stimulus with 640 nm light (9.0×10^2 W cm^{-2}).

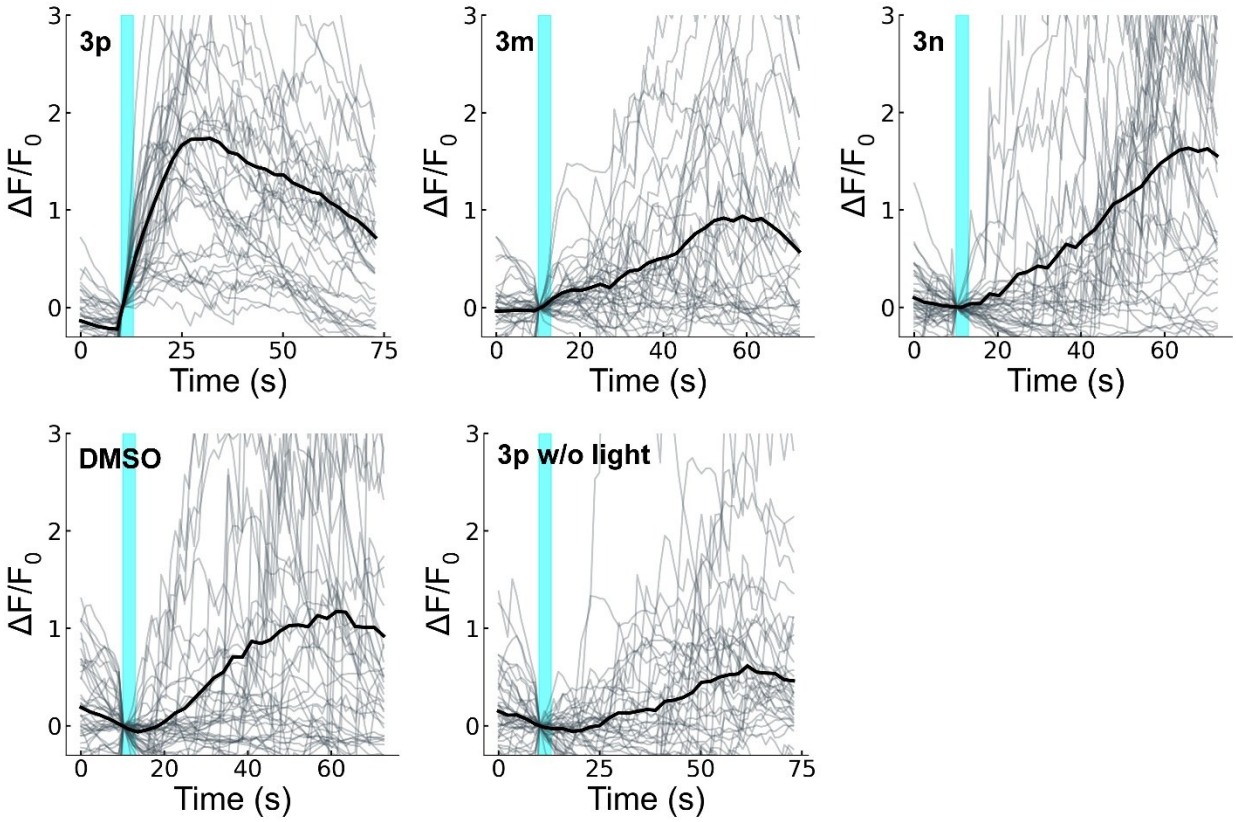

Figure S43. Normalized GCaMP7b fluorescence intensity traces of *Hydra* treated with MJH **3p**, **3m**, **3n**, **DMSO** and light, and **3p** without light. The bold, black-colored traces represent the average trace (n = 25 across five *Hydra*) and the individual traces are shown in grey. For all the plots, the cyan lines indicate the time of stimulus with 640 nm light (9.0×10^2 W cm^{-2} except the one treated with no light, where laser power was set to zero).

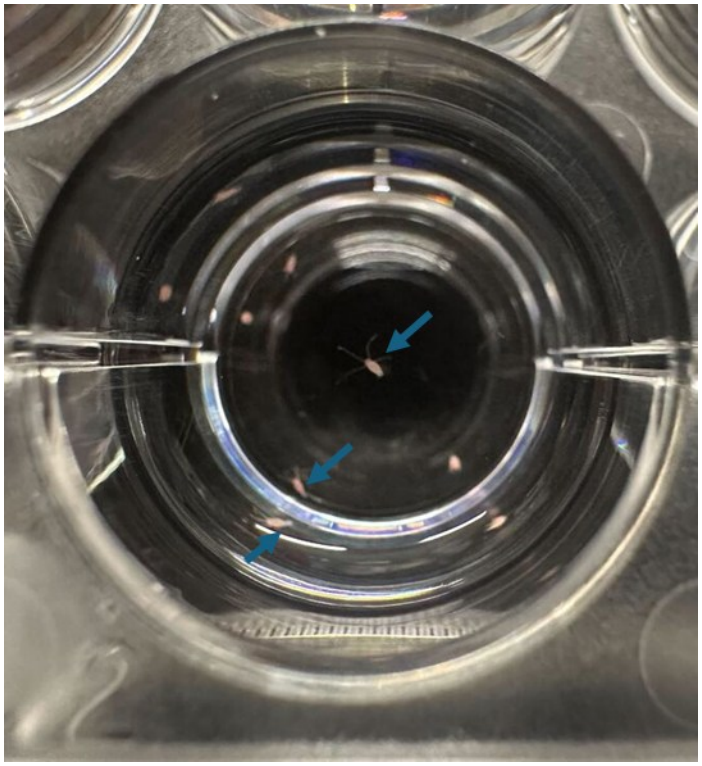

Figure S44. Following treatment with **3p** and laser, the *Hydra* (a few indicated by blue arrows) remained healthy after being cultured for an additional 1 day.

PCC and MOC Calculation

The R_{total} in Figure 4c is Pearson's correlation coefficient (PCC), which can be calculated by the formula given below for a typical image consisting of red and green channels.

$$PCC = \frac{\sum_i (R_i - \bar{R}) \times (G_i - \bar{G})}{\sqrt{\sum_i (R_i - \bar{R})^2 \times \sum_i (G_i - \bar{G})^2}}$$

where R_i and G_i refer to the intensity values of the red and green channels, respectively, of *pixel i*, and $\bar{R}$ and $\bar{G}$ refer to the mean intensities of the red and green channels, respectively, across the entire image. PCC values range from 1 for two images whose fluorescence intensities are perfectly, linearly related, to −1 for two images whose fluorescence intensities are perfectly, but inversely, related to one another. Values near zero reflect distributions of probes that are uncorrelated with one another.

From the PCC results in Figure 4c, R_{total} of **3p** and ER is 0.48 ± 0.04, indicating a moderate colocalization of MJH and ER, while the value of **3p** and mitochondria is 0.39 ± 0.03, showing a moderate but lower colocalization extent compared to ER.

The Manders overlap coefficient (MOC), on the other hand, could be described by the equation:

$$MOC = \frac{\sum_i (R_i \times G_i)}{\sqrt{\sum_i {R_i}^2 \times \sum_i {G_i}^2}}$$

It shows the proportion of colocalized pixels (pixels that show up in both channels) in one specific channel. And in Figure 4c, tM1 and tM2 are MOCs with threshold that are automatically given by the software ImageJ.

As both tM1 and tM2 of **3p** and ER and mitochondria are ~50%, it indicates partially colocalization of **3p** with either ER or mitochondria, which is consistent with the PCC results. Since the IP_3R is located in the ER membrane, our colocalization results showing MJHs partially colocalize with ER could be indirect evidence that the MJHs can activate IP_3 pathway.

Molecular Dynamics Simulation Method

We performed molecular dynamics (MD) simulations to determine the equilibrium distance of dyes below the membrane surface. The simulations are performed in Gromacs[2] using CHARMM36 forcefield.[3,4] The parameters for dyes are generated using the CHARMM-GUI Ligand Modeller.[5] We obtained equilibrium structures of dyes by performing geometric optimization at the HF-3c level of theory using the ORCA package.[6] The membrane with the POPC:POPE:POPG=10:5:1 composition was built using CHARMM-GUI Membrane Builder.[7–10] The initial configurations were prepared using CHARMM-GUI.[11] Additionally, 5 nm of TIP3P water is added with 150 mM NaCl buffer to simulate the ionic strength used in the experiments. We used the Nose-Hoover thermostat[12] to maintain the temperature at 303.15 K and Parrinello-Rahman barostat[13] to maintain pressure at 1 bar. The long-range electrostatics were treated with the particle mesh Ewald (PME) algorithm.[14] Initially, dyes are placed in the middle of the membrane. During the first 225 ps, constraints limit the movement of both lipid heads and the dyes. After removing all constraints, we simulate the system during 80 ns.

References

1. K. Kundu, S. F. Knight, N. Willett, S. Lee, W. R. Taylor and N. Murthy, *Angew. Chem. Int. Ed.,* 2009, **48**, 299–303.
2. M. J. Abraham, T. Murtola, R. Schulz, S. Páll, J. C. Smith, B. Hess and E. Lindahl, *SoftwareX,* 2015, **1–2**, 19–25.
3. B. R. Brooks, C. L. Brooks III, A. D. Mackerell Jr., L. Nilsson, R. J. Petrella, B. Roux, Y. Won, G. Archontis, C. Bartels, S. Boresch, A. Caflisch, L. Caves, Q. Cui, A. R. Dinner, M. Feig, S. Fischer, J. Gao, M. Hodoscek, W. Im, K. Kuczera, T. Lazaridis, J. Ma, V. Ovchinnikov, E. Paci, R. W. Pastor, C. B. Post, J. Z. Pu, M. Schaefer, B. Tidor, R. M. Venable, H. L. Woodcock, X. Wu, W. Yang, D. M. York and M. Karplus, *J. Comput. Chem.,* 2009, **30**, 1545–1614.
4. J. Huang, S. Rauscher, G. Nawrocki, T. Ran, M. Feig, B. L. de Groot, H. Grubmüller and A. D. MacKerell Jr., *Nat. Methods,* 2017, **14**, 71–73.
5. S. Kim, J. Lee, S. Jo, C. L. Brooks III, H. S. Lee and W. Im, *J. Comput. Chem.,* 2017, **38**, 1879–1886.
6. F. Neese, F. Wennmohs, U. Becker and C. Riplinger, *J. Chem. Phys.,* 2020, **152**, 224108.
7. E. L. Wu, X. Cheng, S. Jo, H. Rui, K. C. Song, E. M. Dávila-Contreras, Y. Qi, J. Lee, V. Monje-Galvan, R. M. Venable, J. B. Klauda and W. Im, *J. Comput. Chem.,* 2014, **35**, 1997–2004.
8. S. Jo, J. B. Lim, J. B. Klauda and W. Im, *Biophys. J.,* 2009, **97**, 50–58.
9. S. Jo, T. Kim and W. Im, *PLoS ONE,* 2007, **2**, e880.
10. J. Lee, D. S. Patel, J. Ståhle, S.-J. Park, N. R. Kern, S. Kim, J. Lee, X. Cheng, M. A. Valvano, O. Holst, Y. A. Knirel, Y. Qi, S. Jo, J. B. Klauda, G. Widmalm and W. Im, *J. Chem. Theory Comput.,* 2019, **15**, 775–786.
11. S. Jo, T. Kim, V. G. Iyer and W. Im, *J. Comput. Chem.,* 2008, **29**, 1859–1865.
12. D. J. Evans and B. L. Holian, *J. Chem. Phys.,* 1985, **83**, 4069–4074.
13. M. Parrinello and A. Rahman, *J. Appl. Phys.,* 1981, **52**, 7182–7190.
14. U. Essmann, L. Perera, M. L. Berkowitz, T. Darden, H. Lee and L. G. Pedersen, *J. Chem. Phys.,* 1995, **103**, 8577–8593.

NMR Spectra

^{1}H-NMR spectrum of 3a

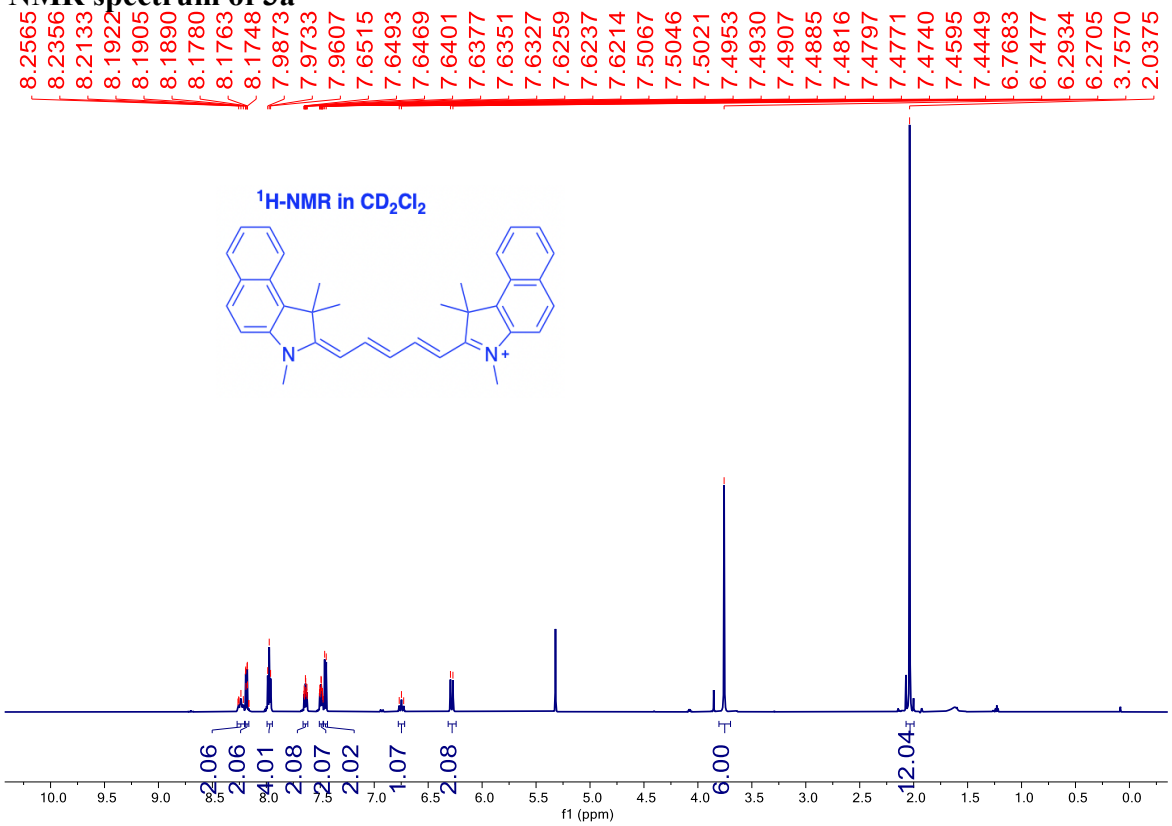

^{13}C-NMR spectrum of 3a

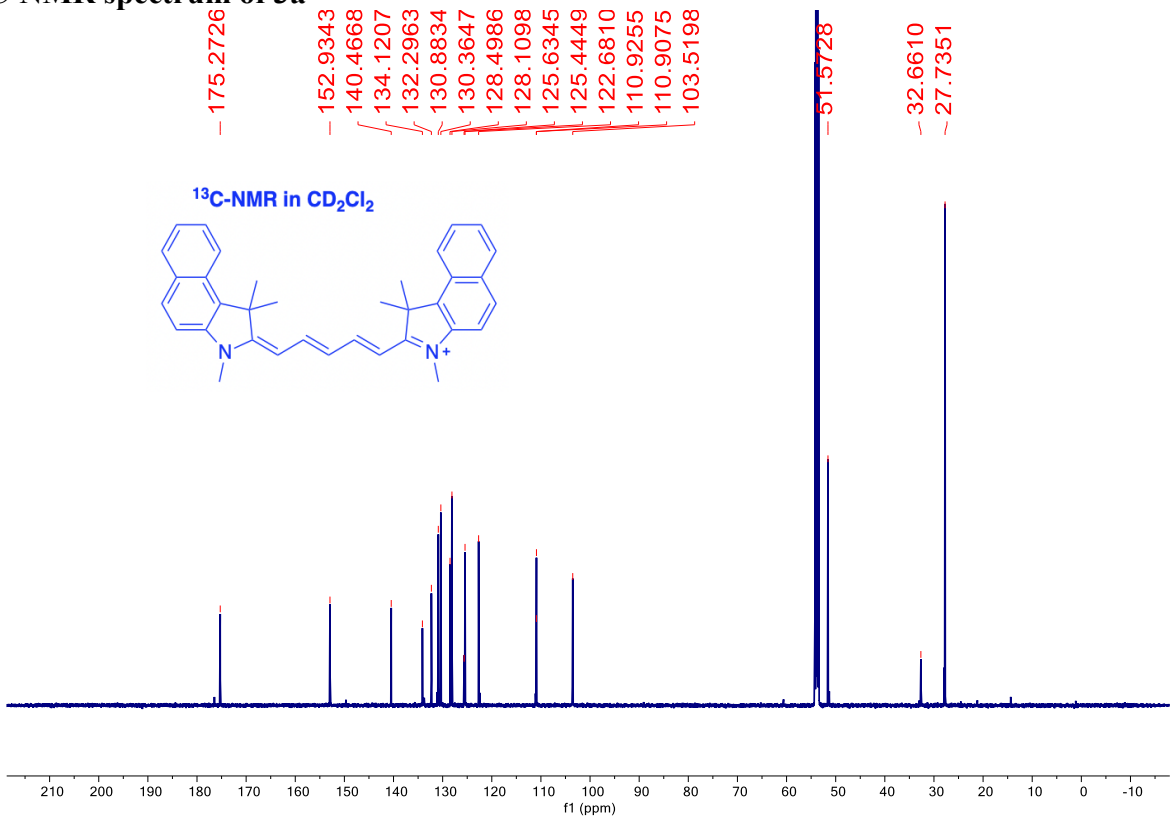

^{1}H-NMR spectrum of 3b

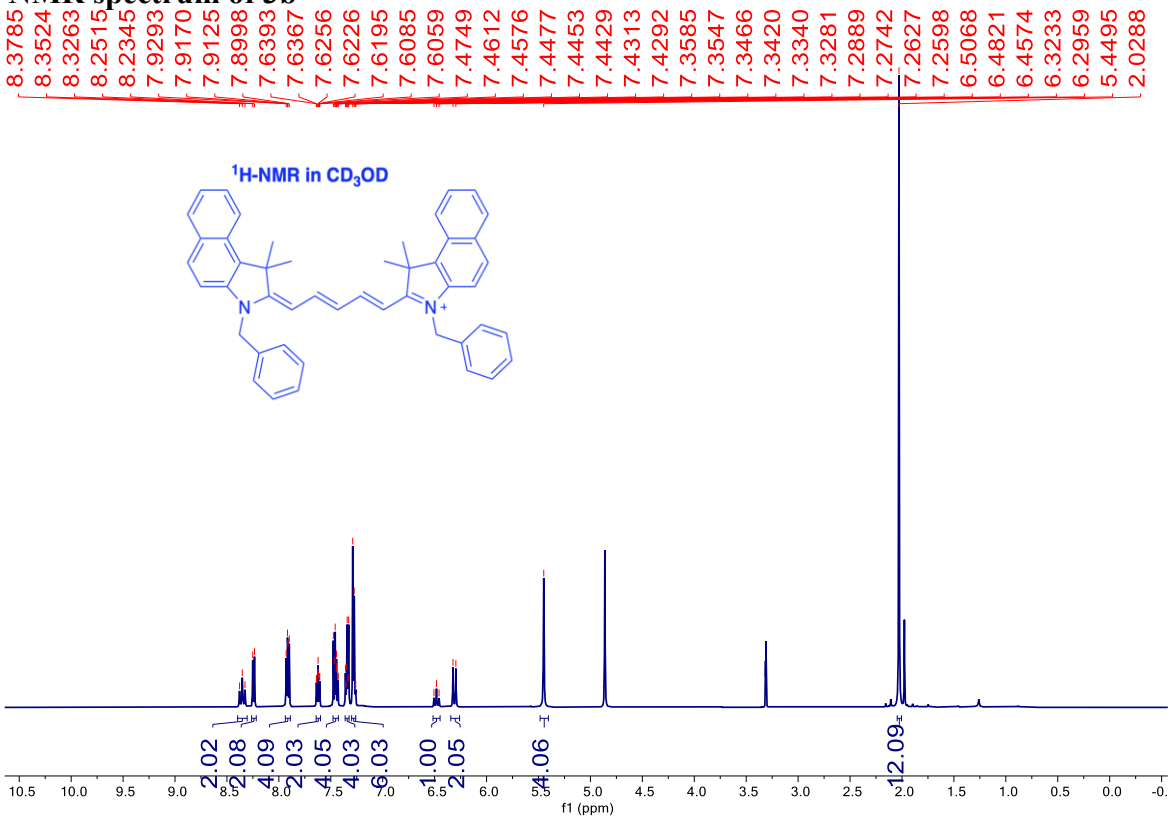

^{13}C-NMR spectrum of 3b

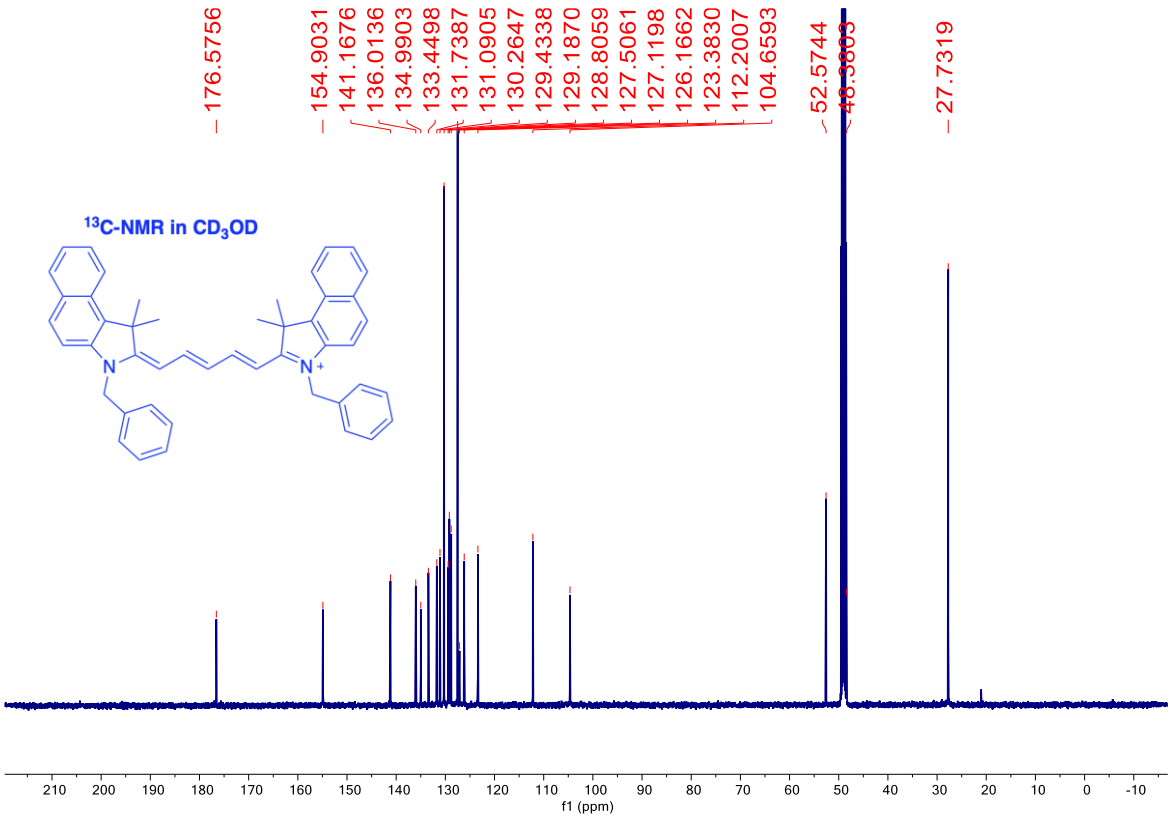

^{1}H-NMR spectrum of 3c

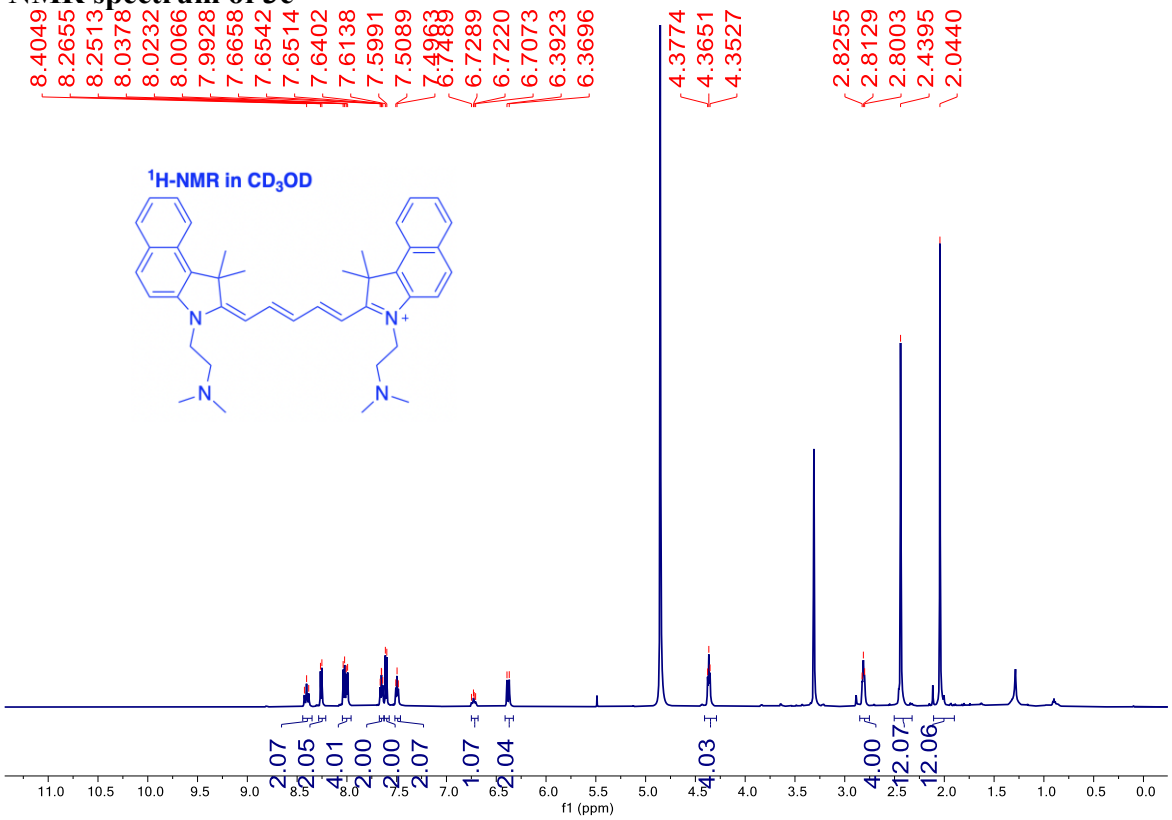

^{13}C-NMR spectrum of 3c

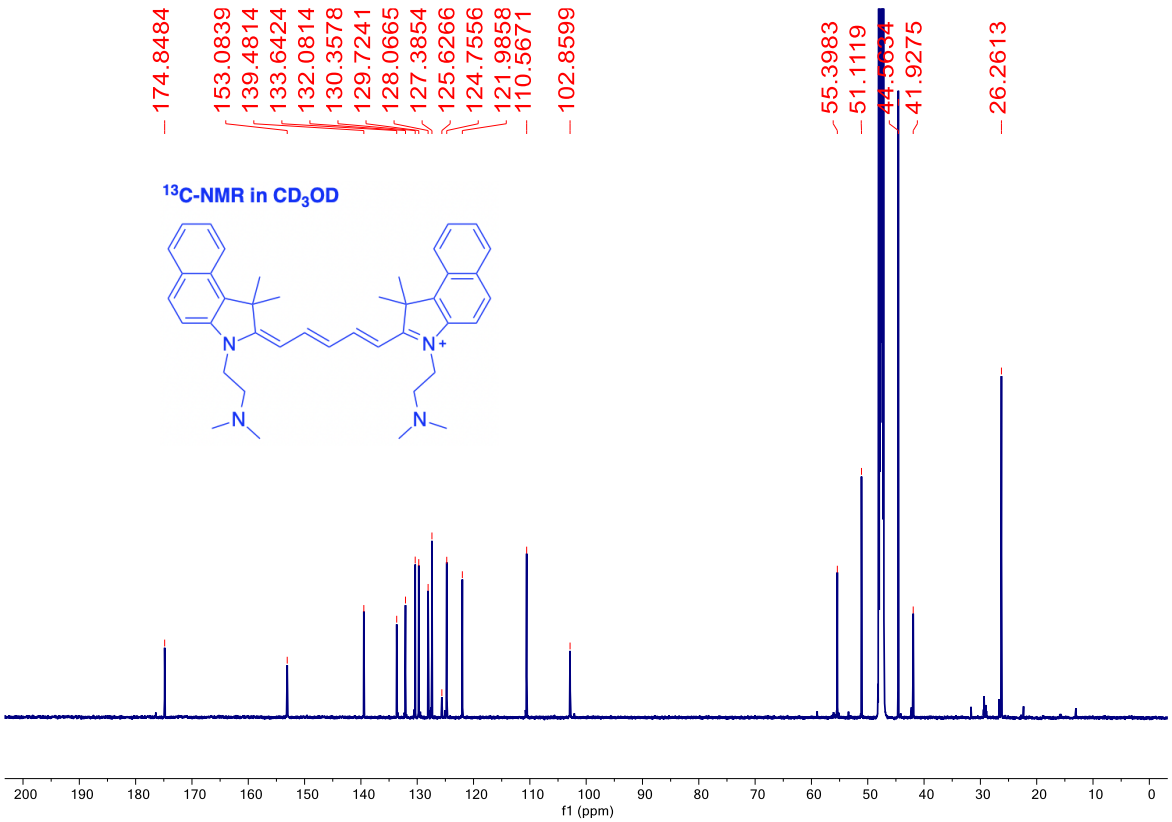

^{1}H-NMR spectrum of 3d

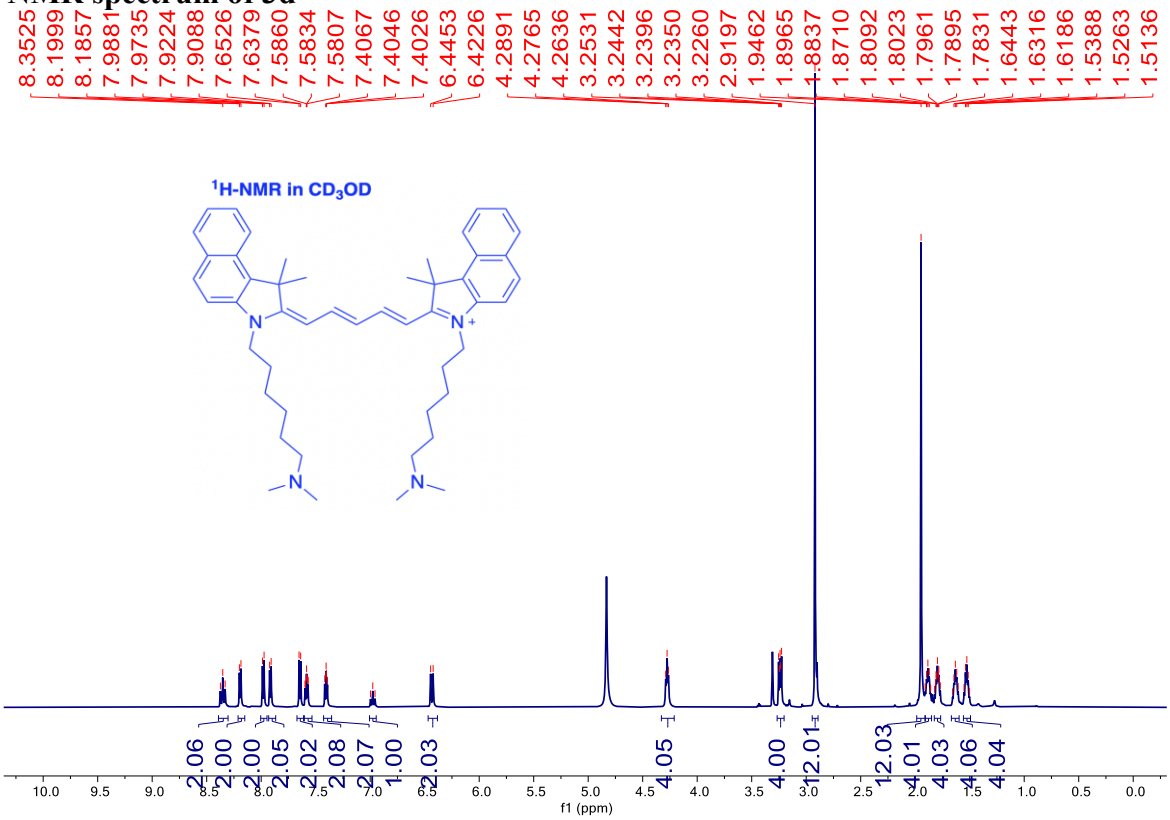

^{13}C-NMR spectrum of 3d

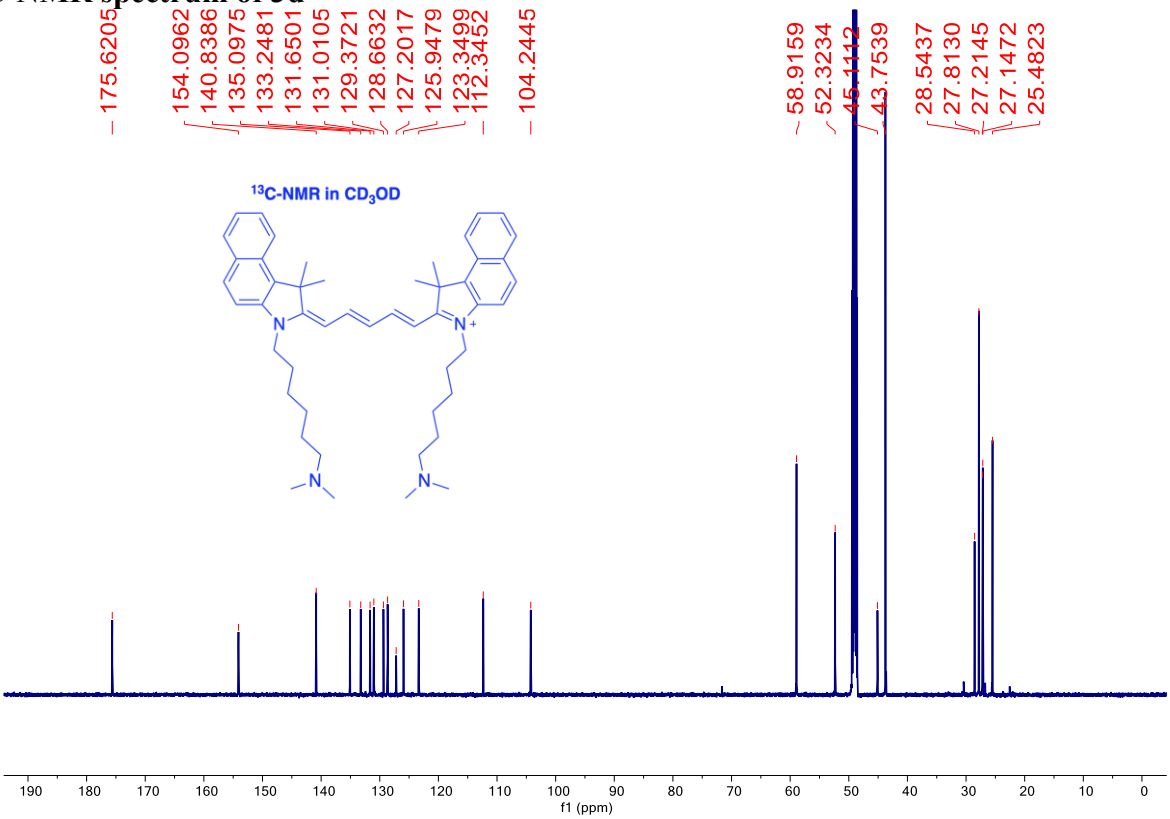

^{1}H-NMR spectrum of 3e

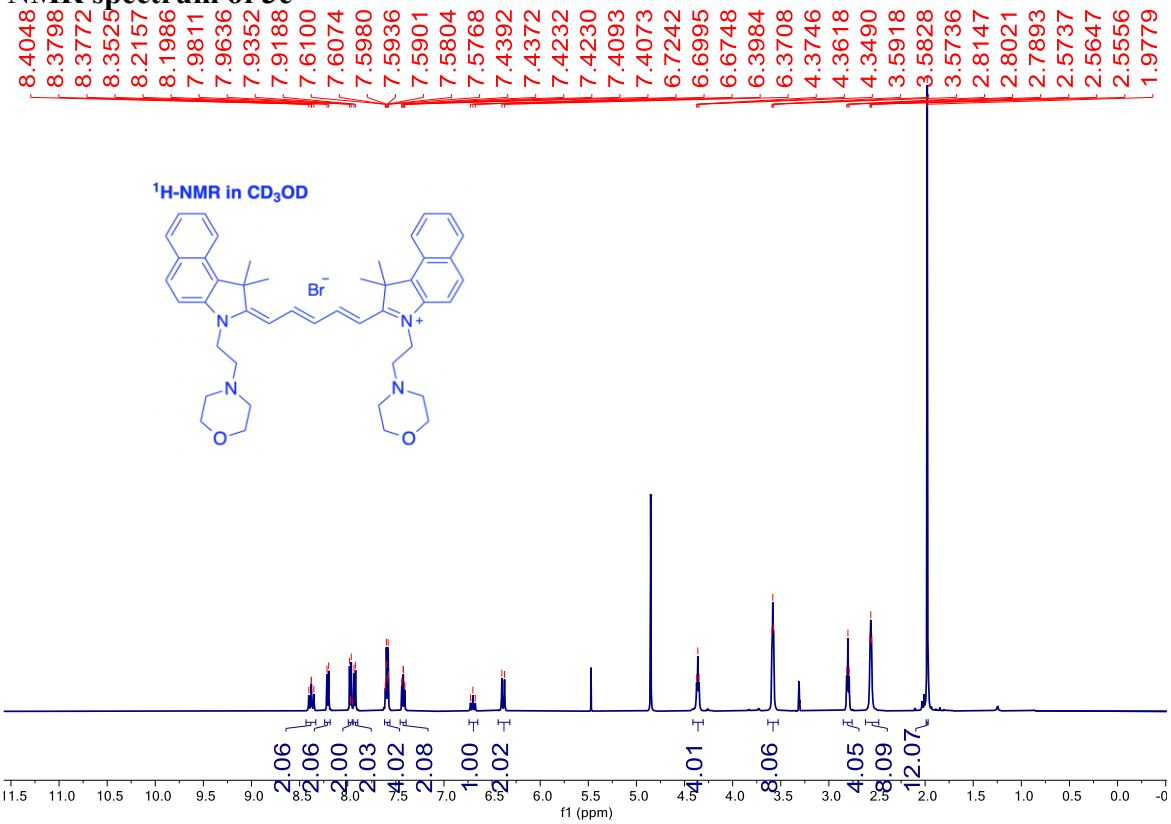

^{13}C-NMR spectrum of 3e

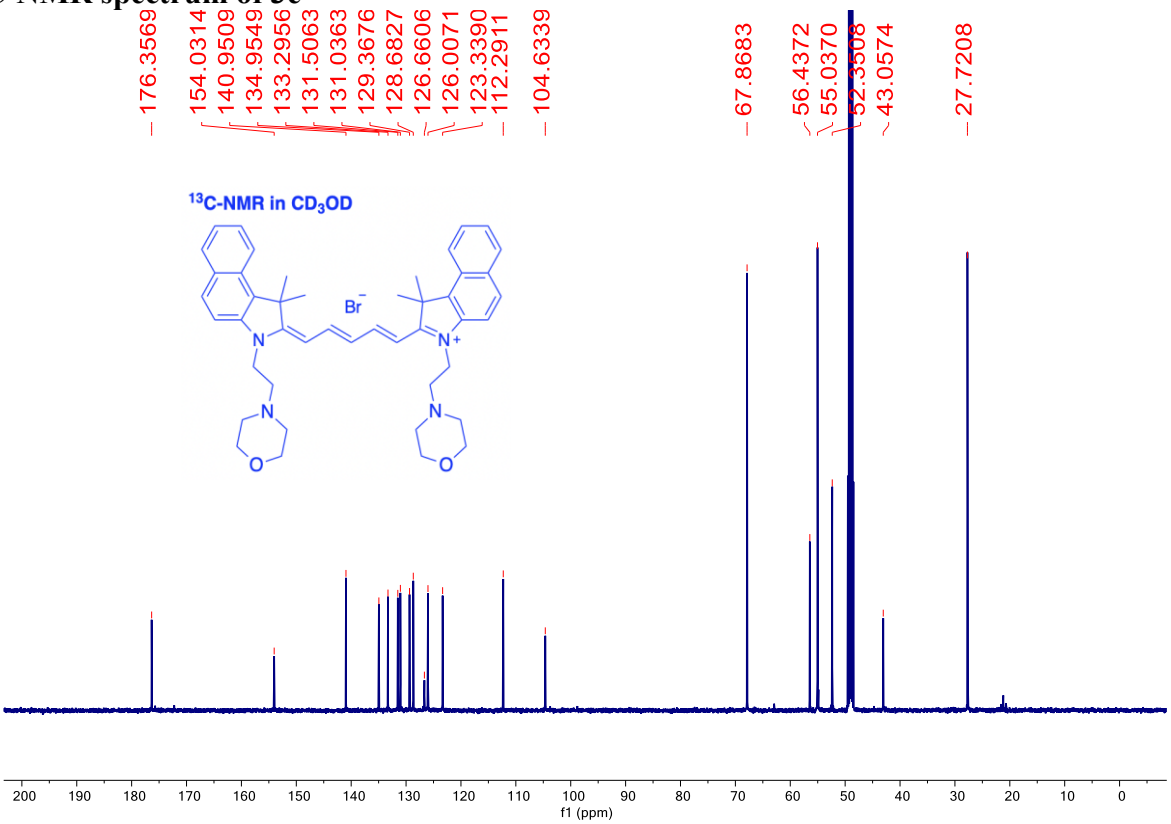

^{1}H-NMR spectrum of 3f

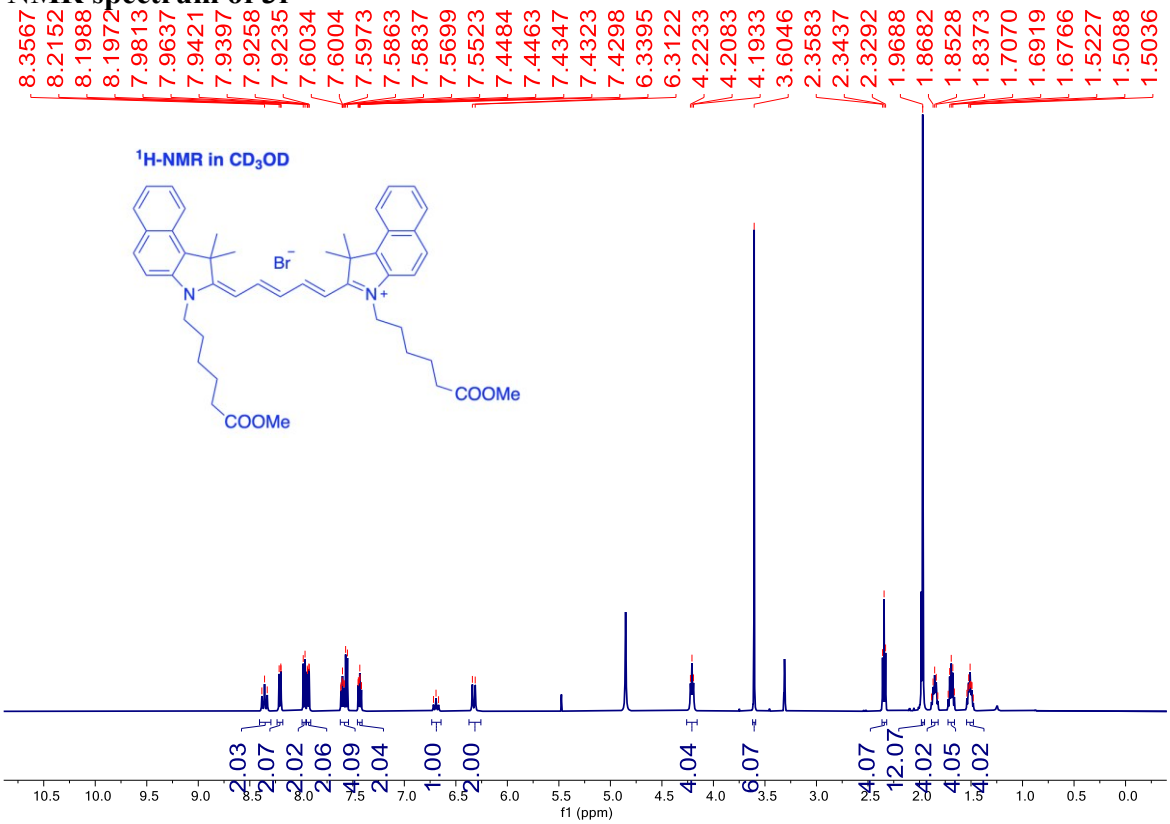

^{13}C-NMR spectrum of 3f

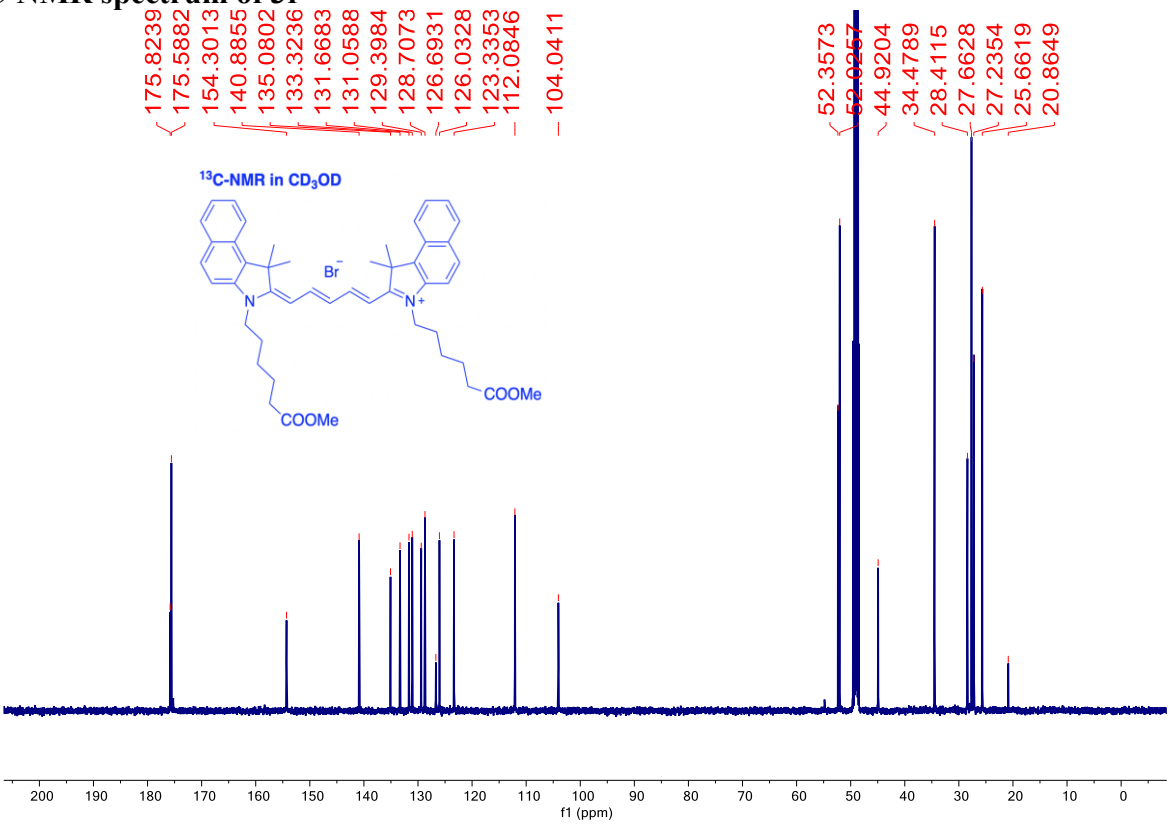

^{1}H-NMR spectrum of 3g

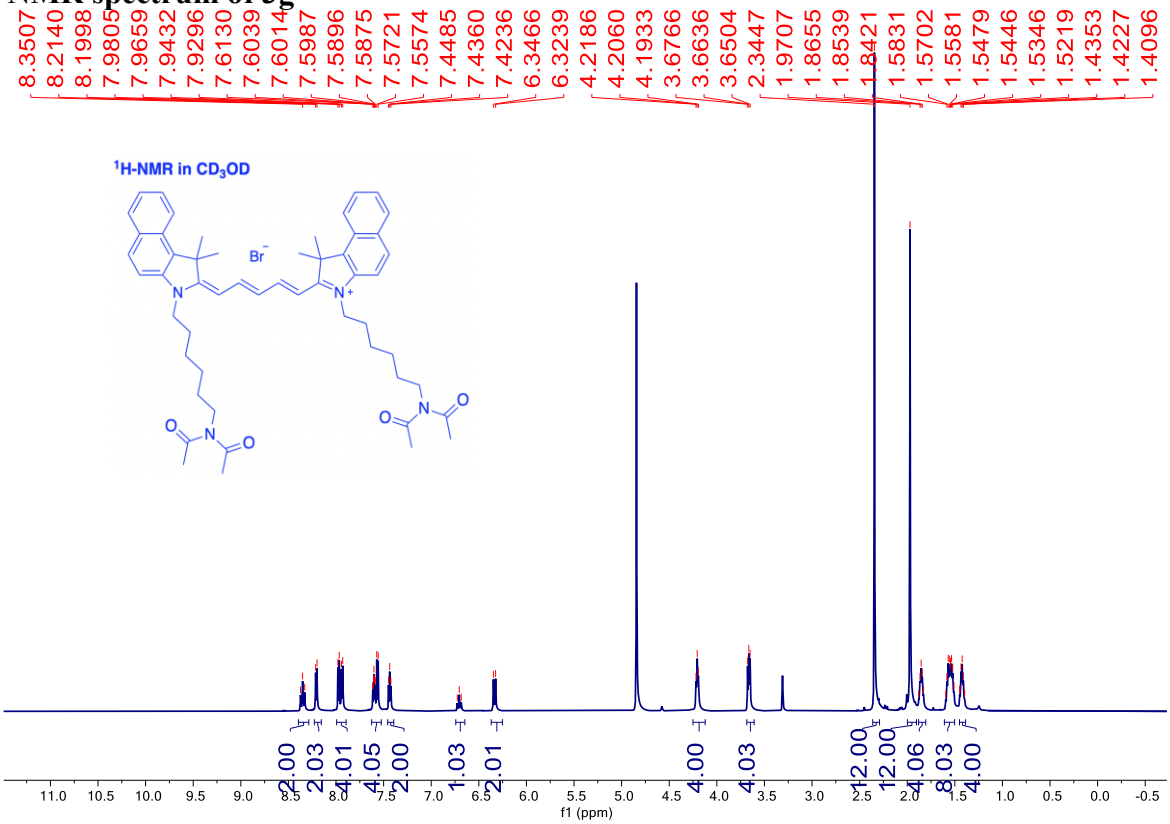

^{13}C-NMR spectrum of 3g

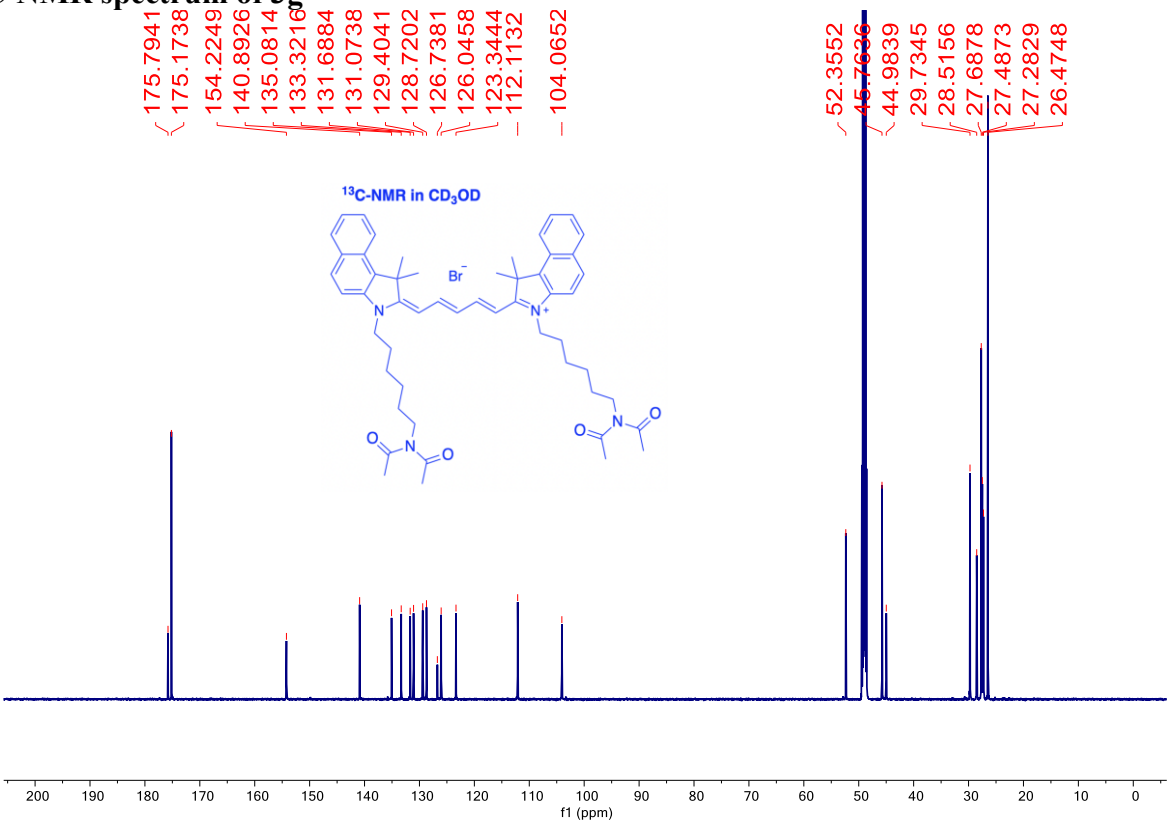

^{1}H-NMR spectrum of 3h

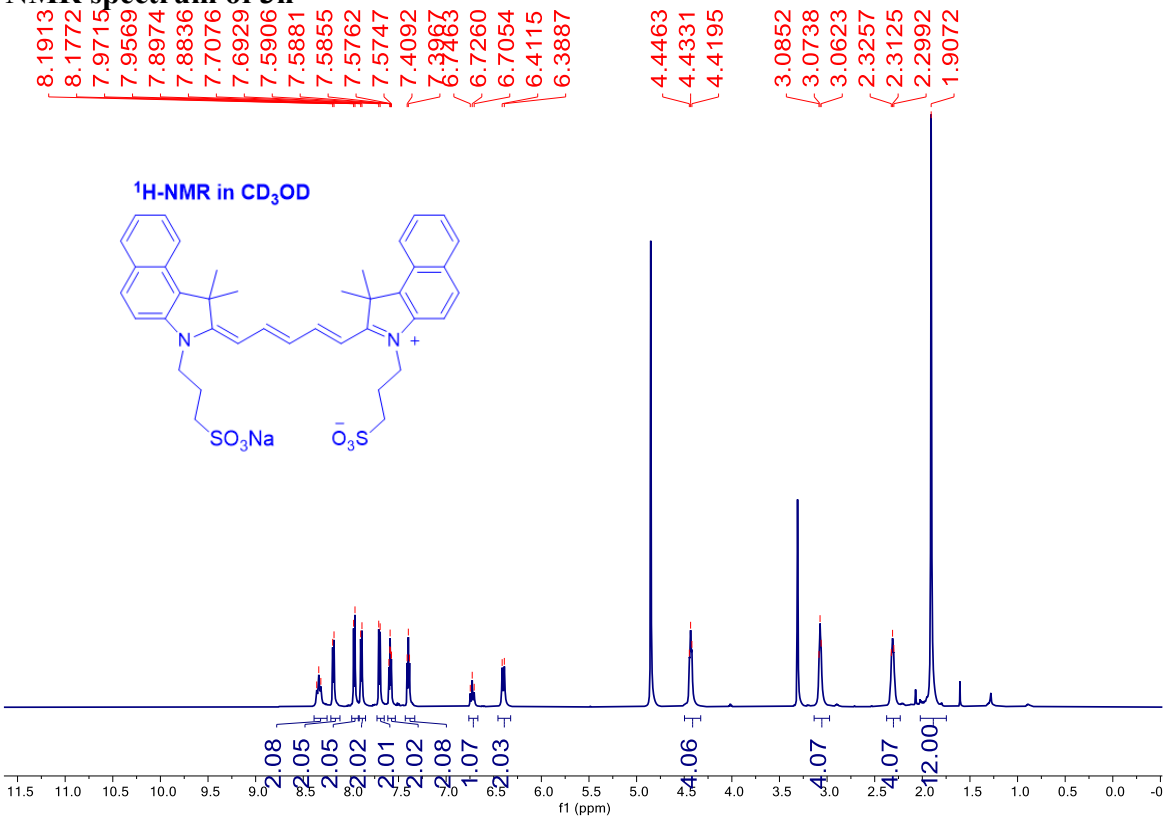

^{13}C-NMR spectrum of 3h

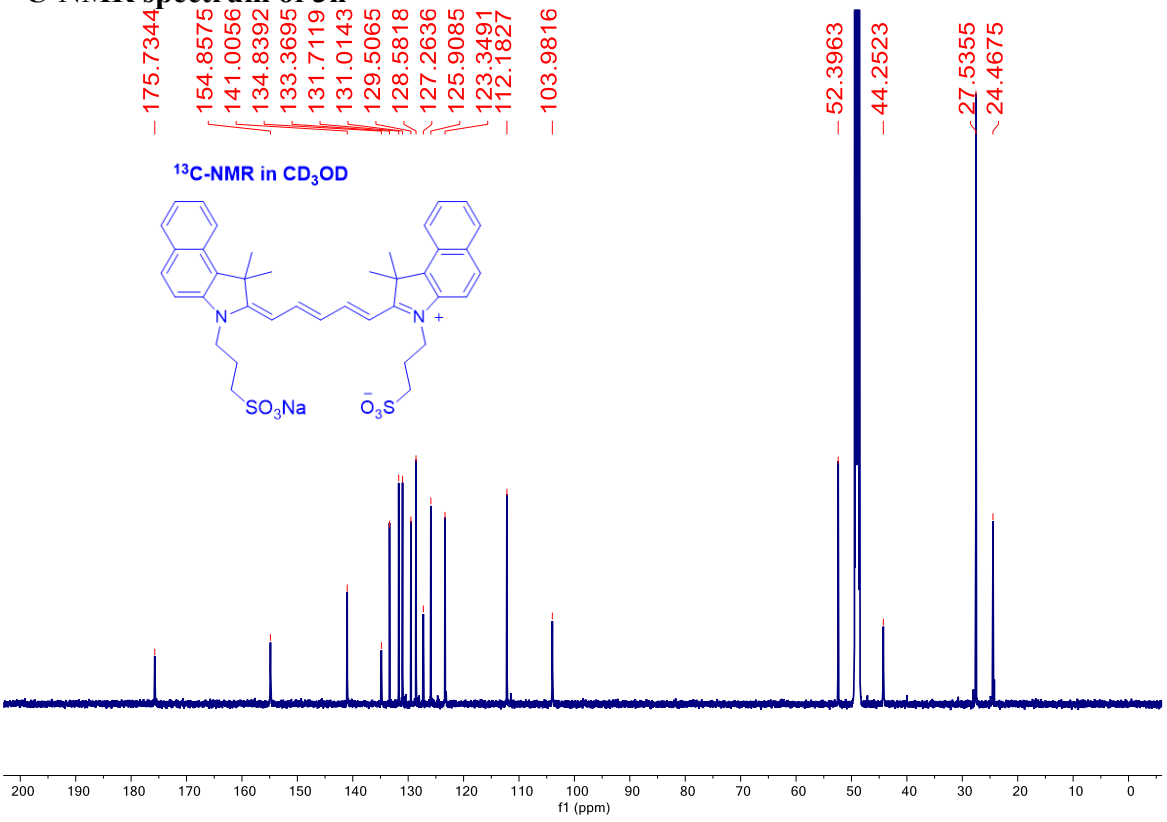

^{1}H-NMR spectrum of 3i

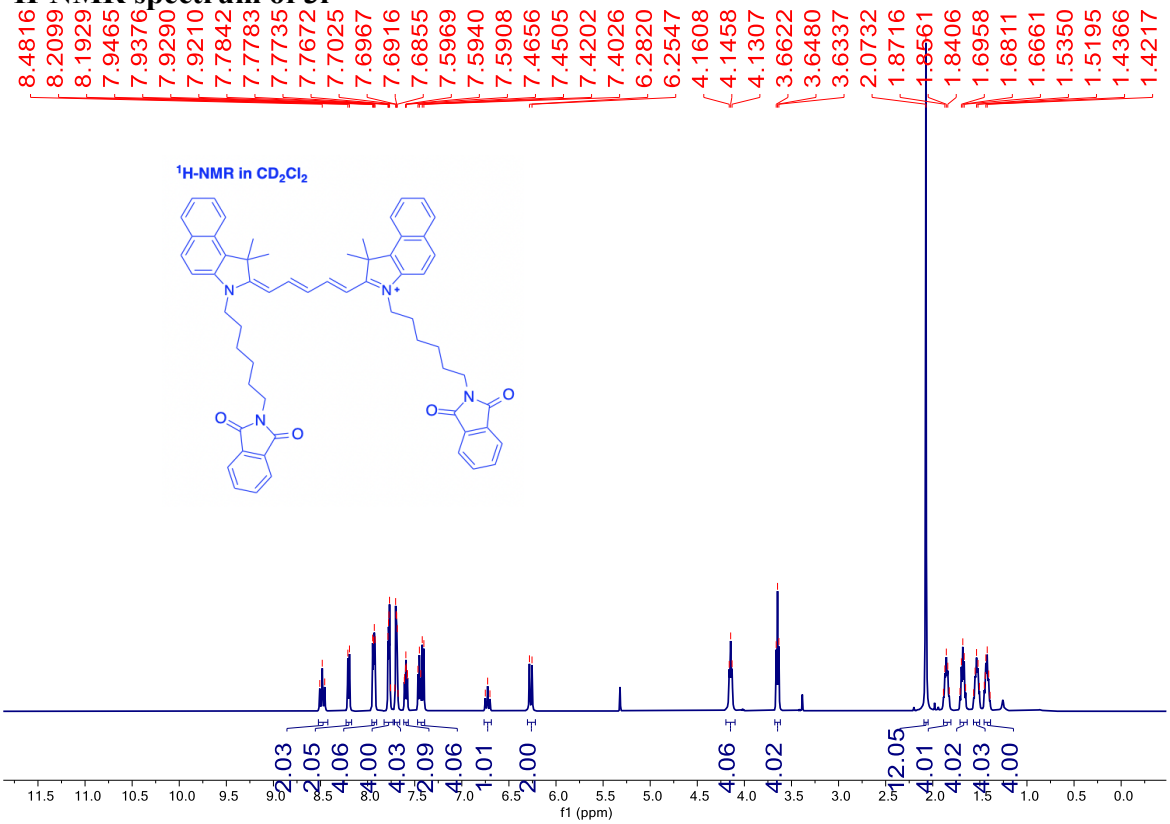

^{13}C-NMR spectrum of 3i

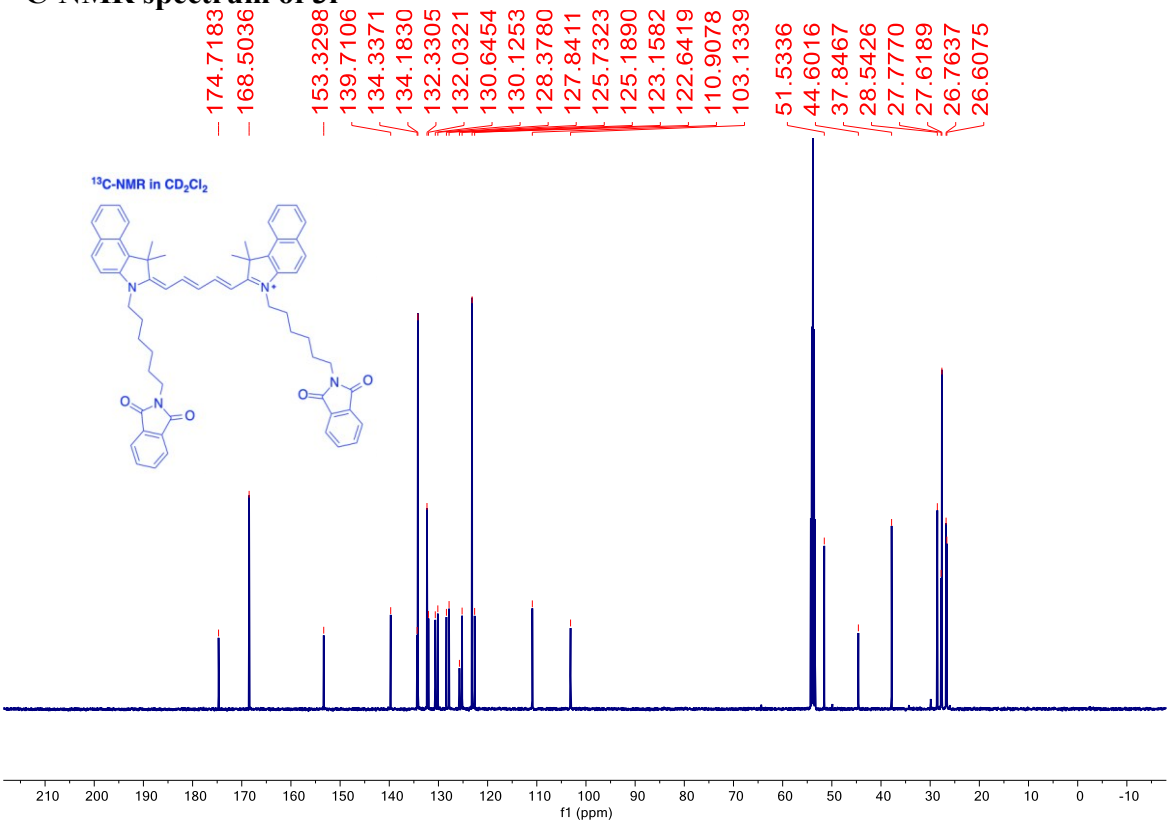

^{1}H-NMR spectrum of 3j

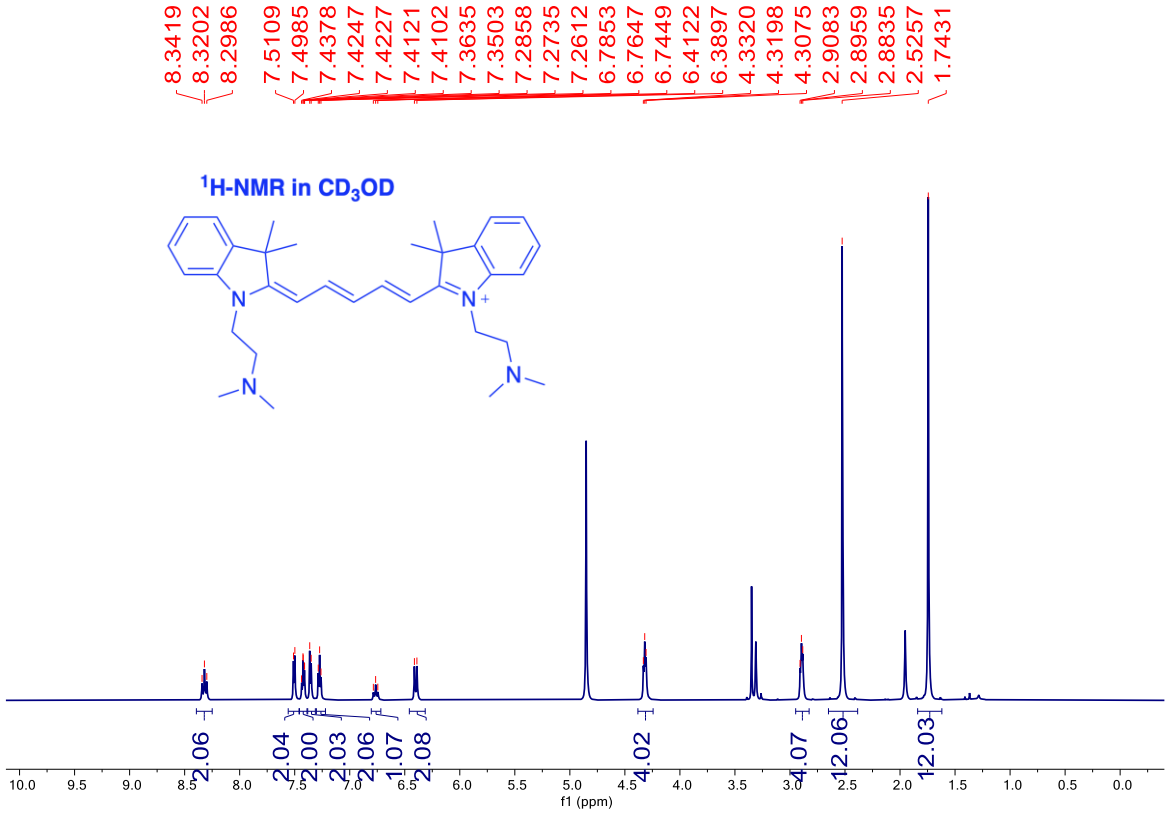

^{13}C-NMR spectrum of 3j

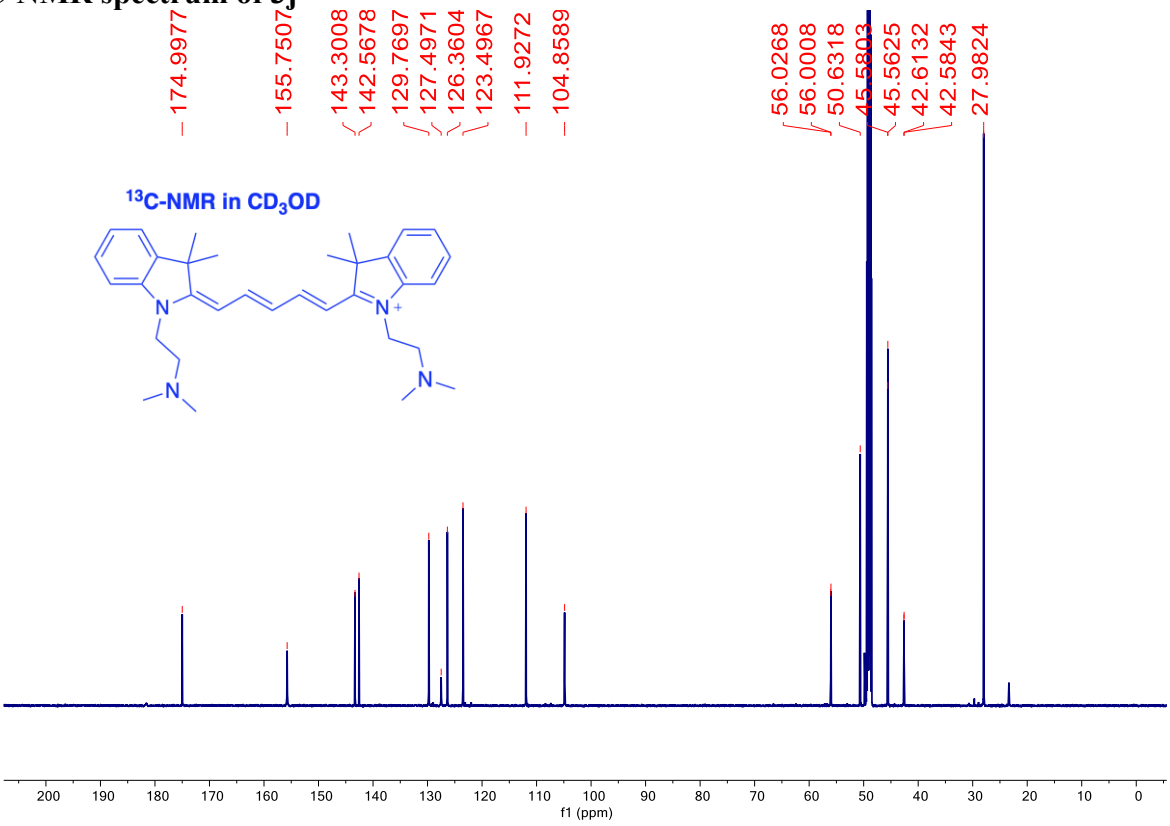

^{1}H-NMR spectrum of 3k

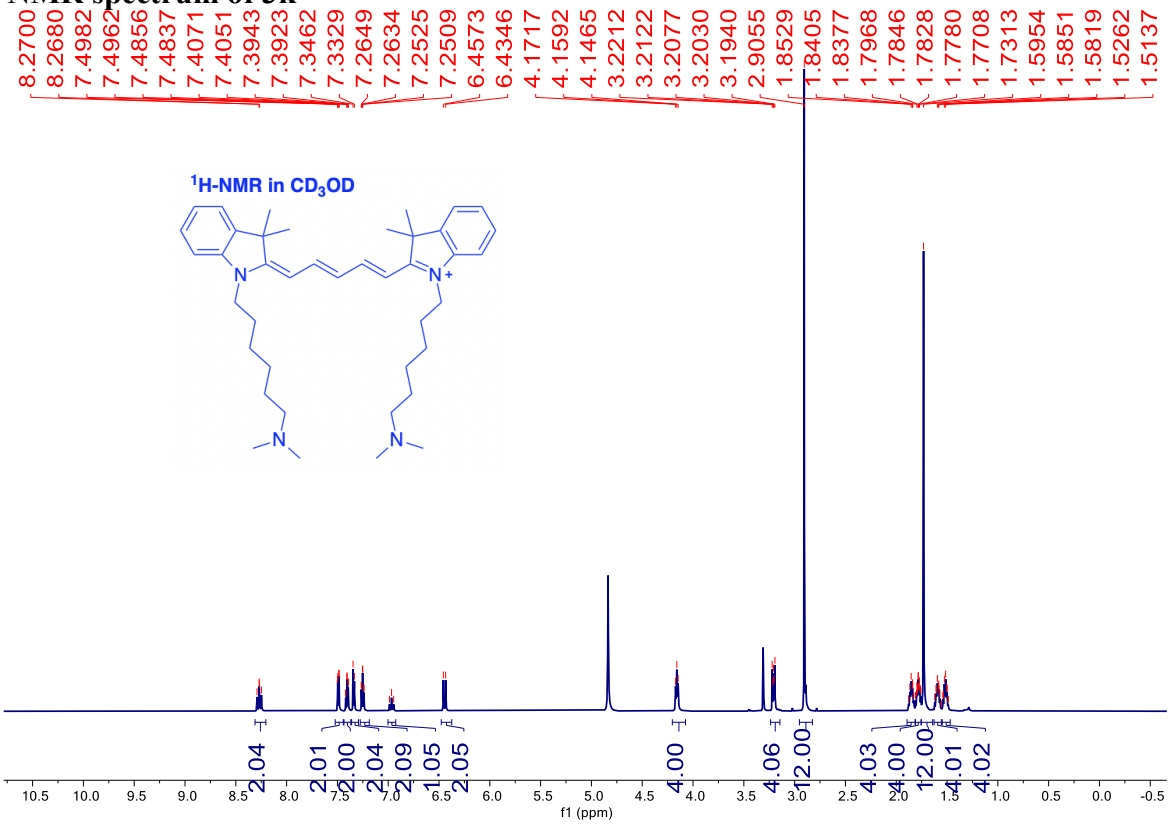

^{13}C-NMR spectrum of 3k

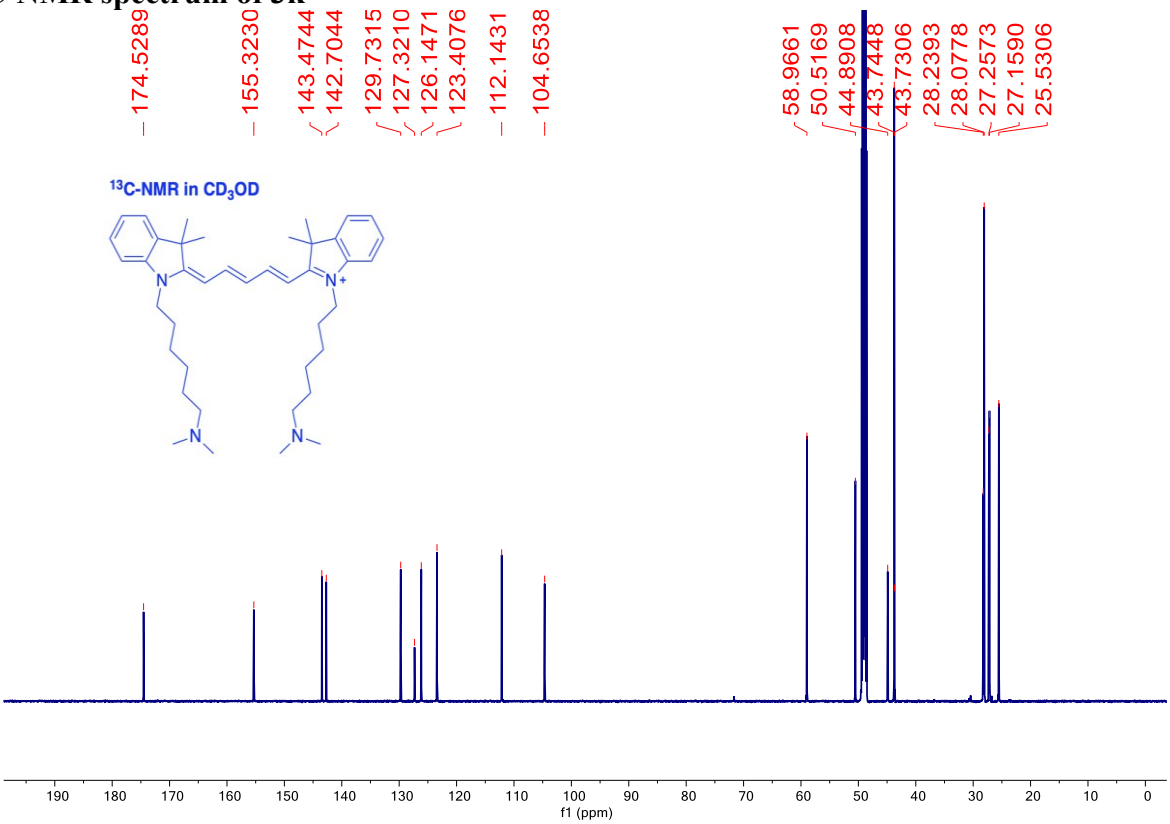

^{1}H-NMR spectrum of 3l

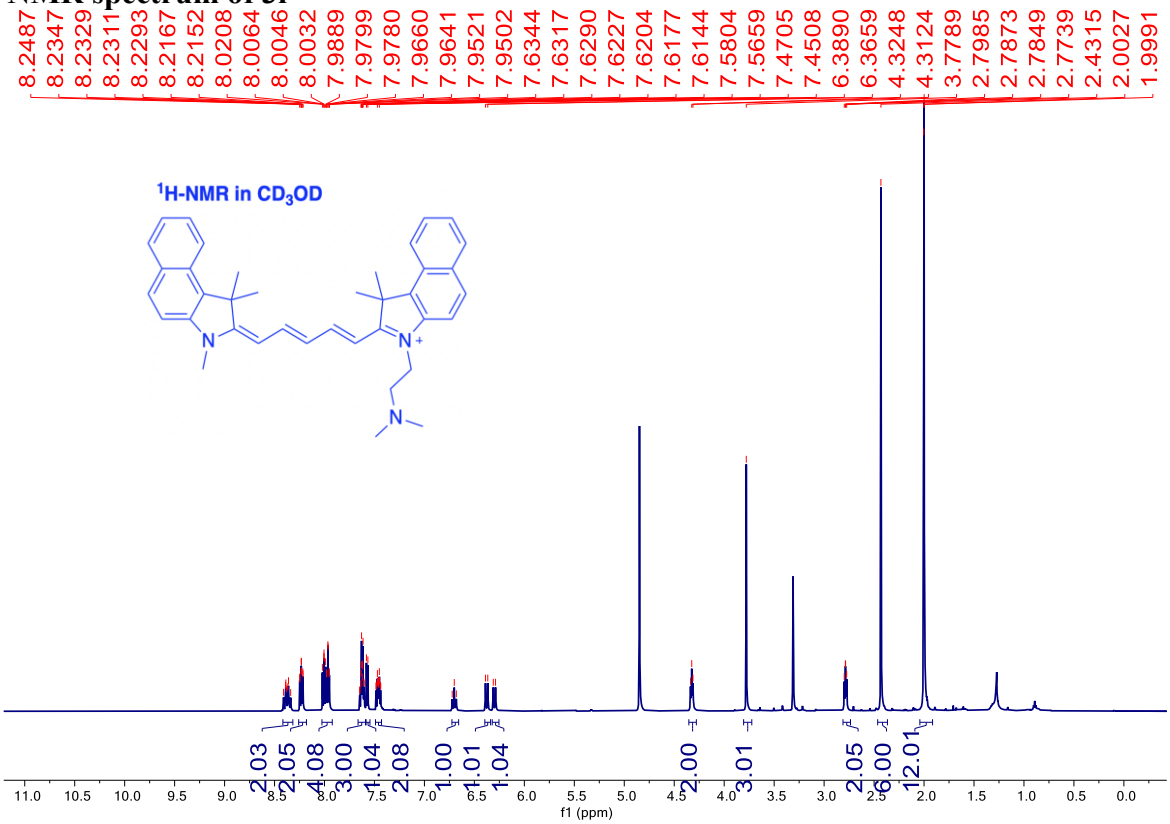

^{13}C-NMR spectrum of 3l

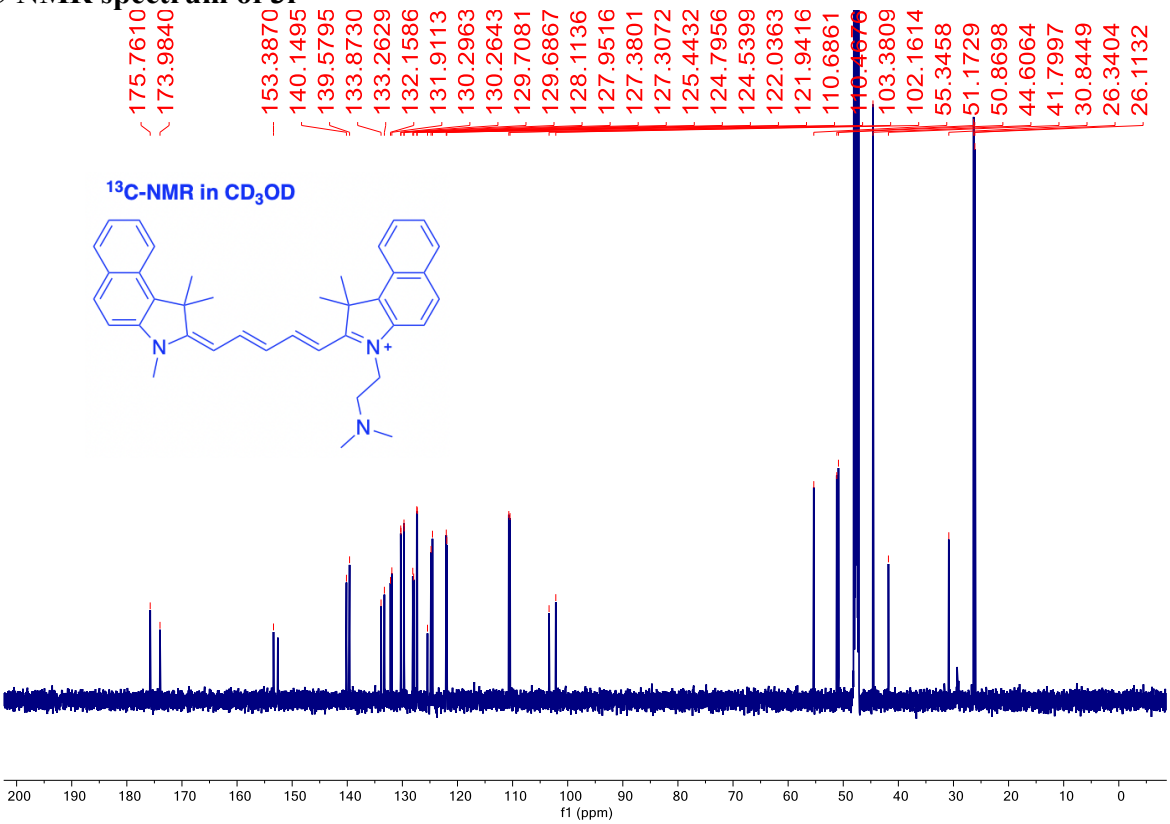

^{1}H-NMR spectrum of 3m

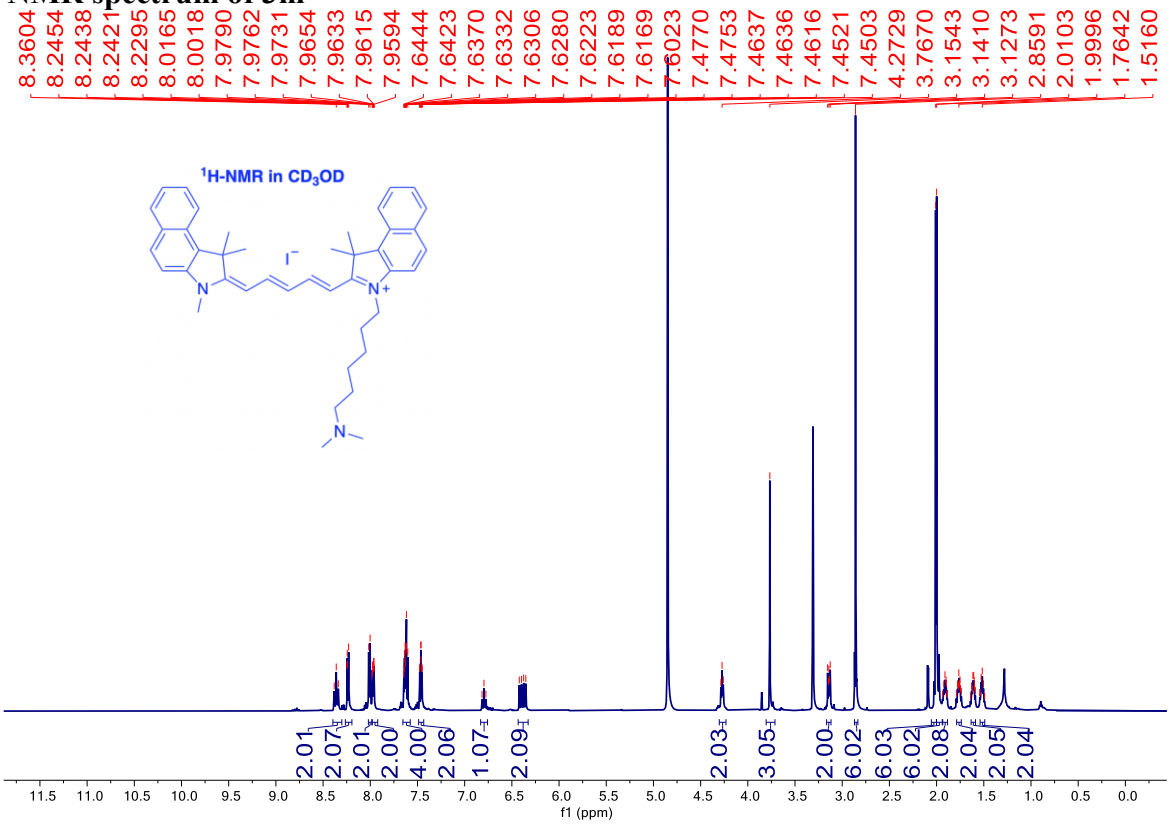

^{13}C-NMR spectrum of 3m

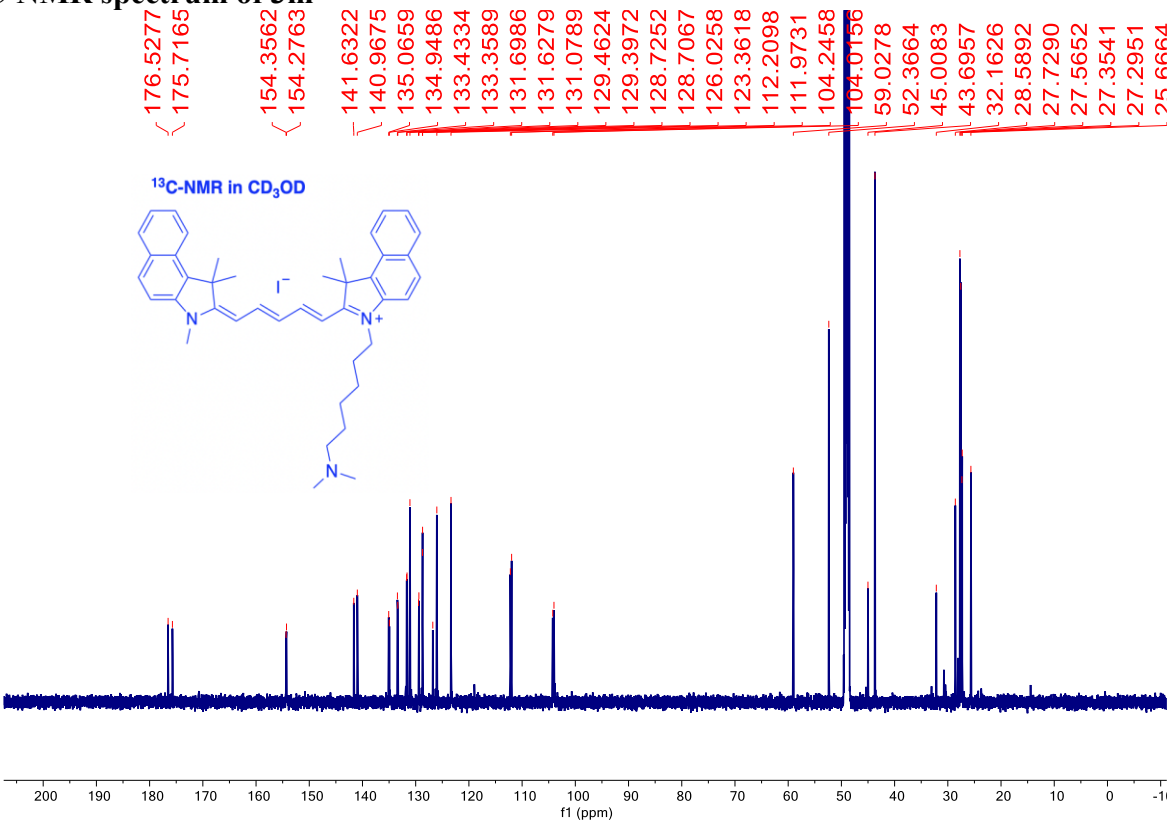

^{1}H-NMR spectrum of 3n

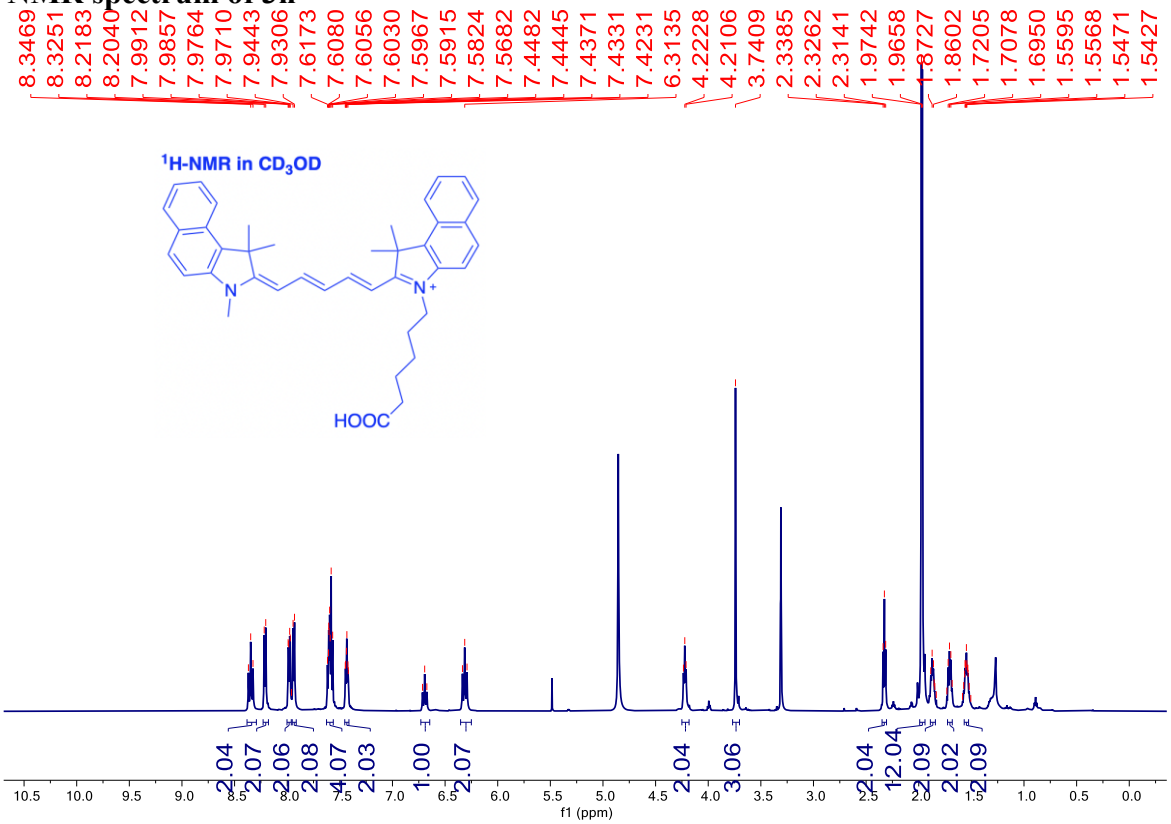

^{13}C-NMR spectrum of 3n

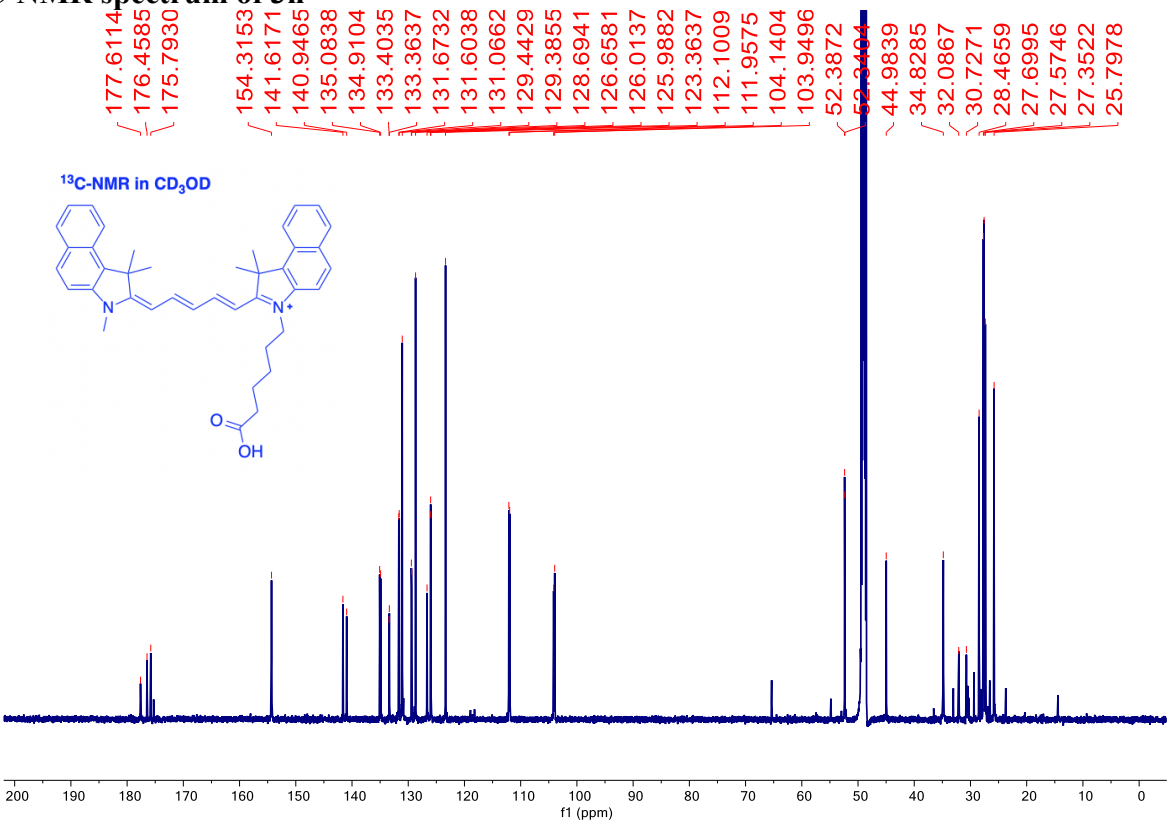

^{1}H-NMR spectrum of 3o

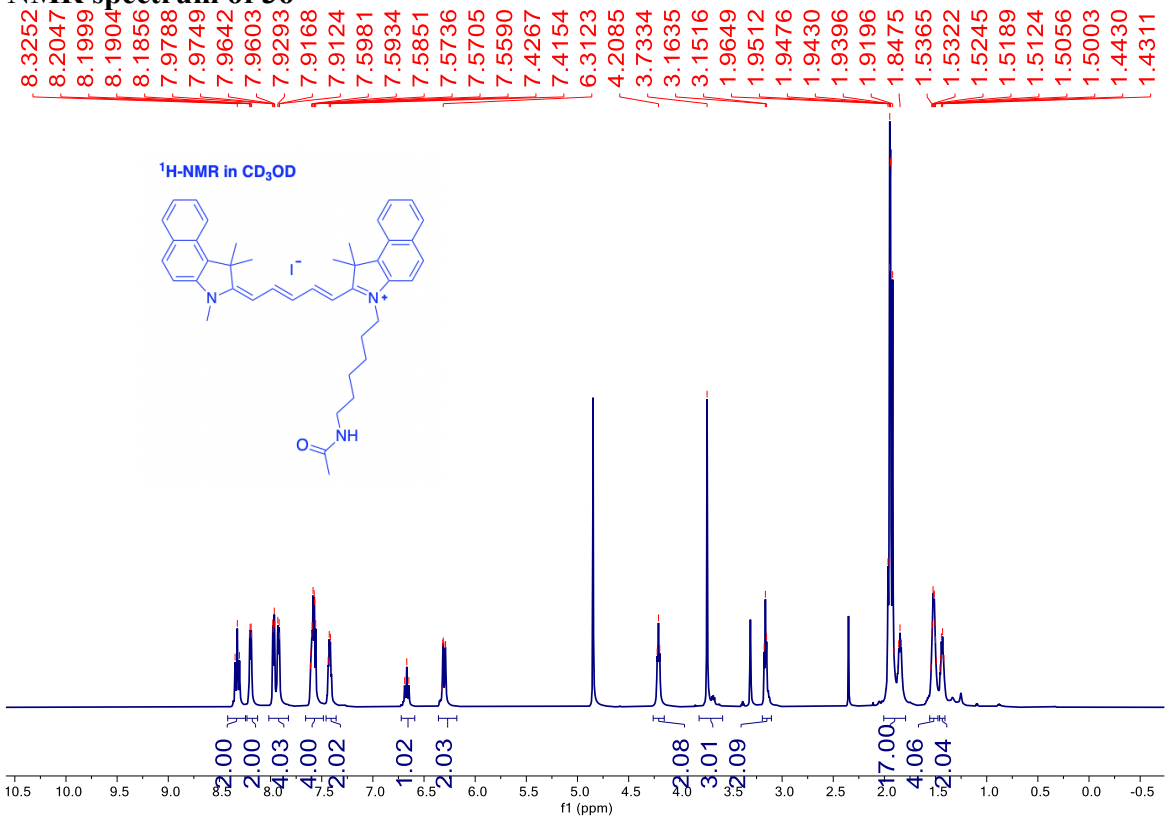

^{13}C-NMR spectrum of 3o

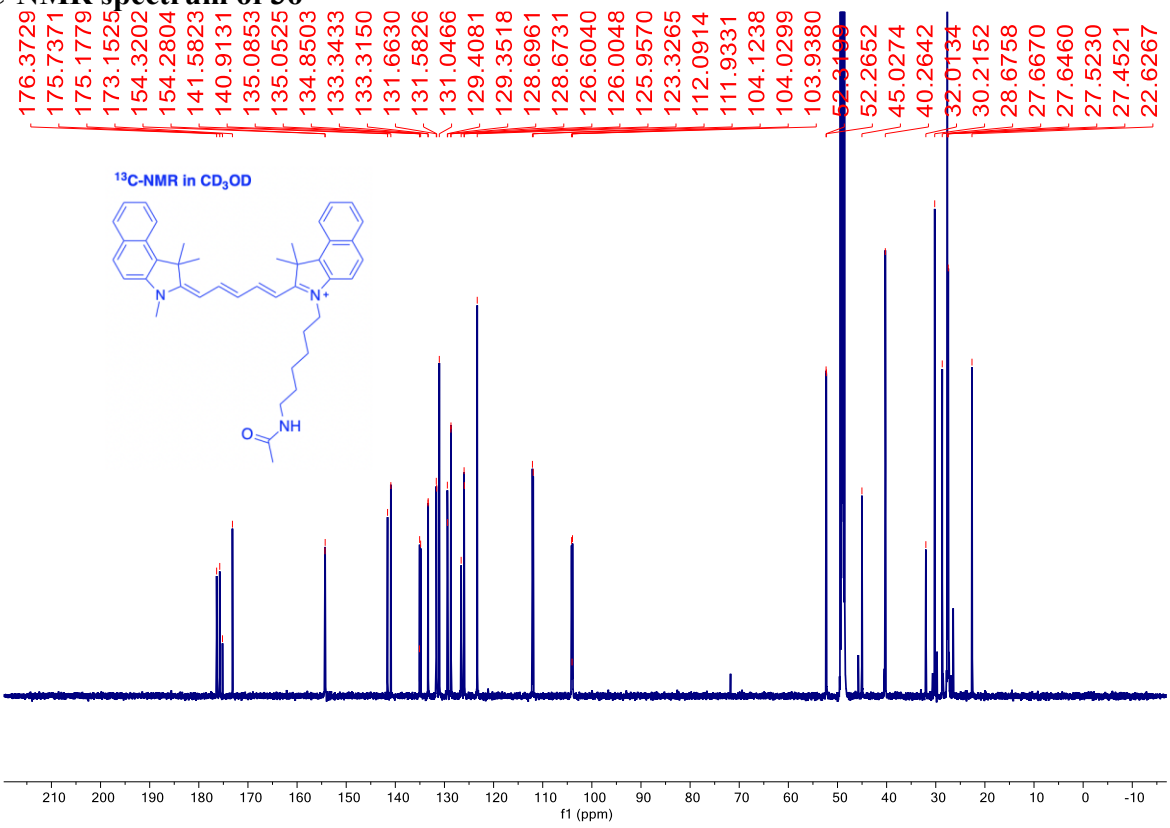

^{1}H-NMR spectrum of 3p

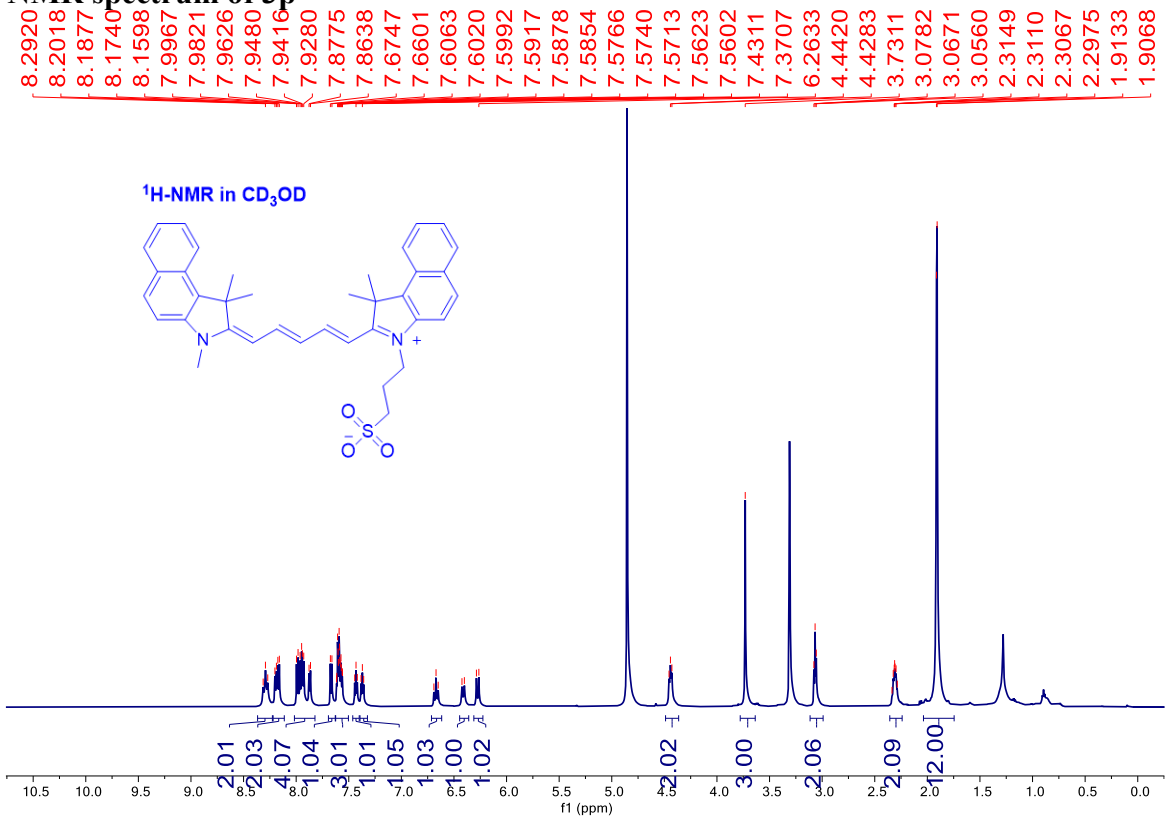

^{13}C-NMR spectrum of 3p

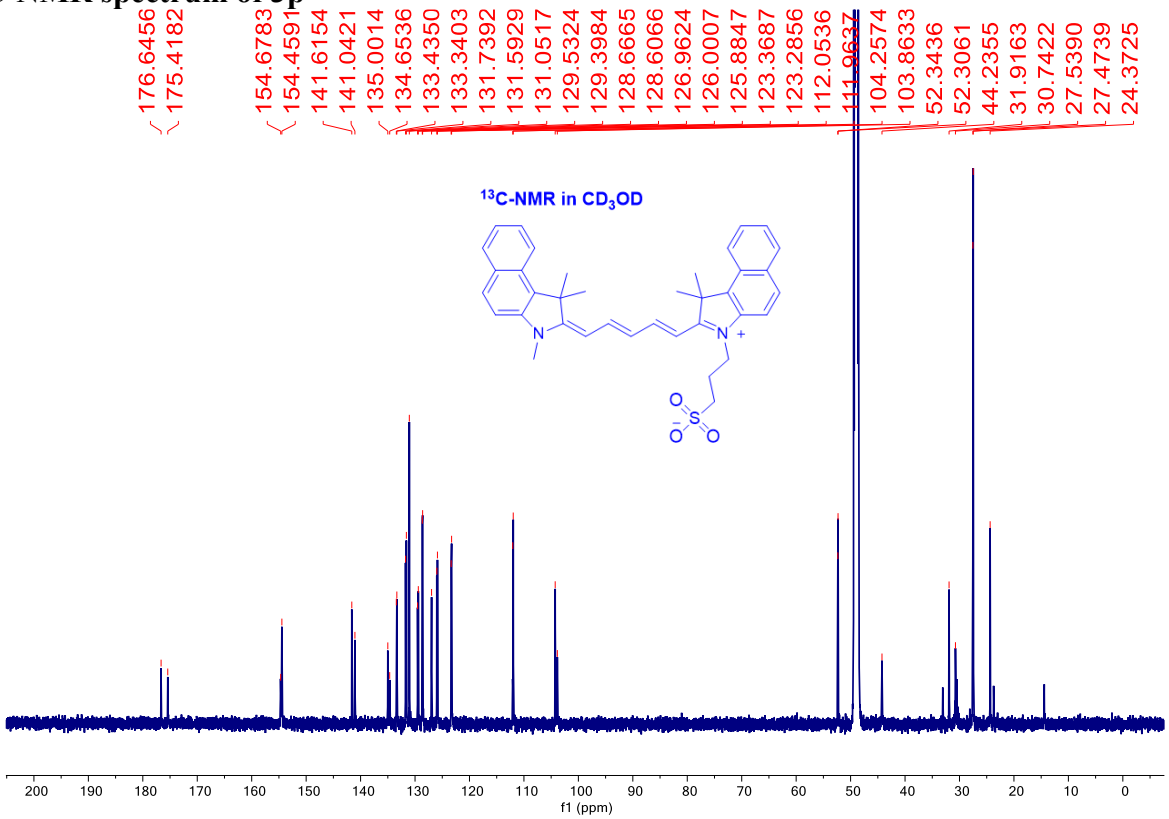

^{1}H-NMR spectrum of 3q

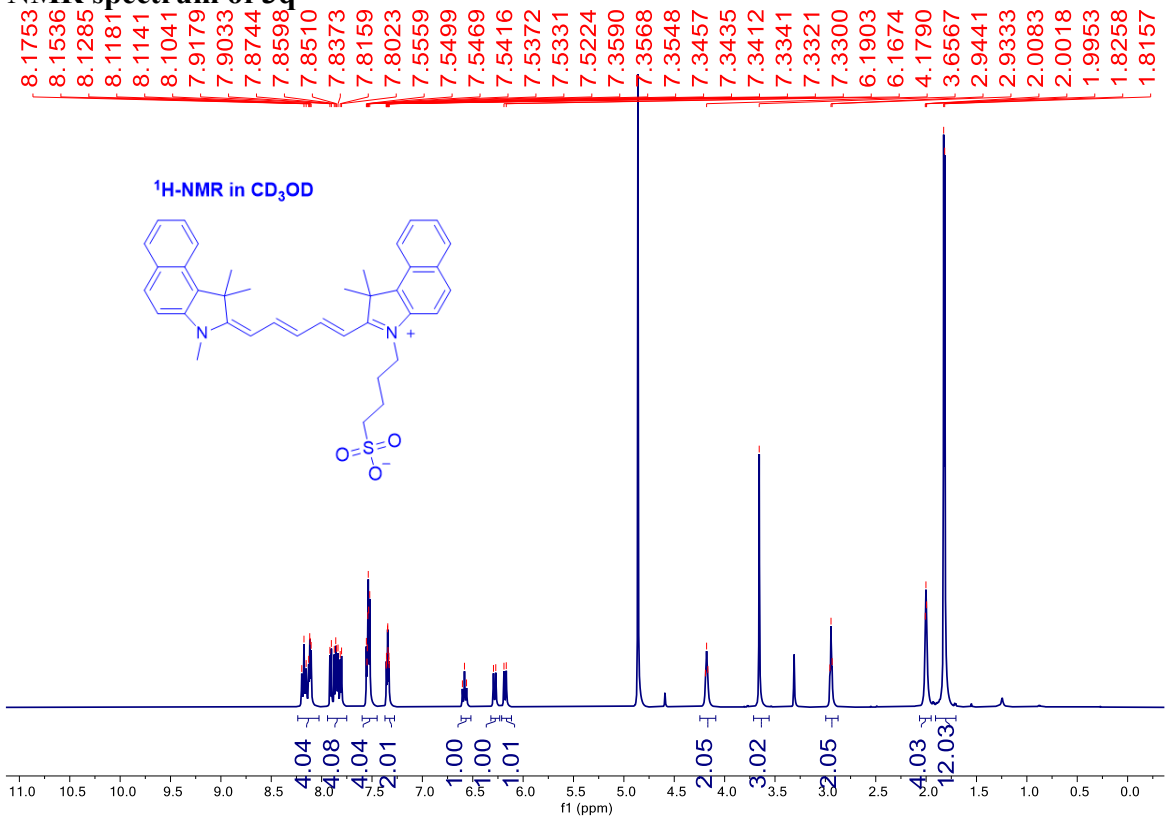

^{13}C-NMR spectrum of 3q

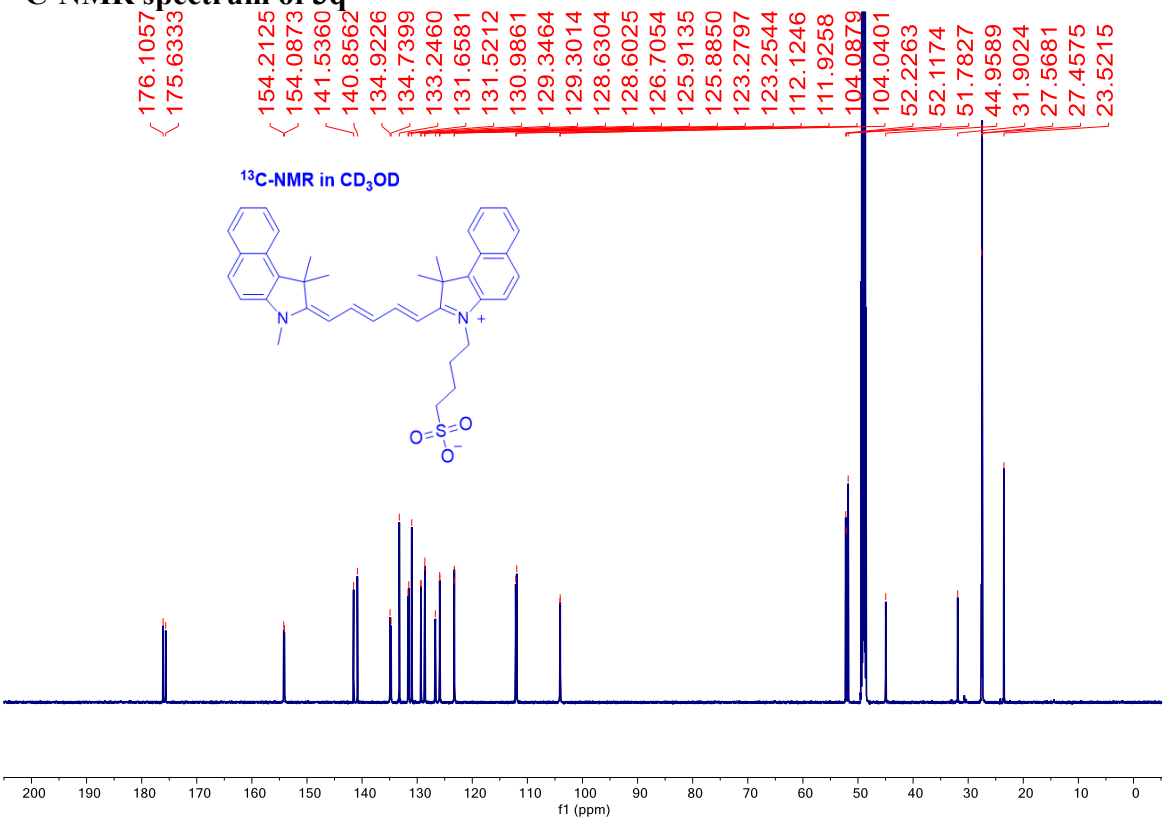

^{1}H-NMR spectrum of 3r

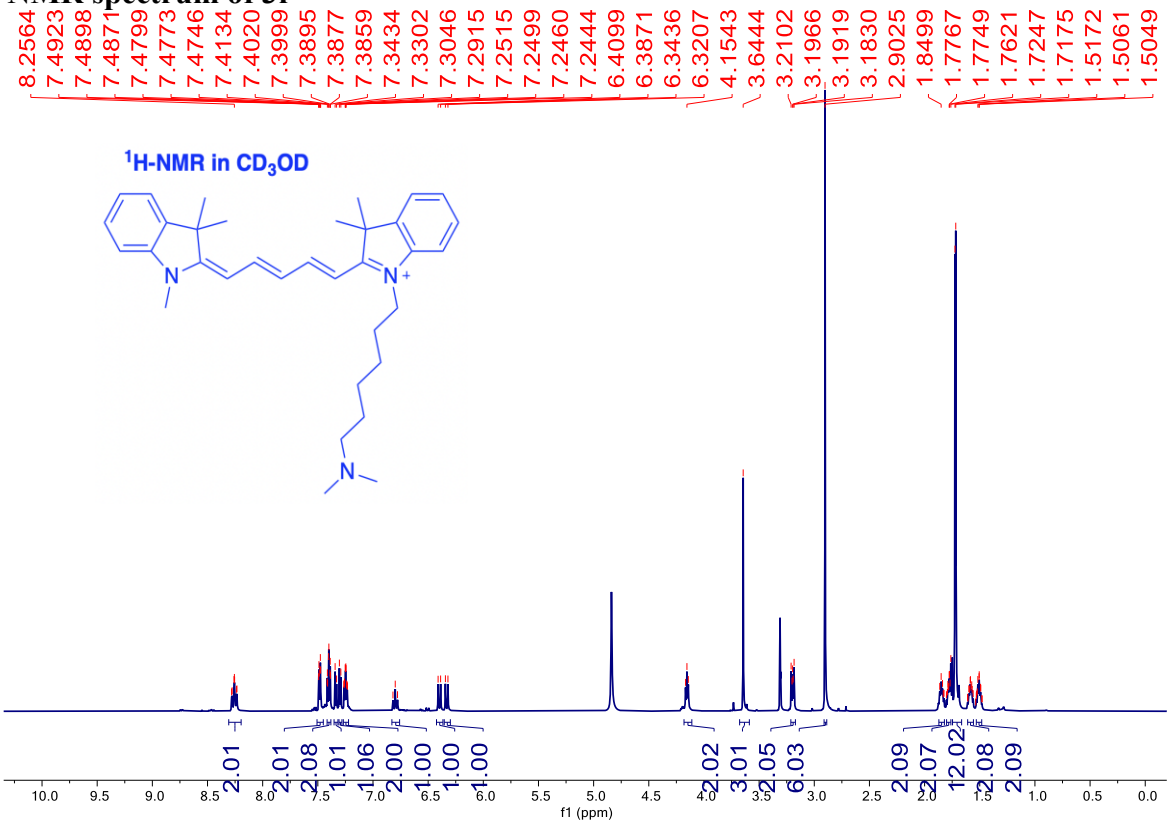

^{13}C-NMR spectrum of 3r

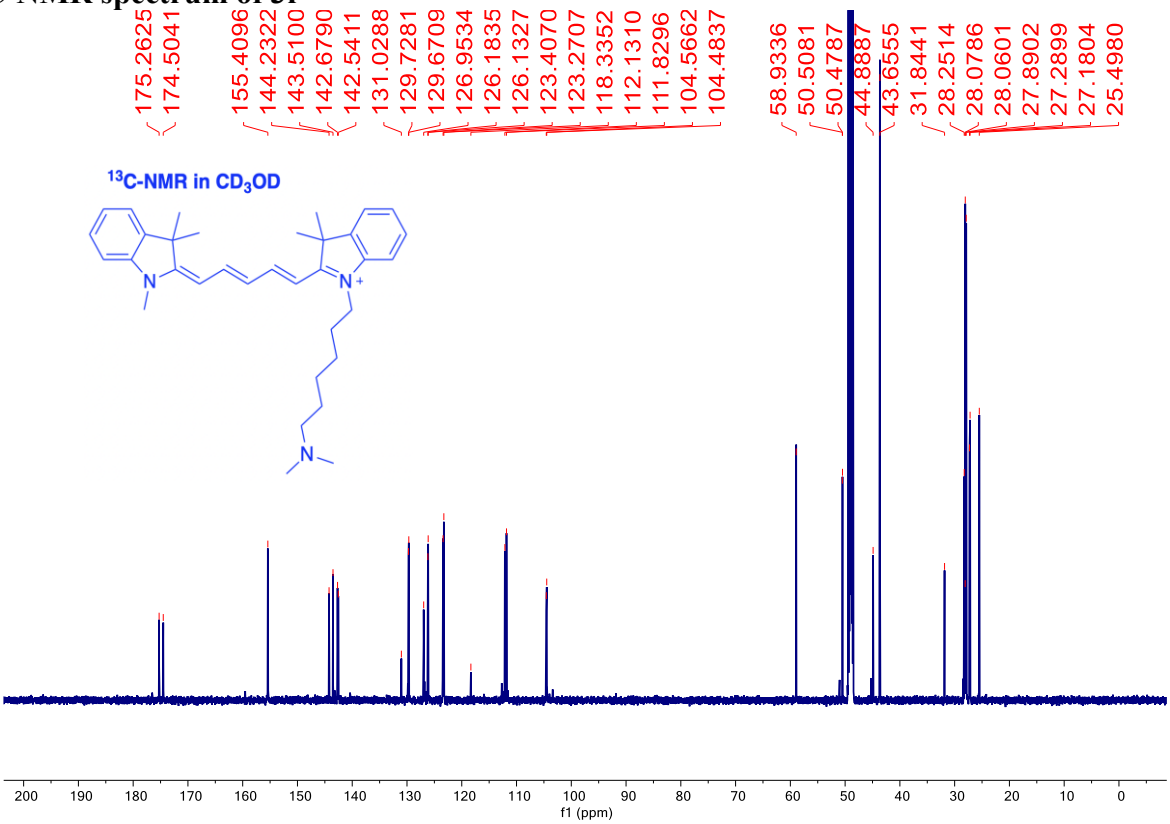

^{1}H-NMR spectrum of 3s

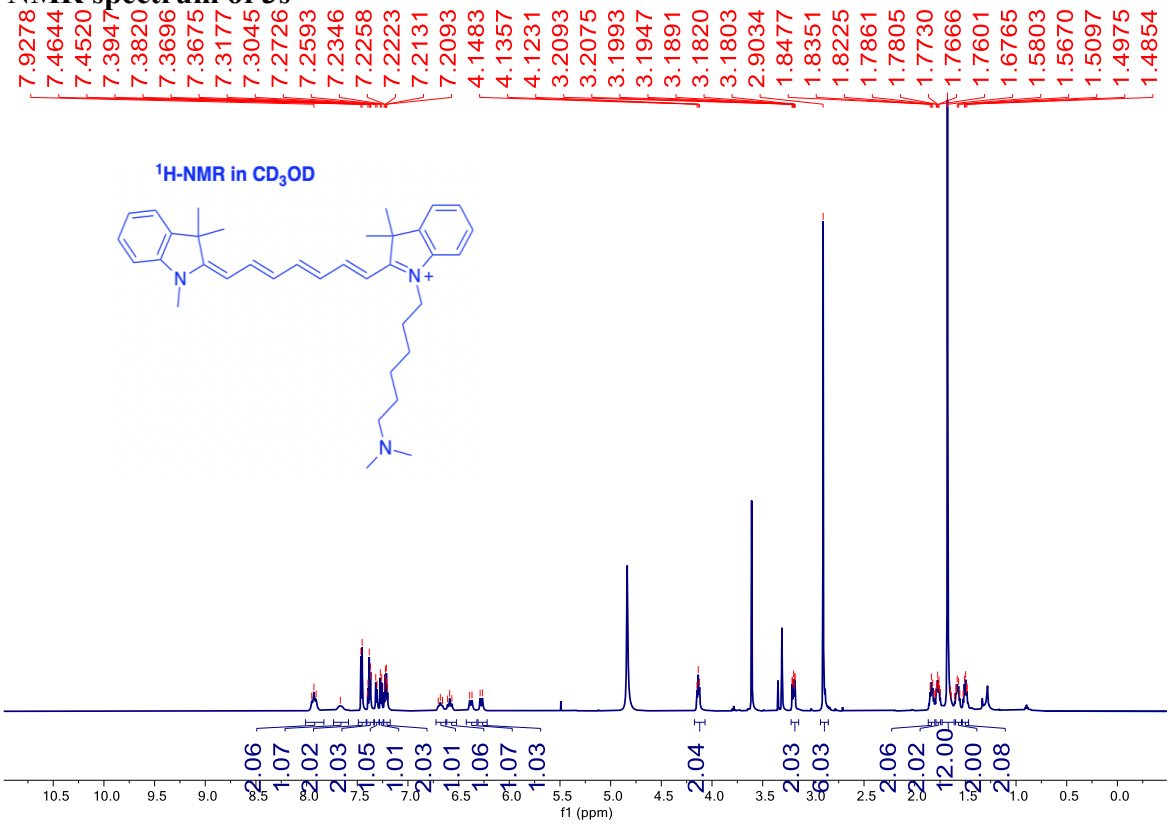

^{13}C-NMR spectrum of 3s

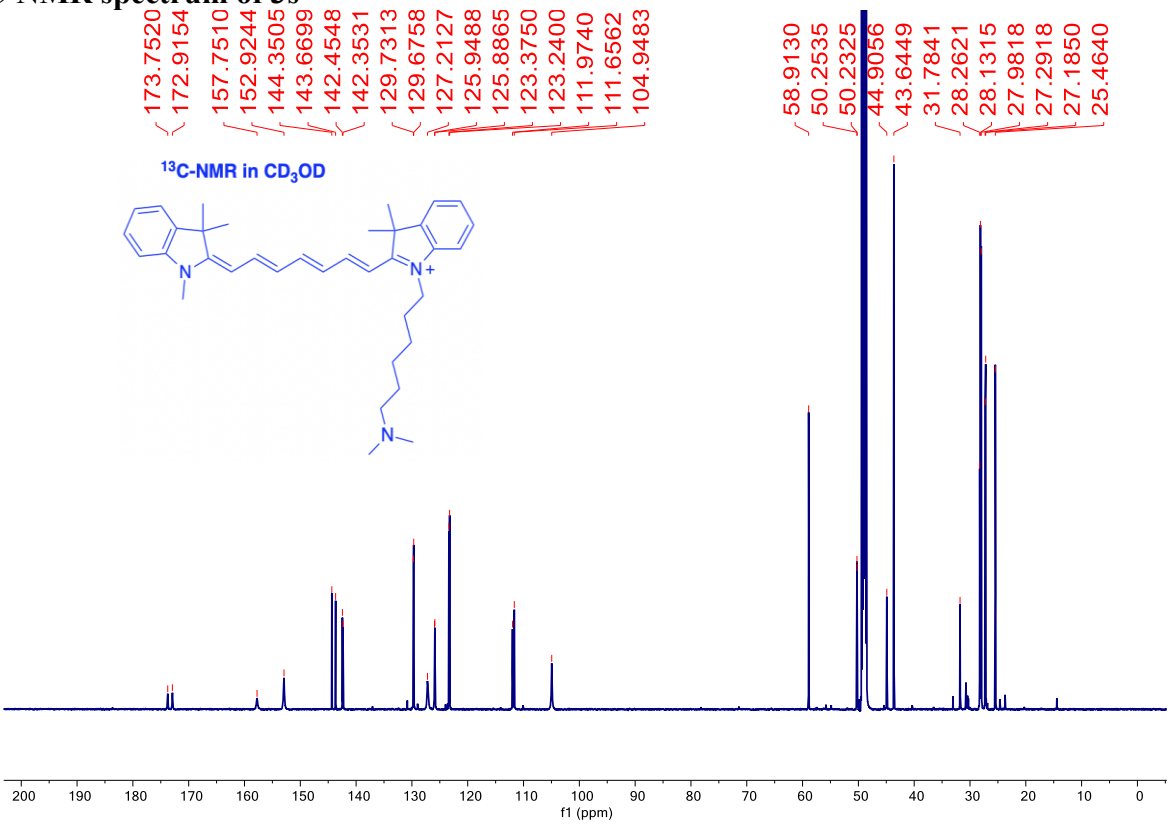

^{1}H-NMR spectrum of 3t

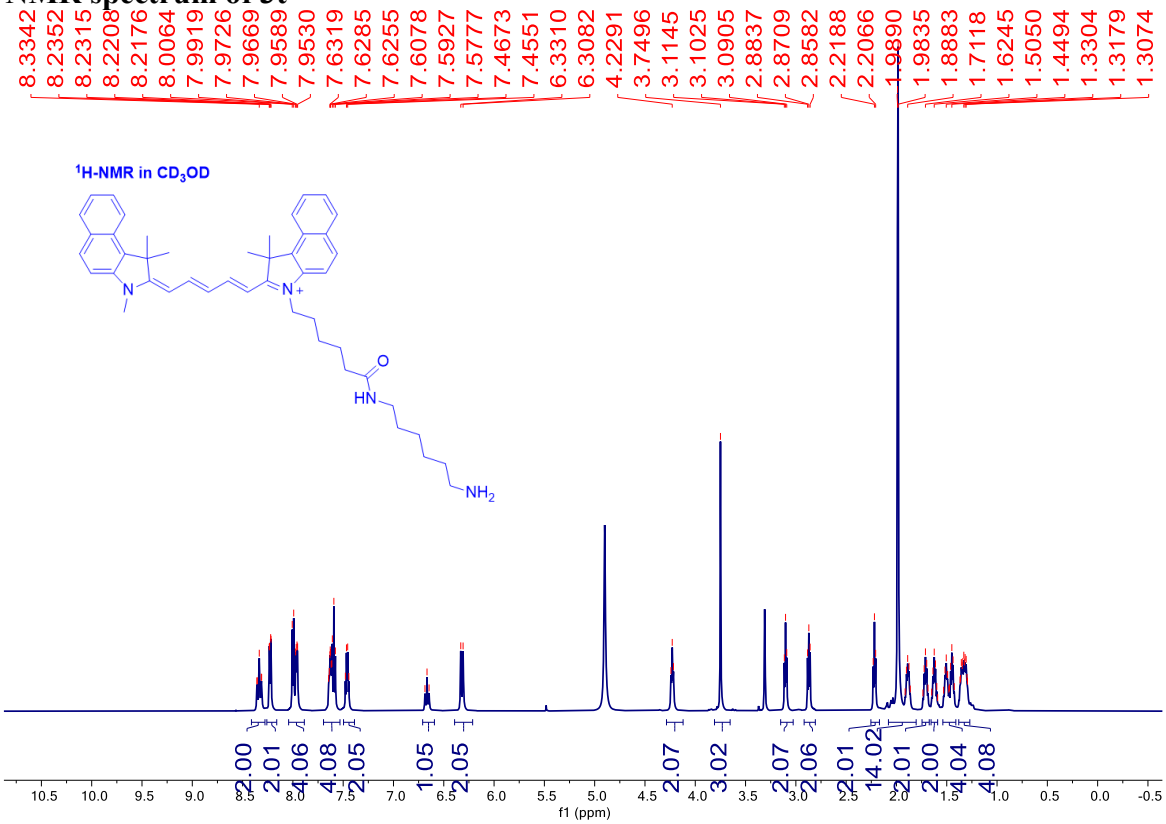

^{13}C-NMR spectrum of 3t